uOttawa

L'Université canadienne
Canada's university

FACULTÉ DES ÉTUDES SUPÉRIEURES ET POSTOCTORALES

uOttawa

L'Université canadienne
Canada's university

FACULTY OF GRADUATE AND POSDOCTORAL STUDIES

Geeta Kulkarni
AUTEUR DE LA THÈSE / AUTHOR OF THESIS

M.Sc. (Microbiology and Immunology)
GRADE / DEGREE

Department of Biochemistry, Microbiology and Immunology
FACULTÉ, ÉCOLE, DÉPARTEMENT / FACULTY, SCHOOL, DEPARTMENT

The Mechanism by which Protein Elongation Factor eEF1A2 Enhances Cell Growth and Oncogenicity

TITRE DE LA THÈSE / TITLE OF THESIS

Jonathan Lee
DIRECTEUR (DIRECTRICE) DE LA THÈSE / THESIS SUPERVISOR

CO-DIRECTEUR (CO-DIRECTRICE) DE LA THÈSE / THESIS CO-SUPERVISOR

EXAMINATEURS (EXAMINATRICES) DE LA THÈSE / THESIS EXAMINERS

Martin Holcik

Lisheng Wang

Gary W. Slater
LE DOYEN DE LA FACULTÉ DES ÉTUDES SUPÉRIEURES ET POSTDOCTORALES /
DEAN OF THE FACULTY OF GRADUATE AND POSTDOCORAL STUDIES

THE MECHANISM BY WHICH PROTEIN ELONGATION FACTOR eEF1A2 ENHANCES CELL GROWTH AND ONCOGENICITY

Geeta Kulkarni

Thesis submitted to the Faculty of Graduate and Postgraduate Studies
In partial fulfillment of the requirements for the degree of

Master of Science
in
Microbiology and Immunology

Department of Biochemistry, Microbiology and Immunology
Faculty of Medicine
University of Ottawa
Ottawa, Ontario, Canada

February 2006

Your file Votre référence
ISBN: 0-494-14919-1
Our file Notre référence
ISBN: 0-494-14919-1

Abstract

EEF1A2 is a putative ovarian and breast oncogene that encodes protein elongation factor eEF1A2. During protein translation, eEF1A2 binds amino-acylated tRNA and recruits it to the ribosome. eEF1A2 also regulates the translocation of the growing polypeptide from the acceptor (A) site to the peptidyl (P) site of the ribosome. Human *EEF1A2* is one of two isoforms of eukaryotic elongation factor 1α (*EEF1A*). *EEF1A1* and *EEF1A2* share more than 90 % DNA and amino acid sequence homology. eEF1A proteins from several species and genera associate with the cellular actin network by binding actin filaments and depolymerizing α-tubulin microtubules. This suggests that eEF1A proteins may contribute to the regulation of cytoskeletal organization in addition to controlling protein translation.

EEF1A2 is increased in copy number in about 25 % of primary ovarian tumors and highly expressed in approximately 30% of ovarian tumors and established cell lines. eEF1A2 mRNA is not detectable in normal ovarian epithelium while about one third of human ovarian tumours have measurable eEF1A2 mRNA. *EEF1A2* gene amplification and protein and mRNA over-expression also occurs in breast tumors. However, the mechanism by which eEF1A2 enhances cell growth and tumorigenesis is currently unknown.

A common signal for cell growth is the upregulation of global protein synthesis. Because eEF1A2 is a translation factor, it may be possible that aberrant eEF1A2 signaling could lead to an increase in cell growth rates via upregulation of certain cell growth regulatory proteins. To understand the mechanism by which eEF1A2 activates cell growth, we derived NIH 3T3 mouse fibroblasts that stably over-express constitutively active AKT, constitutively active PI3K, or c-Myc. We measured mRNA expression of eEF1A2 in these

stable cell lines by quantitative real time PCR. We found that AKT, PI3K or c-Myc expression does not substantially affect the mRNA expression of eEF1A2. We then used a human breast cell line to determine the effect of ectopic eEF1A2 expression on these oncogenes. Our results indicate that eEF1A2 does not affect protein expression of AKT, AKT-2, PI3K (p85 and p110α) or c-Myc. However, eEF1A2 does appear to lead to increased amounts of activated AKT at serine473 and threonine308 residues. This suggests that eEF1A2 may regulate phosphoinositide signaling.

We also derived an eEF1A2 specific antibody. The eEF1A2 specific antibody from rabbit anti-sera was purified by affinity chromatography. The specificity of our polyclonal antibody was analyzed by western blotting on human breast cell lines such as MCF-7 which endogenously express eEF1A2 and BT-549-parental cell lines transduced with flag tagged adenovirus-eEF1A2 (Ad-1A2). The cross-reactivity of eEF1A2 anti-sera against eEF1A1 was assessed by eEF1A2 and eEF1A1 GST fusion proteins. Our data indicate that our eEF1A2 antibody does not cross react with eEF1A1. The eEF1A2 antibody was also efficiently tested on paraffin embedded MCF-7 and BT-549-EV (empty vector) breast cell lines to assess the effectiveness of the eEF1A2 antibody for use in tissue microarrays. This antibody is likely to be utilized in using eEF1A2 as a prognostic marker for breast and ovarian cancer.

ACKNOWLEDGEMENTS

This thesis is by far one of the most significant accomplishments in my life and it would have been impossible without the support of people who believed in me. It is a pleasing facet that I have now an opportunity to manifest my gratitude for all of them. I owe my most sincere gratitude for the enormous scientific directions, trust and work environment provided to me by my thesis supervisor, Dr. Jonathan Lee. Working under his guidance has been an honor and a privilege, one that I am very thankful for. Most importantly, his enthusiasm and integral view on research inspired me to make the right decisions in a given time frame. I would also like to express my gratitude to Dr. Sattar who helped me right from the beginning and provided kind moral support. I am very grateful to my thesis advisory committee members, Dr. Christine Prattt and Dr. Douglas Gray for their intellectual discussions and insights concerning my project. This research has been supported and funded by the US army and CBCRI and I am thankful to them.

I am certainly appreciative of my lab colleagues, Anahita, Nadine, Jessica, Farahnaz and Dixie for providing a friendly environment for a homesick soul and valuable technical assistance, many thanks for being your colleague. My special thanks to Sujeeve for being kind and patient while editing my thesis and for offering me a helping hand through out my project. I am also grateful to Christina for providing me with rides without hesitation to campus even at one o'clock in the morning. I would like to thank Fernando and Kumara for all their help. Hey Fernando, your entertaining movies helped me to extract and precipitate the best out of my stressful brain. Many thanks are due to Dr. Paul Albert for enabling me to access the real time PCR machine and my sincere thanks to Margaret Czesak, for helping

me out with real time PCR. I extend my gratitude to the pathology department at the University of Ottawa for providing me facilities to perform immunocytochemistry. The last but not least, my sincere thanks go to Nicole and Carol Ann for their kind help.

At the heart of my support system is my family and friends back home. The encouragement and support of my mom and my brothers helped me to adapt to a new culture and land. The greatest support and inspiration has undoubtedly showered by my husband and I owe him my loving thanks. His unconditional support, sacrifice and understanding lifted me during the dark times that inevitably present along this road. It is not possible to mention everybody who had an impact to this work, but I certainly appreciate everyone who helped me finish this project with my spirit intact. However, there are those whose spiritual support is even important and those are my parents. I feel a deep sense of gratitude for my late father who formed a part of my vision and goals, his memories are at the roots of my inspiration. Importantly, I would like to dedicate my thesis to my mother because without her I would not have reached here.

TABLE OF CONTENTS

ABSTRACT.....ii

ACKNOWLEDEMENTS.....iv

TABLE OF CONTENTS.....vi

LIST OF FIGURES.....x

LIST OF ABBREVIATION.....xii

INTRODUCTION.....1

PROTEIN SYNTHESIS

Initiation.....3

Elongation.....5

Termination.....7

ELONGATION FACTORS

eEF1A.....7

eEF1A2.....10

AKT/PKB

Background.....11

Structure of AKT.....12

AKT and cell survival.....14

Phosoinositide 3-kinase (PI3K)

Background.....17

Structure and function of PI3K.....18

c-MYC

Background.....21
Structure of c-Myc.....22
c-Myc and cell signaling.....23
SUMMARY.....25
MATERIALS AND METHODS.....26
PLASMID CONSTRUCTS.....27
LIGATION AND TRANSFORMATION.....27
CELL CULTURE FOR NIH 3T3 AND STABLE TRANSFECTIONS.....30
Cell extracts from stably transfected cells.....31
SDS-AGE.....32
REAL-TIME PCR FOR eEF1A2.....33
RNA extraction.....33
Preparation of cDNA and quantitative PCR.....34
CULTURE OF BT-549 CELLS.....37
Cell extracts and SDS-PAGE.....37
DERIVATION OF eEF1A2 ANTIBODY.....38
Affinity chromatography.....39
Cell lines.....42
SDS-PAGE and western blotting.....43
SPECIFICITY OF eEF1A2 ANTIBODY.....44
Production of GST-recombinant proteins:eEF1A2 and eEF1A1.....44
GST plasmid constructs.....44
Expression of GST fusion proteins.....45

Immunoprecipitation.....46

Immunocytochemistry.....47

HYPOTHESIS AND OBJECTIVES.....50

RESULTS.....51

DETERMINING THE EFFECT OF AKT,PI3K AND c-MYC EXPRESSION ON mRNA EXPRESSION OF eEF1A2.....52

Effect of AKT on mRNA expression of eEF1A2.....52

Effect of PI3K on mRNA expression of eEF1A2.....54

Effect of c-Myc on mRNA expression of eEF1A2.....56

DETERMINING THE EFFECT OF eEF1A2 PROTEIN EXPRESSION ON PAN-AKT, AKT-2, pAKT, PI3K(p85 AND p110 SUBUNITS AND c-MYC.....58

Expression of eEF1A2 in BT-549 cell lines.....58

Effect of eEF1A2 expression on activation and protein expression of AKT.....58

Effect of eEF1A2 expression on protein expression of AKT-2.....61

Effect of eEF1A2 expression on protein expression of catalytic and and regulatory subunits of PI3K.....61

Effect of eEF1A2 expression on protein expression of c-Myc.....65

DERIVATION OF eEF1A2 SPECIFIC ANTIBODY

Western blotting.....65

EVALUATION OF THE SPECIFICITY OF eEF1A2 ANTIBODY

Immunoprecipitation.....70

eEF1A2-siRNA and eEF1A2 antibody.....73

GST constructs and eEF1A2 antibody.....73

Immunocytochemistry.....77

DISCUSSION.....78

DETERMINING THE EFFECT OF AKT,PI3K AND c-MYC EXPRESSION ON mRNA EXPRESSION OF eEF1A2.....80

Effect of AKT expression on mRNA expression of eEF1A2.....80

Effect of PI3K expression on mRNA expression of eEF1A2.....83

Effect of c-Myc expression on mRNA expression of eEF1A2..... 86

DETERMING THE EFFECT OF eEF1A2 EXPRESSION ON THE PROTEIN EXPRESSION OF AKT, pAKT, AKT-2, PI3K AND c-MYC.....89

Effect of eEF1A2 expression on protein expression of AKT, AKT-2 and phospho-AKT (pAKT).....89

Effect of eEF1A2 expression on protein expression of catalytic(p110) and regulatory (p85) subunits of PI3K..... 92

Effect of eEF1A2 expression on protein expression of c-Myc..... 94

DERIVATION OF eEF1A2 SPECIFIC ANTIBODY..... 96

Optimization of western blotting.....97

The specificity of eEF1A2 antibody.....98

LIST OF REFERENCES..... 102

LIST OF FIGURES

Figure 1	The initiation phase of protein translation	4
Figure 2	The role of eEF1A in the elongation phase of protein translation	6
Figure 3	Termination phase of protein translation	8
Figure 4	Domain structure of AKT/PKB	13
Figure 5	Multiple mechanisms of cell survival regulation by AKT/PKB	15
Figure 6	Domain structure of phosphoinositide 3-kinase (PI3K)	19
Figure 7	Effect of AKT expression on mRNA expression of eEF1A2	53
Figure 8	Effect of PI3K expression on mRNA expression of eEF1A2	55
Figure 9	Effect of c-Myc expression on mRNA expression of eEF1A2	57
Figure 10	Expression of eEF1A2 in BT-549 cells	59
Figure 11	Effect of eEF1A2 expression on protein expression of AKT and phospho-AKT	60
Figure 12	Effect of eEF1A2 expression on protein expression of AKT-2	62
Figure 13	Effect of eEF1A2 expression on catalytic and regulatory subunits of PI3K	63
Figure 14	Effect of eEF1A2 expression on protein expression of c-Myc	64
Figure 15	Derivation of eEF1A2 antibody	66
Figure 16	Derivation of eEF1A2 antibody (optimization for western blotting)	68
Figure 17	Derivation of eEF1A2 antibody (Final optimization for	

western blotting) 69

Figure 18 Derivation of eEF1A2 antibody (MCF-7 and BT-549 cells) 71

Figure 19 Immunoprecipitation 72

Figure 20 Specificity of eEF1A2 antibody (The eEF1A2-siRNA and eEF1A2 antibody) 74

Figure 21 Specificity of eEF1A2 antibody (eEF1A2 anti-sera against eEF1A2 and eEF1A1 GST proteins) 75

Figure 22 Immunocytochemistry 76

ABBREVIATION

aa-tRNA	Aminoacyl tRNA
ATCC	American type culture collection
Ad-eEF1A2	Adenovirus eEF1A2
bHLHzip	Basic helix-loop-helix leucine zipper
BSA	Bovine serum albumin
°C	Degree celcius
cDNA	Complementary deoxyribonucleic acid
CMV	Cytomegalovirus
CsCl	Cesium chloride
C_T	Threshold cycle
C-terminal	Carboxy terminal
DAB	Diaminobenzidine
Ddwater	Double distilled water
DEPC	Diethyl pyrocarbonate
DMSO	Dimethyl sulfoxide
DMEM	Dulbecco's Modified Eagle Medium
DNA	Deoxyribonucleic acid
dNTP	Deoxyribonucleoside trisphosphate
DNAse	Deoxyribonuclease
DTT	Dithiothreitol
E.coli	*Escherichia coli*
ECL	Enhanced chemiluminescence
EDTA	Ethylenediamine tetraacetic acid
eIFs	Eukaryotic initiation factors
eRF	Eukaryotic release factor
EV	Empty vector
eEF1A	Eukaryotic elongation factor 1A
FBS	Fetal bovine serum
GDP	Guanosine diphosphate
GPCR	G-protein coupled receptor
GTP	Guanosine triphosphate
GST	Glutathione S-transferase
HCl	Hydrochloric acid
HEPES	N-[2-Hydroxyethyl]piperazine-N′-[2-ethanesulfonic acid] sodium salt
Hr	Hour

HRP	Horseradish peroxidase
IAA-NHS	Iodoacetic Acid –N-Hydroxysuccinimide Ester
ILK	Integrin-linked kinase
IPTG	Isopropyl-β-D-thiogalactopyranoside
Kb	Kilobases
KLH	Keyhole limpet hemocyanin
LBA	Luria-Bertani agar
M	Molar
Met-tRNA	Methionine- tRNA
Min	Minute
mRNA	Messenger ribonucleic acid
mTOR	Mammalian target of rapamycin
NBF	Neutral buffered formalin
ng	Nanogram
N-terminal	Amino terminal
OD	Optical density
PAGE	Polyacrylamide gel electrophoresis
PBS	Phosphate buffered saline
PCR	Polymerase chain reaction
PDK	Phosphoinositide-dependent kinase
PIC	Protein inhibitor cocktail
PI3K	Phosphatidylinositol 3-Kinase
PKB	Protein Kinase B
PMSF	Phenylmethylsulfonyl fluoride
PtdIns	Phosphatidylinositol
PVDF	Polyvinylidene difluoride
qRT-PCR	Quantitative reverse transcriptase PCR
RIPA	Radioimmunoprecipitation buffer
RNA	Ribonucleic acid
RNAse	Ribonuclease
RPM	Rounds per minute
RT	Room temperature
SDS	Sodium dodecyl sulphate
Ser	Serine

TBS	Tris-buffered saline
TBS/T	Tris-buffred saline with 1%Tween-20
TE	Tris-EDTA
TEMED	N, N, N′, N′-tetramethyl-ethylenediamine
Thr	Threonine
Tris	Trihydroxymethylamino-methane
tRNA	Transfer ribonucleic acid
ug	Microgram
umol	Micromolar
UTR	Untranslated region
UV	Ultraviolet

INTRODUCTION

Introduction

The idea that protein translation can impact oncogenesis is exciting but not fully explored. Translational elements in regulation of cell proliferation and transformation have been investigated over the past few years. Translational factors are highly conserved throughout evolution and their roles as oncogenes and enhancing tumorigenicity can lead to new insights related to cell growth control. Recent research has mainly focused on exploring the link between cancer development and proteins engaged in protein synthesis. The eukaryotic initiation factor, eIF4E, was the first protein translation factor implicated in malignancy (Watkins and Norbury, 2002). Moreover, our laboratory recently identified the eukaryotic elongation factor, *EEF1A2*, as a putative breast and ovarian oncogene. Cell growth and proliferation rates rely upon the rate of protein synthesis. The deregulation of protein synthesis is a common feature of tumorigenesis and has been seen in various cancers. For example, eIF4E over-expression is found in a wide variety of human tumors (Watkins and Norbury, 2002). Furthermore, eEF1A2 has also proved to be involved in tumorigenesis (Anand *et al.* 2002). The major goal of the current study is to elucidate the mechanism by which eEF1A2 enhances cell growth and oncogencity.

Proteins are important in that they are structural and functional components of living entities. Living systems require that proteins are manufactured in a systematic and specific manner. Thus, protein synthesis is a highly complex process that requires numerous components to function effectively and flawlessly in order to translate one mRNA into a corresponding protein. This process utilizes large quantities of cellular energy. The translation of mRNA is conceptually divided into three stages: initiation,

elongation and termination.

PROTEIN SYNTHESIS

Initiation

Translation initiation in mammalian cells is an intricate process comprising a set of proteins known as eukaryotic initiation factors (eIFs) (Fig1A-B) (Kapp and Lorsch, 2004). The main purpose of this process is to position the 80S ribosome correctly on the mRNA. At first, the 80S ribosome dissociates into the 40S and 60S ribosomal subunits. eIF1, eIF3 and eIF1A attach and recruit the 40S subunit of the ribosome to the mRNA, whilst the 60S subunit associates with eIF3A (Gingras *et al.* 1999; Hershey *et al.* 1991). Thus the binding of mRNA to the 40S ribosome needs several initiation factors, eIF4F, a multimer, and a functional complex made up of eIF4E, eIF4A, eIF4B and eIF4G. The met-tRNA is recruited to the 40S ribosome by a GTP bound eIF2. eIF2 becomes inactive upon GDP binding and this happens as a recycling process which is governed by a guanine nucleotide exchange factor, eIF2B (Abbott and Proud, 2004). eIF4E attaches to the 5′-cap of the mRNA to form complexes with eIF4G and thus binds the 7-methyl guanosine cap at the 5′ end of the mRNA. The eIF4E binding proteins (4E-BP), 4E-BP1, 4E-BP2 and 4E-BP3, prevents eIF4E from binding with the mRNA and eIF4G (Thornton *et al.* 2003). The ternary complex of GTP, eIF2 and met-tRNA with the 40S ribosomal subunit further scans for the start codon (AUG) along the 5′-untranslated region (5′ UTR) (Abbott and Proud, 2004). The AUG codon then associates with the UAC anticodon of methionine charged aa-tRNA (met-tRNA). The 60S ribosomal subunit further associates with the ternary complex to form the 80S initiation complex. Thus the 80S ribosome

Figure 1. The initiation phase of protein translation.

A complex of eIF1, eIF1A, eIF3 and tRNA-met binds to the 40S subunit of the ribosome. The eIF4F (eIF4B, eIF4A, eIF3) multimer complex binds to the 7' methyl cap. The 43S mRNA initiation complex attaches to the mRNA near the cap and scans for an AUG codon. After recognizing the start codon, eIF5 catalyzes the hydrolysis of GTP and releases all initiation factors from the ribosome complex while leaving the tRNA-met bound to the AUG codon. The 60S ribosomal complex associates with 40S ribosome to form 80S initiation complex which can proceed into elongation process.

(The figure is taken from Kapp and Lorch , 2004, with kind permission from *Annu Rev Biochem*)

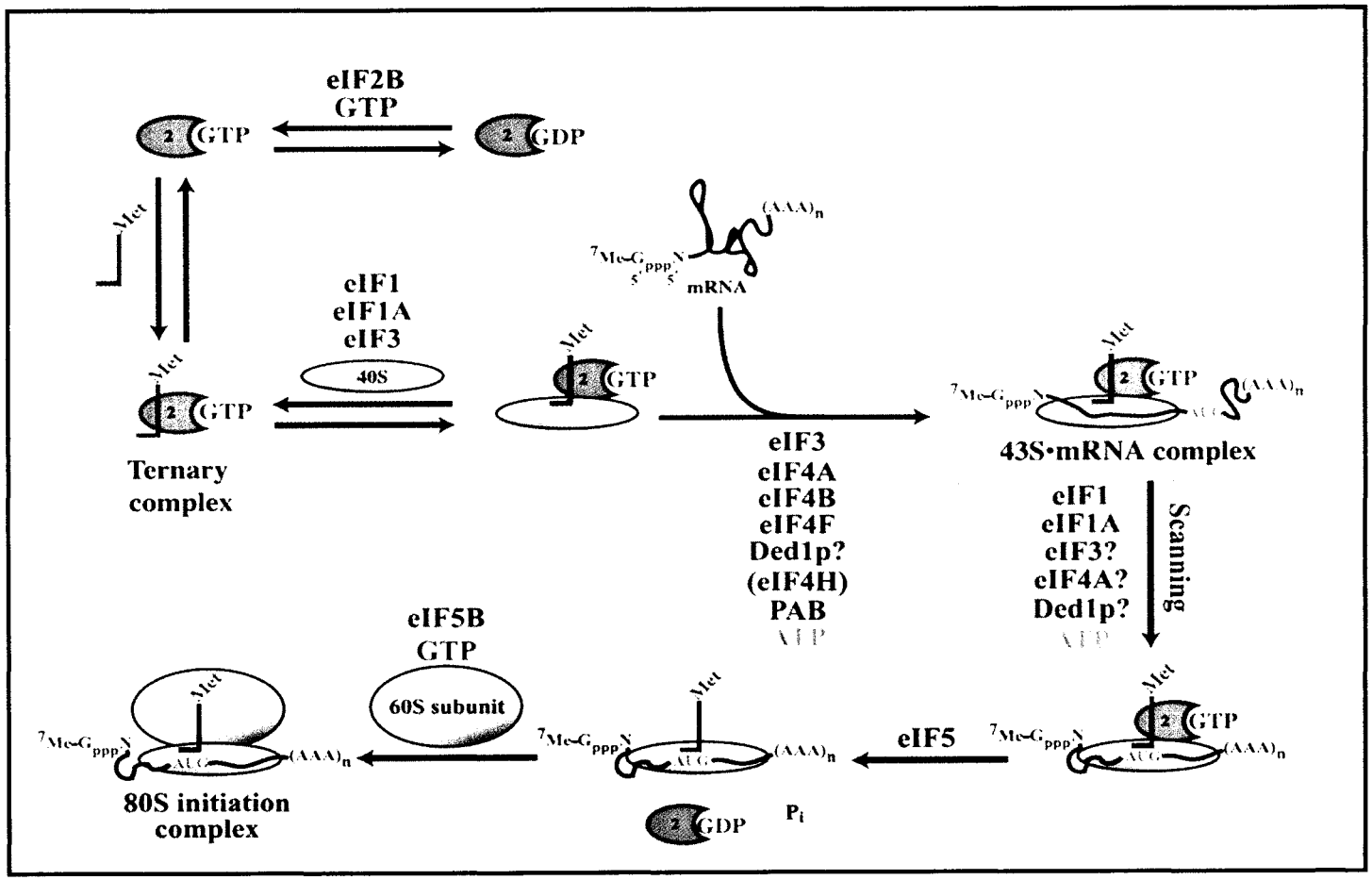
eIF2B
GTP
GTP
GDP
Met
eIF1
eIF1A
eIF3
40S
Met
GTP
Ternary
complex
mRNA
eIF3
eIF4A
eIF4B
eIF4F
Ded1p?
(eIF4H)
PAB
ATP
43S•mRNA complex
eIF1
eIF1A
eIF3?
eIF4A?
Ded1p?
ATP
Scanning
eIF5B
GTP
60S subunit
80S initiation
complex
eIF5
GDP
Pi

with the start codon is positioned in the ribosomal P-site (peptidyl site) and is ready to proceed to the elongation phase of protein translation.

Elongation

During the elongation process, the polypeptide grows in length as additional amino acids are sequentially added to the growing polypeptide chain in the order specified by the sequence of mRNA (Fig.2) (Abbott and Proud, 2004). The acylated tRNA molecules are associated to their respective amino acids and form complexes termed as aminoacyl-tRNAs. This process occurs in the cytoplasm and depends on aminoacyl-tRNA (aa-tRNA) synthetase enzymes (Gingras *et al.* 1999; Hershey *et al.* 1991). eEF1A recruits aa-tRNA to the A-site (acceptor or aminoacyl binding site) of the ribosome (Hershey *et al.* 1991). This process is cyclic and governed by GTP hydrolysis. The guanidine nucleotide-exchange factor eEF1B stimulates the regeneration of active eEF1A-GTP complexes where eEF1A protects the aminoacyl ester bond against hydrolysis. eEF1B is comprised of α, β, and γ subunits which are encoded by three different genes respectively (Thornton *et al.* 2003; Hershey *et al.* 1991). eEF1 translation factors regulate the shuttling of aa-tRNA while the peptide bond forms between the amino acids at the P-site and the A-site under the control of eEF2. In particular, eEF2-GTP binds near the A site of the ribosome and forces aa-tRNA from the A site to the P site which stimulates the ribosome to move one codon down the mRNA towards the 3′ direction. Thus the elongation factor eEF2 is essential for the translocation of the peptidyl-tRNA from the A-site to the P-site of the ribosome (Abbott and Proud, 2004). This translocation process as well as the movement of the ribosome along the mRNA is GTP-dependent. The peptidyl transferase in the 60S ribosomal subunit catalyses the

Figure 2. The role of eEF1A in the elongation phase of protein translation.

Eukaryotic elongation factor 1A bound to GTP, shuttles amino-acelated tRNA (aa-tRNA) to the A- site of ribosome. The proper codon-anticodon interactions triggers GTP hydrolysis and eEF1A-GDP releases from the ribosome. eEF1A further interacts with eEF1B which lead to the regeneration of eEF1A-GTP. (The figure is taken from Abbott and Proud, 2004, with kind permission from *Trends Biochem Sci*)

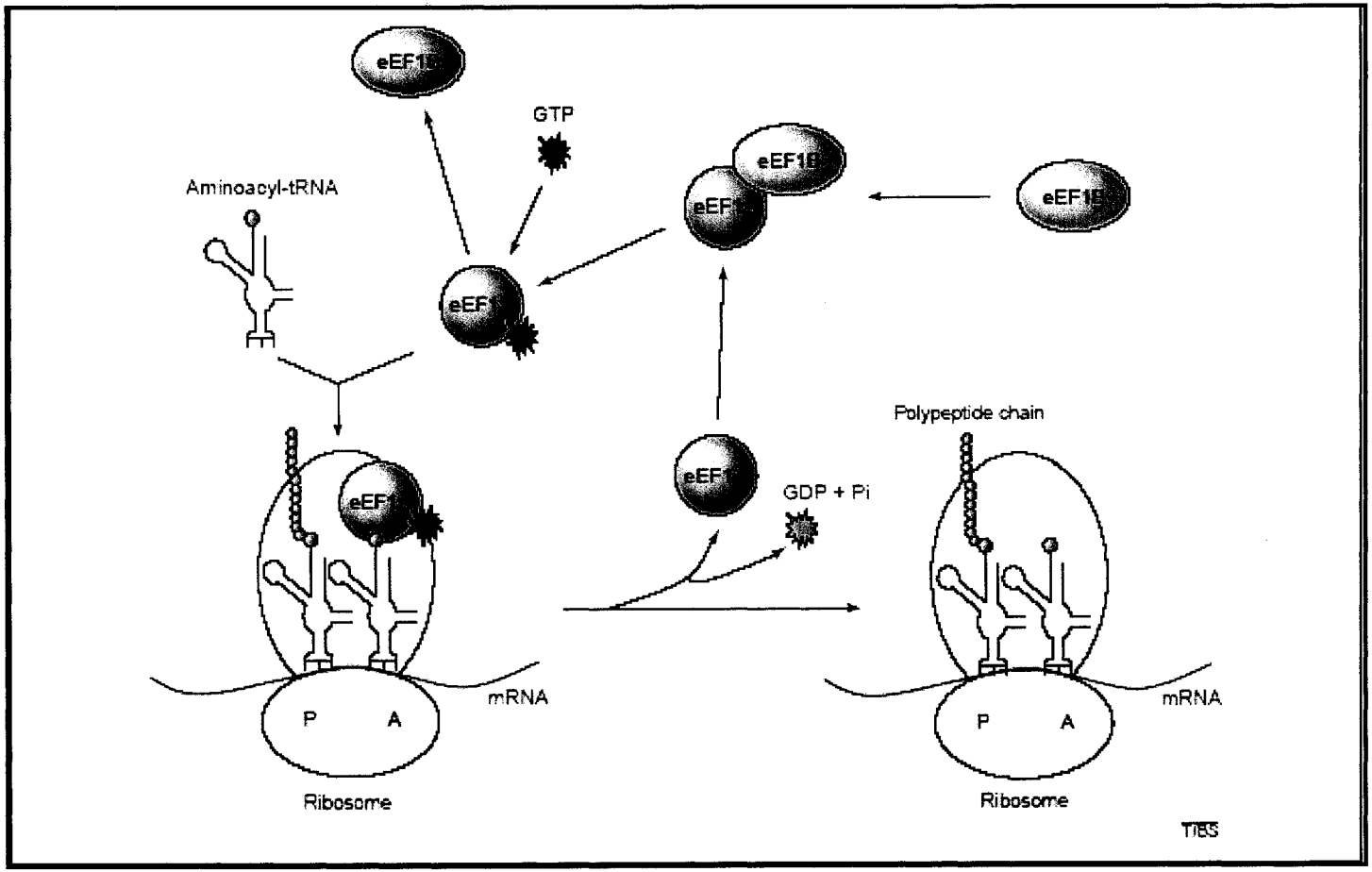
eEF1
GTP
Aminoacyl-tRNA
eEF1B
eEF1
eEF1B
eEF1
eEF1
Polypeptide chain
GDP + Pi
mRNA
P
A
Ribosome
mRNA
P
A
Ribosome
TIBS

formation of a peptide bond between amino acids in the A-site and the P-site of the ribosome (Hershey *et al.* 1991). The deacylated tRNA from the P-site is compelled to the exit site (E-site) and then released from the ribosome to recycle back to the cytosol and to further reacylate there. The dissociation of eEF2 makes the A site vacant for the recruitment of new aa-tRNA by eEF1A. The eEF1A and eEF2 proteins are recycled since the GTP hydrolysis is required to complete the elongation process until a stop codon on the mRNA arrives into the A-site (Kapp and Lorsch, 2004).

Termination

The final step of translation is termination which occurs when the stop codon (UAA, UAG, or UGA) arrives at the A-site of the ribosome (Fig.3) (Kapp and Lorsch, 2004). Eukaryotic release factor1 (eRF1) imitates an aa-tRNA and attaches to the A-site in the presence of stop codons. This is also a GTP-dependent process (Mansilla *et al.* 2002). The binding of eRF1 complex to the ribosome triggers the cleavage of the bond between the peptide and tRNA and that promotes the release of the newly synthesized polypeptide from the E-site to the cytoplasm. Furthermore, eRF3 catalyzes eRF1 and dissociates eRF1 from the ribosome by GTP hydrolysis (Kapp and Lorsch, 2004).

ELONGATION FACTORS

eEF1A

The eukaryotic translation elongation factor 1 (eEF1A, formerly EF-1α and in eubacteria, EF-Tu) is a soluble and highly abundant multifunctional protein which recruits aa-tRNA to the ribosome (Kapp and Lorsch, 2004; Munshi *et al.* 2001; Ransom-Hodgkins *et al.* 2000). eEF1A is a well-conserved protein and forms 1-3% of the total

Figure 3. Termination phase of protein translation.

Upon stop codon recognition (UAA, UGA, UAG), eukaryotic release factor 1 (eRF1) enters the A-site of the ribosome. eRF1 resembles the letter "Y" and structurally mimics an aa-tRNA. eRF1 binding to the stop codon stimulates the hydrolysis of peptidyl-tRNA. This leads to the release of the polypeptide chain from the tRNA and the ribosomal complex into the cytoplasm. The tRNA further moves to the E-site of the ribosome from where it is then released into the cytoplasm. eRF3 stimulates the dissociation of eRF1. The remaining ribosome complex contributes in translational reinitiation or gets recycled is unclear. (The figure is taken from Kapp and Lorch, 2004, with kind permission from *Annu Rev Biochem*)

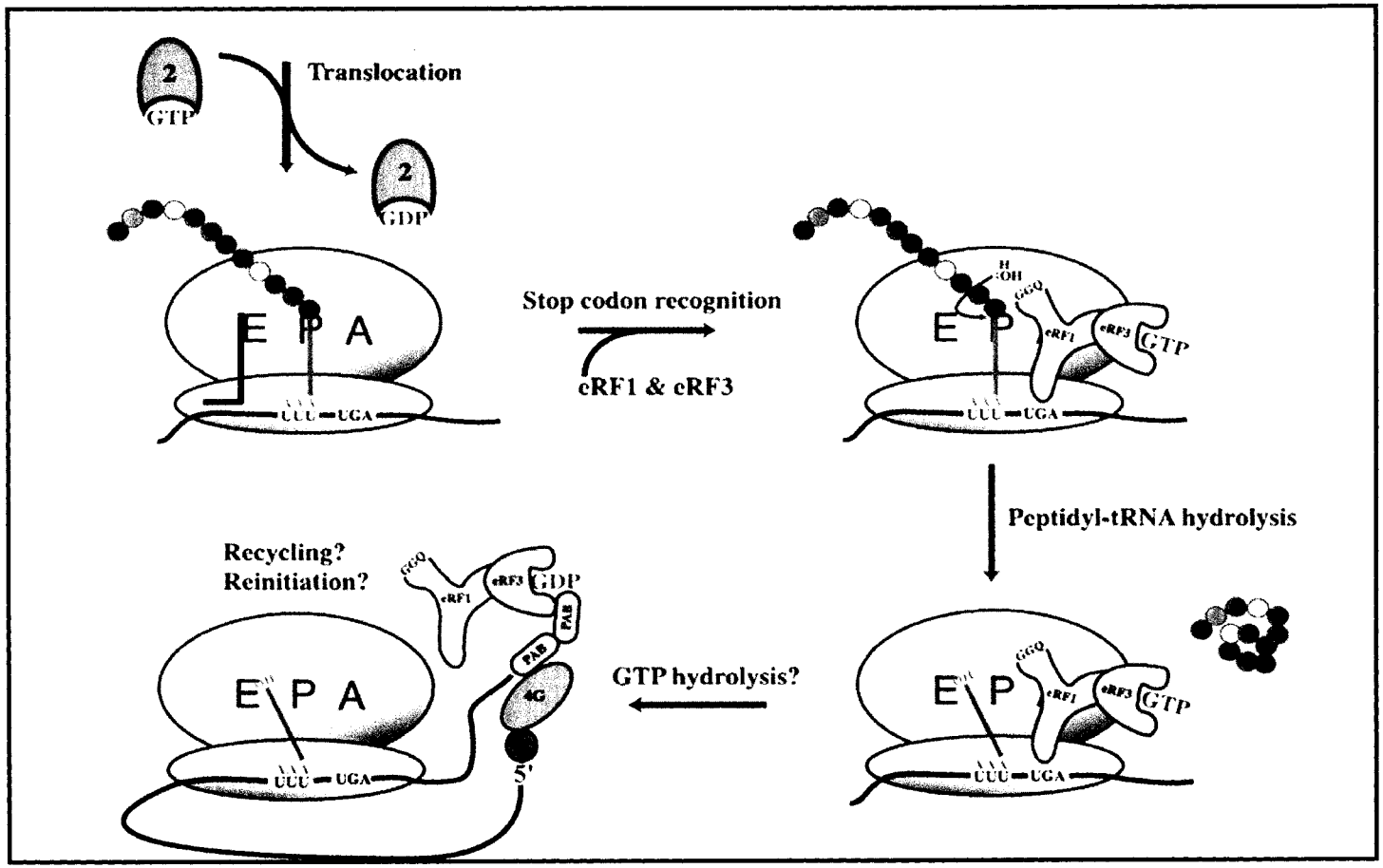
2
GTP
Translocation
2
GDP
E P A
UUU UGA
Stop codon recognition
eRF1 & eRF3
H
OH
GGQ
eRF1
eRF3 GTP
E P
UUU UGA
Peptidyl-tRNA hydrolysis
Recycling?
Reinitiation?
GGQ
eRF1
eRF3 GDP
PAB
PAB
4G
5'
E P A
UUU UGA
GTP hydrolysis?
GGQ
eRF1
eRF3 GTP
E P
UUU UGA

cytoplasmic protein content of the eukaryotic cell (Kahns *et al.* 1998). eEF1A levels reduce during aging in mouse as well as human fibroblasts. On the other hand, the constitutive expression of eEF1A2 in *Drosophila melanogaster* increases the life span of the fruit fly (Lamberti *et al.* 2004; Thornton *et al.* 2003; Kahns *et al.* 1998). Numerous studies implicate that eEF1A plays a major role in tumorigenesis (Lamberti *et al.* 2004; Anand *et al.* 2002; Thornton *et al.* 2003; Munshi *et al.* 2001; Ransom-Hodgkins *et al.* 2000). The involvement of eEF1A in prostate carcinoma was suggested by the identification of PTI-1(prostate tumor inducing gene-1). PTI-1 is a fusion between the *Mycoplasma hyopheumoniae* 23S ribosomal RNA gene and a mutated form of human *EEF1A1* (Lamberti *et al.* 2004). eEF1A forms complexes with tubulin and actin filaments and depolymerizes microtubules (Lamberti *et al.* 2004; Kahns *et al.* 1998). eEF1A proteins are also upregulated in metastatic cells relative to nonmetastatic cells (Lamberti *et al.* 2004) suggesting the eEF1A activity is coordinated with cell replication (Thornton *et al.* 2003). The S6 kinase can phosphorylate eEF1A and upregulate the activity of eEF1A by two-to threefold in *in vitro* assays (Chang *et al.* 1997). It has been recently reported that eEF1A can recognize structural errors by interacting with newly synthesized polypeptides and with properly folded full-length proteins, while mediating ubiquitin-mediated degradation of proteins that are incapable of folding precisely in the cytosol (Lamberti *et al.* 2004; Hotokezaka *et al.* 2002). eEF1A has also been suggested to be an activator of phosphatidylinositol-4 kinase (Kahns *et al.* 1998).

Thus, besides functioning as a vehicle for aa-tRNA transport to the ribosome, eEF1A appears to play additional roles in cell growth and transformation. There are two isoforms of eEF1A, eEF1A1 and eEF1A2, which are differentially expressed (Kahns *et al.* 1998).

These two isoforms share more than 90% homology at the amino acid level (Lee, 2003; Anand *et al.* 2002). *EEF1A1* maps to the chromosome 6q14 while *EEF1A2* is located on 20q13.3 (Lund *et al.* 1996). eEF1A1 is expressed ubiquitously in human tissues, however at a lesser extent in eEF1A2 expressing tissues. Conversely, eEF1A2 is expressed primarily in terminally differentiated cells in brain, heart and skeletal muscle (Kahns *et al.* 1998). The ectopic expression of rat eEF1A2 can protect muscle cells from caspase-3 mediated apoptosis (Ruest *et al.* 2002). These two isoforms have somewhat different but overlapping functions (Kahns *et al.* 1998). According to Kahns and colleagues, eEF1A2 has a stronger affinity for GDP relative to eEF1A1 and this higher affinity may help eEF1A2 in efficient actin binding (Kahns *et al.*1998). The eEF1A1 isoform is shown to be replaced by eEF1A2 in mouse and rat muscle at ~21 days after birth (Abbott and Proud, 2004). eEF1A1 expression is upregulated in cell lines obtained from human head and neck cancer which were resistant to the anticancer agent, Cisplatin (Thornton *et al.* 2003). Anand and colleagues have shown the amplification of the *EEF1A2* gene in breast tumors (Anand *et al.* 2002). Therefore, the upregulated expression of eEF1A1 and eEF1A2 in human cancers leads to the theory that the over expression of eEF1A may contribute to resistance to anticancer therapy (Thornton *et al.* 2003).

eEF1A2

The *wasted* mutation in mice has been shown to be a 15.8 kb deletion that eliminates eEF1A2 activity. This consequently resulted in mice developing profound neuromuscular problems culminating in death by 30 days of age (Abbott and Proud, 2004; Chambers *et al.* 1998). This evidence shed light on the function of eEF1A2. *EEF1A2* is a putative oncogene which encodes a protein elongation factor, eEF1A2 (Thornton *et al.* 2003; Anand *et*

*al.*2002). It is mapped to 20q13.3 chromosome and frequent amplification at 20q has been demonstrated in various cancers (Lund *et al.* 1996; Lee, 2003; Watanabe *et al.* 2002). In addition, ectopic expression of wild type eEF1A2 can transform mouse and rat fibroblasts and induce tumor formation when xenografted into mice. The same group also found amplification of *EEF1A2* in 25-30% of primary ovarian tumors and solid breast tumors. Furthermore, NIH 3T3 cells over-expressing ectopic eEF1A2 can form colonies in soft agar relative to controls (Anand *et al.* 2002). These observations suggest that eEF1A2 is a putative oncogene. However, the mechanism by which it enhances cell growth and oncogenicity is unclear.

AKT/ PKB

Background

AKT, a serine/ threonine kinase, is a critical enzyme in signal transduction pathways involved in cell proliferation and cell survival (Khwaja, 1999). AKT-8, an acute transforming retrovirus, was described in 1977 (Kandel and Hay, 1999). *v-akt*, a gene transduced by AKT-8, was identified and termed as c-AKT in 1991 (Kandel and Hay, 1999; Marte and Downward, 1997). This kinase is also known as RAC (a protein kinase related to protein kinases **A** and **C**) or PKB (protein kinase B) (Kandel and Hay, 1999; Franke, 1999). AKT maps to the human chromosome 16p13.3 (Stephens *et al.* 1998). There are three mammalian AKT isoforms; AKT1, AKT2 and AKT3. All three isoforms share 85% sequence identity while their protein products share the same structural organization. The three isoforms have conserved serine and threonine residues (Kandel and Hay, 1999). The serine and threonine residues present in AKT1, AKT2 and

AKT3 are serine473/threonine308 (ser473/thr308), ser474/thr309 and ser472/thr302 respectively (Kandel and Hay, 1999). All three isoforms are ubiquitously expressed in mammals. However, their expression levels differ among tissues (Kandel and Hay, 1999). AKT1 /PKBα is mainly expressed in most of tissues and in regenerating neurons while the expression of AKT2/PKBβ is observed mainly in skeletal muscle and in intestinal and reproductive organs (Franke, 1999; Kandel and Hay, 1999). AKT3/PKBγ is observed in the testis and brain (Nakatani *et al.* 1999). AKT1 gene amplification is observed in gastric carcinomas while elevated AKT1 kinase activity is associated with ovary, breast and prostate carcinomas (Sun *et al.* 2001). AKT2 gene amplification is observed in ovarian carcinomas with an aggressive tumor phenotype (Paez and Sellers, 2003). AKT3 mRNA levels and enzymatic activity are elevated in breast cancer cell lines and tumors lacking the estrogen receptor (Paez and Sellers, 2003).

Structure of AKT

The primary structure among AKT family members is conserved, with the exception of the carboxyl-terminal tail (Paez and Sellers, 2003; Datta *et al.* 1999; Marte and Downward, 1997). All AKT isoforms comprise of an amino-terminal pleckstrin homology (PH) domain, a central catalytic domain with the specificity for serine-threonine residues, and a regulatory domain at the carboxyl terminal (Fig. 4) (Datta *et al.*1999; Franke, 1999; Kandel and Hay, 1999). The PH domain is highly conserved amongst the three isoforms of AKT and it mediates lipid-protein and / or protein-protein interactions. The PH domain is a 100-120 amino-acid motif which was first identified as

Figure 4. Domain structure of AKT/PKB.

AKT/PKB contains amino terminal pleckstrin homology(PH) domain , a central kinase domain with the threonine308 (Thr308) phosphorylation site and a carboxyl-terminal regulatory domain with the serine473 (ser473) phosphorylation site.

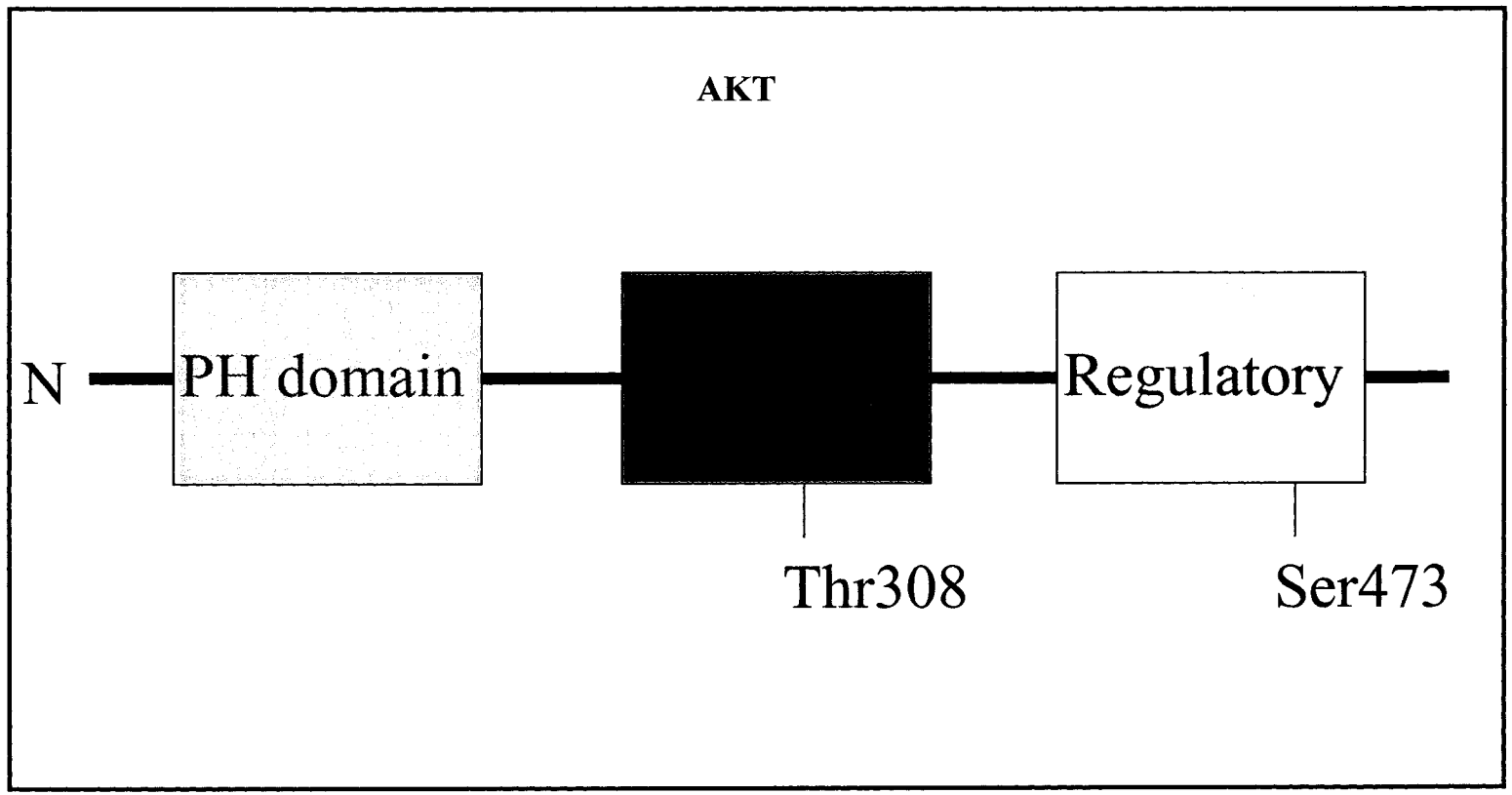
AKT
N
PH domain
Regulatory
Thr308
Ser473

an internal repeat in pleckstrin, the main phosphorylation substrate for protein kinase C (PKC) in platelets (Chan *et al.*1999). The carboxyl terminal tail region includes a hydrophobic and proline-rich domain termed as a regulatory domain (Paez and Sellers, 2003).

AKT and cell survival

AKT is activated by a wide variety of growth stimuli such as platelet derived growth factor (PDGF), epidermal growth factor (EGF), insulin, and nerve growth factor (NGF) (Lawlor and Alessi, 2001; Ouyang *et al.* 2000; Marte and Downard, 1997). Numerous studies document that AKT is activated by phosphatidylinositol 3-kinase (PI3K) dependent pathways. PI3K generates D3-carbon phosphorylated phosphoinositide products, PI(3,4,5) P_3 (PIP_3) and PI(3,4) P_2 or PIP_2 . PIP_3 binds to the PH domain of AKT and triggers the translocation of AKT to the plasma membrane, where AKT can be constitutively activated by growth factors (Datta *et al.* 1999). The elevated phosphoinositides act as second-messenger molecules and activate phosphoinositide-dependent kinases (PDKs), PDK1 and PDK2 (Fig.5). At the plasma membrane, AKT is phosphorylated at the thr308 residue by PDK1, whereas ser473 is phosphorylated by PDK2 (Paez and Sellers, 2003; Datta *et al.*1999). Thr308 phosphorylation is essential for activation of AKT, while phosphorylation of ser473 is necessary for maximal activity of AKT (Zdychova and Komers, 2005). Integrin-linked kinase (ILK) can also phosphorylate AKT on ser473 in a PI3K-dependent manner (Vanhaesebroeck and Alessi, 2000). Conversely, PI3K independent activation of AKT at ser473 occurs by oxidative stress induced by mitogen activated protein kinase-activated protein kinase-2 (MAPKAP kinase-2) while Ca^{2+}/calmodulin-dependent kinase kinase

Figure 5. Multiple mechanisms of cell survival regulation by AKT/PKB.

The extracellular growth factors (GF) activate phosphoinositide 3- kinase (PI3K). This leads to the activation of AKT. Activated AKT/PKB phosphorylates downstream targets such as glycogen synthase kinase (GSK-3), Bad, caspase-9, mammalian target of rapamycin (mTOR) and endothelial nitric oxide synthase (eNOS) as well as transcription factors: forkhead related transcription factor (FKHR) and nuclear factor κB (NFκB).

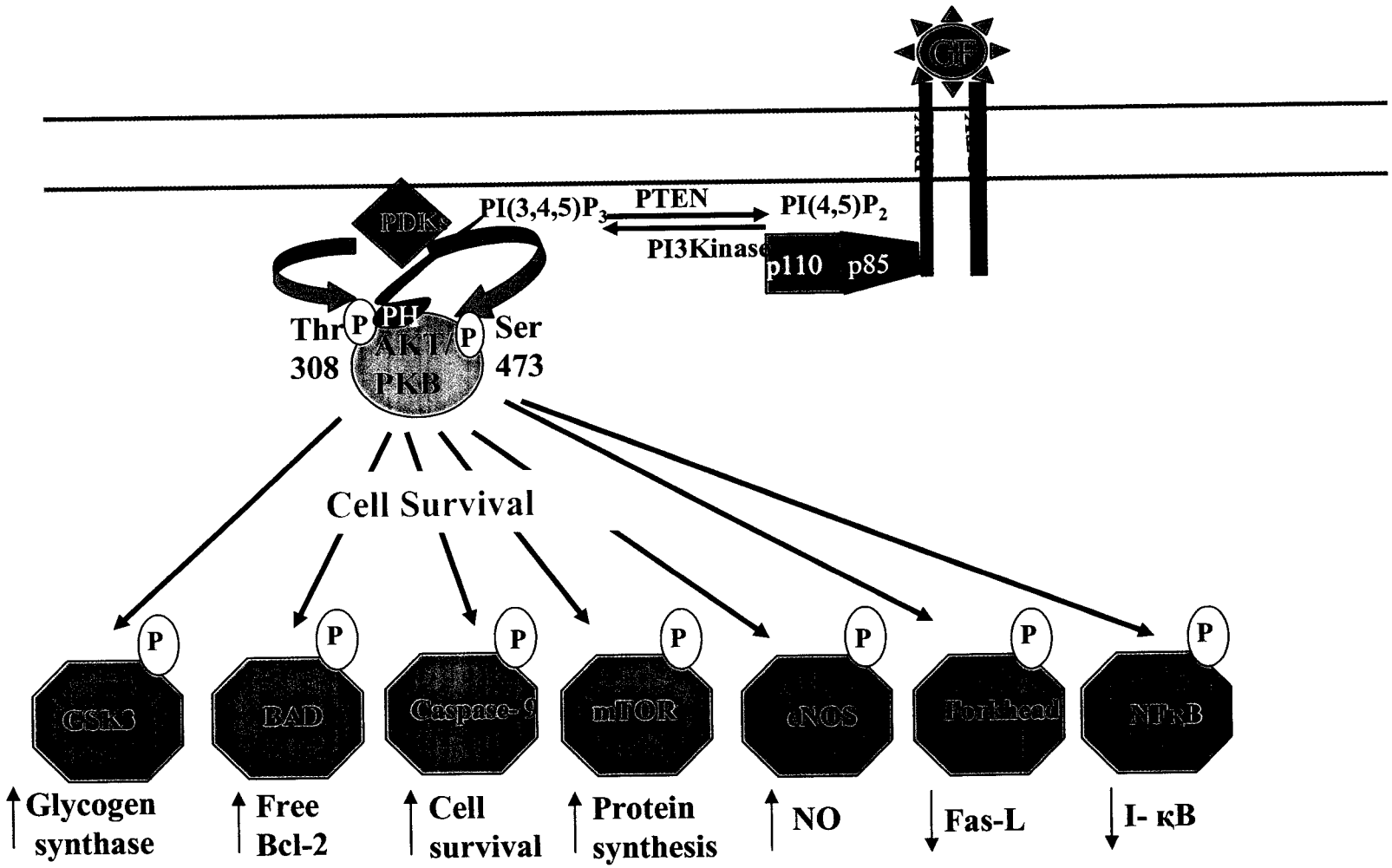
GF
PDK1
PI(3,4,5)P3
PTEN
PI(4,5)P2
PI3Kinase
p110
p85
PH
AKT/
PKB
Thr
308
P
Ser
473
Cell Survival
GSK3
BAD
Caspase-9
mTOR
eNOS
Forkhead
NFκB
Glycogen synthase
Free Bcl-2
Cell survival
Protein synthesis
NO
Fas-L
I- κB

(CaM-KK) can phosphorylate AKT on thr308 (Franke, 1999). The substrate of PDK1, protein kinase A, also triggers phosphorylation and activation of AKT. On the other hand, negative regulators of AKT, such as elevated ceramide levels, dephosphorylate AKT (Franke, 1999). Phosphatase activity of PTEN (phosphatase and tensin homologue deleted on chromosome 10) and SHIP (SH2-containing inositol phosphatase) also inhibit membrane localized activation of AKT (Franke, 1999; Kandel and Hay, 1999). After activation, AKT detaches from the plasma membrane and further translocates to the nucleus, where it activates transcription factors or stimulates certain cell regulatory targets in the cytosol (Meier *et al.* 1997). The mostly possible downstream targets of AKT include glycogen synthase kinase (GSK3), BAD, human caspase 9, forkhead and nuclear factor- κB (NF-κB) transcription factors, mammalian target of rapamycin (mTOR), and endothelial nitric oxide synthetase (eNOS) (Paez and Sellers, 2003) (Fig.5). For example, one of the downstream targets of AKT is Bad, a pro-apoptotic Bcl-2 family member protein. Normally, Bad inhibits the anti-apoptotic Bcl-2 protein. However, once BAD is phosphorylated by active AKT, the phosphoserine residue of BAD forms a binding site for 14-3-3 molecules and localizes BAD to the cytosol and neutralizes its pro-apoptotic activity (Paez and Sellers, 2003). The 14-3-3 proteins can also retain pro-apoptotic forkhead-related transcription factors in the cytoplasm, reducing the transcription of the Fas ligand (Franke, 1999). NF-κB is regulated through an inhibitory cofactor I- κB, which sequesters NF-κB in the cytoplasm. Active AKT can trigger phosphorylation and eventual degradation of I- κB via IκBα kinases (IKKs) (Zdychova and Komers, 2005). Active AKT can also mediate Ca^{2+}-independent as well as dependent activation of eNOS (Fulton *et al.* 1999). Heat shock protein 90 (HSP90), which refolds certain denatured proteins, can maintain AKT kinase activity (Fujita *et al.*

2002). In addition, Ras and AKT signal transduction pathways play a significant role in protein synthesis by regulating mRNA translation and cellular transformation (Mamane *et al.* 2004). Activated AKT can phosphorylate mTOR which phosphorylate eIF4E-BP, a binding protein for the protein initiation factor and thus releasing eIF4E to further modulate translation (Zdychova and Komers, 2005; Mamane *et al.* 2004).

PHOSPHOINOSITIDE 3-KINASE (PI3K)

Background

Phosphatidylinositol (PtdIns) is a component of eukaryotic cell membranes and is involved in cell survival, proliferation, glucose transport and cytoskeletal organization. Phosphoinositides are derivatives of PtdIns (Vanhaesebroeck and Alessi, 2000). The phosphoinositide 3-kinase (PI3K) enzymes are ubiquitous lipid kinases which regulate several key signal transduction pathways controlling critical cellular processes which are implicated in carcinogenesis (Cantley, 2002; Walker *et al.* 1999). The PI3K family is a group of enzymes that generate lipid "second messengers" that arbitrate signal transduction. These second messengers are thus the products of PI3K-catalyzed reactions and include, phosphatidylinositol-3, 4, 5-triphosphate (PIP_3), $PI(3,4)P_2$ /(PIP_2) or PI3P (Cantrell, 2001). PIP_3 further stimulates phosphoinositide-dependent kinases (Vanhaesebroeck and Alessi, 2000) (Fig.5). The signal transduction pathways remain active until phosphatase enzymes, such as PTEN, dephosphorylate the PI3K lipid second messengers (Cantley, 2002; Vanhaesebroeck and Alessi, 2000). All PI3K enzymes have lipid kinase activity (where it phosphorylates the D3 carbon of the inositol ring) and protein kinase activity (Walker *et al.* 1999). PI3Ks are classified as Class IA, IB, II and III enzymes (Vanhaesebroeck and

Alessi, 2000; Vanhaesebroeck and Waterfield, 1999). Class IA enzymes include any one of the catalytic subunits (p110α, p110β, or p110δ) complexed with any one of the regulatory subunits (p85α, p85β or p55γ) (Cantrell, 2001). Class IB PI3K enzymes comprise p110γ catalytic and the p101 regulatory subunit. The p110δ and p110γ isoforms differ from the other PI3K subunits in that they have a tissue-restricted expression. The p110γ isoform is expressed only in white blood cells, while p110δ is expressed in white blood cells and breast tissue (Vanhaesebroeck and Alessi, 2000; Vanhaesebroeck and Waterfield, 1999). Class II enzymes are differentiated by a C2 domain and usually use PtdIns and PtdIns(4)P as substrates while class III enzymes phosphorylate only PtdIns and lack the Ras binding domain (Walker *et al.*1999). Class IV PI3K-related kinases contain a kinase domain that is similar to the kinase core domain of PI3K and PI4Ks. The kinase domain is mainly involved in serine/threonine protein kinase activity (Vanhaesebroeck and Waterfield, 1999). Class I enzymes are extensively studied enzymes and are activated by tyrosine kinases such as growth factor receptors and cytokine receptors, whereas the Class IB enzymes are activated by G Protein Coupled Receptors (GPCRs). Class II PI3Ks are considered to be activated by some tyrosine kinase receptors, integrins, and GPCRs while the class III PI3Ks seem to be constitutively activated (Cantrell, 2001; Vanhaesebroeck and Alessi, 2000; Walker *et al.* 1999; Vanhaesebroeck and Waterfield, 1999).

Structure and function of PI3K

PI3K enzymes contain an amino terminal region, which interacts with regulatory protein subunits (p85), a Ras binding domain, a C2 domain, a helical domain and a carboxyl terminal catalytic subunit domain (kinase domain) (Fig.6) (Samuels *et al.* 2004;

Figure 6. Domain structure of phosphoinositide 3-kinase (PI3K).

The PI3K structure comprises of an amino terminal regulatory subunit domain (31-108 aa), a ras binding domain (173-292 aa) followed by a C2 domain (350-485 aa), a helical domain (519-794 aa) and a carboxyl terminal kinase or catalytic domain (796-1015 aa).

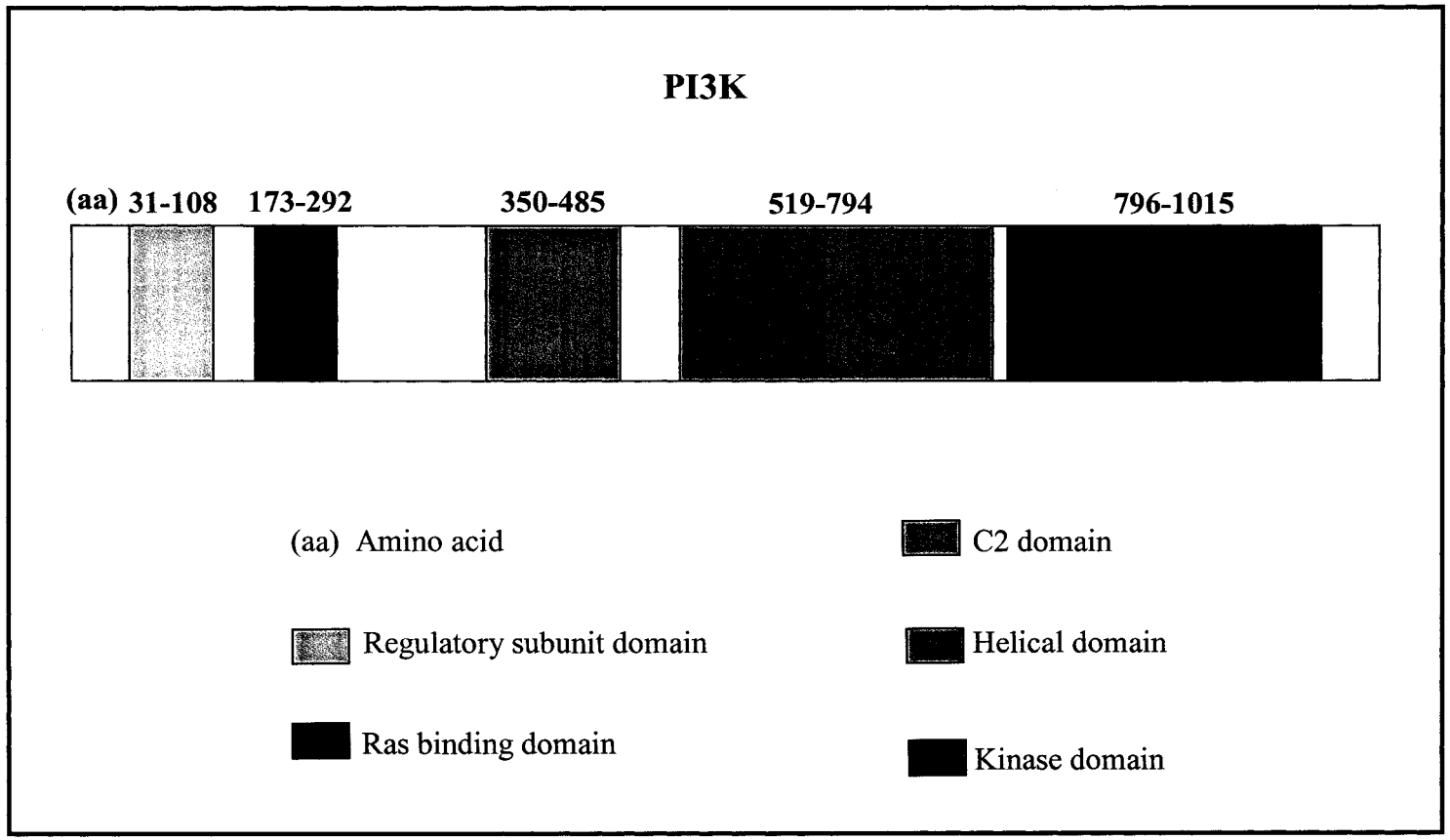
PI3K
(aa) 31-108
173-292
350-485
519-794
796-1015
(aa) Amino acid
Regulatory subunit domain
Ras binding domain
C2 domain
Helical domain
Kinase domain

Vanhaesebroeck *et al.* 2001). Ras interacts with PI3K via the Ras binding domain. The C2 domain is involved in membrane trafficing of PI3K, generation of second messengers and protein phosphorylation. The helical domain acts as a structural spine around which the other domains are attached. The kinase domain is essential for the catalytic function of PI3K (Vanhaesebroeck *et al.* 2001). PI3Ks are heterodimers corresponding regulatory subunit, p85, and a catalytic subunit, p110. The amino terminal regions of p85α and p85β consist of an SH3 domain, a proline-rich sequence, and a Bcr homology domain (Okkenhaug and Vanhaesebroeck, 2001). Regulatory subunits do not contain lipid kinase activity but are phosphoprotein substrates for many cytoplasmic and receptor tyrosine kinases (Vivanco and Sawyers, 2002). The p110 subunit is homologous to protein kinases and acquires both serine-threonine protein kinase as well as phosphoinositide kinase activities. The formation of the p85/p110 heterodimer helps in recruiting PI3K enzyme to the plasma membrane and /or interacts with activator proteins that induce PI3K activation (Paez and Sellers, 2003; Okkenhaug and Vanhaesebroeck, 2001).

The activator proteins have tyrosine-phosphorylated amino acid sequences containing both receptor and non-receptor tyrosine kinases (RTK) (Fig.5). In addition, the heterodimer can be activated by direct interaction between p110 and one of several cellular proteins such as p21-ras or G proteins (cdc42) (Krasilnikov, 2000). PI3K kinase is activated by growth factor receptors via binding of a regulatory subunit to phosphotyrosine residues present on the receptor. This facilitates the catalytic subunit of PI3K to phosphorylate phosphoinositides at the D3-position of the inositol ring to generate PI3P, PI(3,4)P_2 and PI(3,4,5)P3 (Kandel and Hay, 1999) (Fig.5). PI3Ks are activated by the oncogene Ras, which is mutated in human cancers. It has been publicized that Ras-

dependent PI3K activation is essential for many cell processes required for cell transformation (Vivanco and Sawyers, 2002; Cantrell, 2001; Rodriguez-Viciana, 1994). PI3K activation stimulates many signal transducers important in cell transformation, such as AKT, protein kinase C (PKC) and small GTP hydrolyzing proteins, such as Rac and ILK (Vivanco and Sawyers, 2002; Cantrell, 2001; Stephens *et al.* 1998). The upregulation of PI3K signaling can occur by an increase in PI3K signaling resulting from activating gene mutations, amplification and over-expression of PI3Ks or upstream receptors that activate PI3Ks. For example, mutations that trigger the epidermal growth factor receptor (EGFR), which is normally over-expressed in cancer (Paez and Sellers, 2003; Vivanco and Sawyers, 2002), have been revealed to elevate the levels of the PI3K lipid products (Paez and Sellers, 2003). The negative regulators of PI3K, such as wortmannin and LY294002 can disturb the ATP binding pocket of PI3K and PI3K-like enzymes (Paez and Sellers, 2003). The tumor suppressor proteins, PTEN, also negatively affects the activation of PI3K (Hara *et al.* 2005; Paez and Sellers, 2003; Vivanco and Sawyers, 2002).

c-MYC

Background

The cellular myc gene (c-Myc) is a homolog of a retroviral v-Myc (avian **my**elocytomatosis retrovirus), discovered in 1982 (Facchini and Penn, 1998). c-Myc gene maps to the chromosome 8q24. The ubiquitous expression of c-Myc is observed in embryonic and in post –developmental tissues that have a high proliferative potential (Mamane *et al* 2004). The c-Myc proto-oncogene is a potent inducer of both cell proliferation as well as apoptosis and deregulated expression of the gene has been detected

in many tumors. The proto-oncogene form of c-Myc can be stimulated to its oncogenic form by chromosomal translocation or mutations that trigger the rate of transcription elongation (Kato and Dang, 1992.) c-Myc is a member of the basic helix-loop-helix (HLH) leucine zipper (bHLHzip) family. This family also consists of other myc related genes, homologous to c-Myc, such as N-Myc, L-Myc, S-Myc and B-Myc. These genes are involved in neuroblastomas (N-Myc), lung cancers (L-Myc), and neoplastic transformations (S-Myc and B-Myc) (Kato and Dang, 1992; Resar *et al.* 1993). c-Myc encodes a protein that plays a key role in regulation of the cell cycle and cell growth, while over- expression of c-Myc can transform normal cells into tumor cells (Facchini and Penn, 1998). The dysregulated expression of *c*-Myc is involved in a wide variety of human cancers (Facchini and Penn, 1998). The amplification of c-Myc gene is seen in almost one third of breast and colon carcinoma while it is also elevated in lung and ovarian carcinomas (Blancato *et al.* 2004; Plisiecka-Halasa *et al.* 2003; Liao and Dickson, 2000; Facchini and Penn, 1998). c-Myc is also involved in osteosarcomas, glioblastomas and myeloid leukemias (Facchini and Penn, 1998).

Structure of c-Myc

c-Myc is a transcription factor that binds to the E box motif containing a specific DNA sequence, CAC (G/A) TG (Liao and Dickson, 2000; Kato and Dang, 1992). c-Myc is seen to be phosphorylated *in vivo* and this phosphorylation plays a key role in regulating its function (Peckham and Cleveland, 1995). The c-Myc protein in cells is present in two isoforms, c-Myc1 and c-Myc2, with molecular weights of 67kDa and 64kDa respectively. However, there is no functional difference ascribed to these forms (Peckham and Cleveland, 1995). The structure of c-Myc is comprised of HLH, leucine zipper (LZ)

and basic (B) domains present at the C-terminal region. These three domains are commonly found in many transcription factors. The LZ and HLH domains can mediate protein-protein interactions while the basic region contacts with the major groove of DNA (Peckham and Cleveland, 1995). The N-terminal end of c-Myc contains a transactivation domain (TAD) which is also involved in protein binding. The TAD domain comprises of two regions which are well conserved in all members of the myc family. These regions are called Myc homology boxes I and II (MBI and MBII) and mainly regulate the activity of c-Myc by transactivation and transsuppression of genes respectively (Liao and Dickson, 2000). c-Myc can interact with Max or with the members of Mad family (Mad 1, 2, 4 and Mxi1) (Hurlin *et al.* 1995b). c-Myc heterodimerizes with Max and this interaction further facilitates transcription activation while c-Myc/ Mad heterodimerization leads to the transcription repression of genes. c-Myc has a short life span (20-30 min) and is a low abundant protein in the cell while Max is a relatively abundant protein with a longer life span. Max either homodimerizes with itself or heterodimerizes with Mad and can then bind to DNA. Interestingly, the competition between c-Myc and Mad for Max to bind to the similar target sequences governs the activity of c-Myc (Grandori *et al.* 2000). The decision of cell division or cell differentiation is dependent upon the formation of c-Myc/Max or Mad/Max (or Mxi1/Max) complexes respectively (Peckham and Cleveland, 1995). c-Myc is expressed in proliferating cells while the mRNA and /or protein levels of c-Myc are almost undetectable in terminally differentiated cells (Johansen *et al.* 2001).

c-Myc and cell signaling

c-Myc is involved in regulation of specific target genes by transactivation or repression, however its precise role in human tumorigenesis is yet unclear. c-Myc induces

expression of the following genes; ornithine decarboxylase (ODC), cyclin A and E , cyclin-dependent kinase 4 (Thomas-Tikhonenko *et al.* 2004; Liao and Dickson, 2000; Facchini and Penn, 1998), prothymosine α (Eilers *et al.* 1991), and eIF4E (Kato and Dang, 1992). c-Myc represses expression of lymphocyte function associated antigen -1(LFA-1), plasminogen–activator inhibitor -1(PAI-1), C/EBPα (Johansen *et al.* 2001) and c-Myc itself (Peckham and Cleveland, 1995). Putative gene targets of c-Myc such as ODC and α-prothymosin have a CACGTG sequence located downstream of the transcriptional start site (Peckham and Cleveland, 1995). The catalytic subunit of human telomerase, hTERT, is mainly involved in extending lifespan of primary human cells. Interestingly, c-Myc can transactivate the hTERT promoter and consequently participate in the immortalization of cells (Lutz *et al.* 2002; Gewin and Galloway, 2001; Liao and Dickson, 2000).

The c-Myc gene encodes a protein that, after translation, localizes to the cell nucleus and functions as a transcription factor, although the cellular distribution of c-Myc is not restricted to the nucleus. Pietilainen and colleagues documented that immunohistochemistry on 95% of breast cancer cases show positive staining of c-Myc in the cytoplasm while 12% of the cases illustrate c-Myc in the nucleus or both nucleus and cytoplasm (Liao and Dickson, 2000). The localization of the c-Myc protein in a cell and its relativity to its activity are still inconclusive. It has been documented that *Drosophila* c-Myc is an important regulator of certain factors involved in protein synthetic and metabolism machinery (Guo *et al.* 2000). Interestingly, c-Myc can regulate the protein synthetic machinery such as translation factors eIF-2α, eIF4E, eIF4G, elongation factor-2 (EF-2) and ribosomal protein genes (Guo *et al.* 2000; Dang, 1999; Rosenwald 1996).

SUMMARY

To summarize, *EEF1A2* is a putative ovarian and breast oncogene which is increased in copy number in about 25 % of primary ovarian tumors and highly expressed in approximately 30% of ovarian tumors and established cell lines. eEF1A2 mRNA is detected in about one third of human ovarian tumours. However, the mechanism by which eEF1A2 exert tumorigenesis is undetermined. Since eEF1A2 is a translation factor, it may upregulate the production of proteins that activate cell growth. AKT, PI3K and c-Myc are known oncogenes which are amplified in breast and ovarian cancers. In this current study, we speculated that eEF1A2 regulates cell growth through the AKT, c-Myc or PI3K-dependent pathways or vice versa.

MATERIALS AND METHODS

Materials and Methods

PLASMID CONSTRUCTS

We obtained pcDNA3-HAPKB-D308D473 and pcDNA3-p110CAAX, which encode for a constitutively active AKT and PI3K (Phosphatidylinositol 3- kinase) respectively, from Dr. Luc Sabourin's laboratory (University of Ottawa), while pMGC11567-c-Myc (Murine c-Myc) was a gift from Ken Garson (ORCC). Mutations in pcDNA3-HAPKBD308D473 were present in *KpnI* (T308D at 1934 base pairs) and *NheI* (S473D at 2429 base pairs). The pcDNA3.1 vector (Invitrogen), containing the neomycin resistance marker and a human cytomegalovirus (CMV) promoter, was used to construct pcDNA3.1-HAPKB (AKT) and pcDNA3.1-c-Myc plasmids. HAPKB-D308D473 was excised from pcDNA3 by *EcoRI* and *Xho1* restriction digest and subcloned into pcDNA3.1. Murine c-Myc was excised from pMGC11567-c-Myc by *Eco RI* and *NotI* restriction digests and subcloned into pcDNA3.1.

LIGATION AND TRANSFORMATION

Plasmids, pcDNA3-HAPKB and pMGC11567-c-Myc, were digested with *EcoRI/XhoI* and *EcoRI/NotI* respectively, and electrophoresed on 1% agarose gels. The inserts (HAPKB and c-Myc respectively) were cut under ultraviolet light (UV) following ethidium bromide staining. Vector pcDNA3.1 was also electrophoresed and excised out of a 1% agarose gel. Vector and inserts were purified by GFX ^{TM} PCR, DNA and Gel band purification kit (Amersham Biosciences, UK) according to manufacturer's instructions. Purified DNA was again electrophoresed on 1% agarose gel to confirm the molecular

weight. The following formula was used to determine the appropriate concentration of vector to insert ratio. Commonly used ratios for vector: insert are 1:3 and 1:6.

$$\text{Quantity of insert (ng)} = \frac{\text{Quantity of vector (40-100ng)} \times \text{Size of insert (kb)} \times \text{ratio (3 or 6)}}{\text{Size of vector (kb)}}$$

The standard 20ul ligation reaction mixture comprised of vector, insert, 1ul of T4 ligase and 2ul T4 ligase buffer (New England Biolabs, U.S.A.). Ligation reactions were kept overnight at 16°C. The negative control ligation reaction was performed in similar way without the inserts. The next day, ligation reactions were spun down for 1 minute at 4000 rpm and transformations were carried out as follows. *E.coli* strain DH5α were used as competent cells for transformations. Aliquots of 200ul of thawed (on ice) competent cells were mixed with half of the ligation reactions. The competent cells were then incubated on ice for 30 min. and heat shocked for 1.5 min. at 42°C followed by cooling on ice for another 1.5 min. 300ul of S.O.C. media (Invitrogen) were added and cells were shaken at 225 rpm for 45 min. at 37°C. The resulting bacteria were centrifuged at 4000 rpm for 2 min. and the bacterial pellet was resuspended in 100ul of S.O.C. media and plated on Luria-Bertani (LB) agar plates containing 50ug/ml ampicillin. The plates were incubated at 37°C for 14 hrs and colonies were picked and used to inoculate starter cultures (i.e. 5ml of LB broth containing 50ug/ml ampicillin for 6 to 8 hrs at 37°C with gentle shaking). The plasmid DNA was then isolated by miniprep kits (Qiagen) as per manufacturer's instructions and purified DNA was digested with respective enzymes and run on 1% agarose gels to confirm the desired plasmid constructs. All plasmids DNA (pcDNA3.1-HAPKB, pcDNA3-p110CAAX and pcDNA3.1-c-Myc) were also sequenced by ABI prism 3100 genetic analyzer to ensure no errors were introduced in the amplification process. Once the orientation of plasmid constructs

(pcDNA3.1-HAPKB, pcDNA3.1-c-Myc) were confirmed, 15% glycerol stocks were prepared and stored at

-80°C. 5ml starter cultures were performed as described previously and added to 500ml of LB broth with 50ug/ml of ampicillin and grown for 14 hrs under the same conditions. Amplification and purification of plasmids (pcDNA3.1-HAPKB, pcDNA3-p110CAAX and pcDNA3.1-c-Myc) was then performed by using "Qiagen maxi-prep plasmid purification kit" (Qiagen) protocol according to manufacturer's instructions followed by cesium chloride purification.

The DNA isolated by Maxi-prep was resuspended in 8ml CsCl (1g/ml) and 300μl ethidium bromide (10mg/ml). The mixtures were vortexed carefully and then transferred to 15ml Beckman ultracentrifuge tubes. These tubes were heat sealed, balanced and spun down in Beckman TL-100 ultracentrifuge overnight at 55000 rpm for 16 hrs at 25°C. Tubes were checked for pink band around middle of the tubes. A 26 gauge needle was inserted into the top of the tube to generate an air pocket. An 18 gauge needle was attached to a 5cc syringe and inserted 1cm below the pink DNA band. This procedure was performed in the fume hood. The band was extracted and poured in a falcon tube with 5ml Tris- EDTA buffer (TE, 10mM Tris-Cl, pH 8.0, 1mM EDTA). The DNA in TE was mixed thoroughly with 5ml butanol and solvent layer (ethidium bromide) was removed. The process was repeated until the upper phase became clear. Precipitation of CsCl salt was prevented by adding 15ml of ddH_2O to DNA, followed by 1 volume of 95% ethanol. Tubes were kept at -20°C for half an hour and then spun down at 3000 rpm for 30 min. at 4°C. The supernatants were removed and DNA pellets were left to air dry. The pellets were suspended in 500μl TE (pH8.0) and plasmids were stored at -20°C. Cesium chloride purified plasmids were further

used for the stable transfections in NIH 3T3 cells.

CELL CULTURE FOR NIH 3T3 AND STABLE TRANSFECTIONS

NIH 3T3, a mouse fibroblast cell line, was used to generate stable cell lines. Cell lines were maintained in the Dulbecco's Modified Eagle Media (DMEM, Gibco) supplemented with 10% FBS (Fetal Bovine serum, Gibco), 1% antibiotic/antimycotic (Gibco) to prevent bacterial and fungal growth. Cell lines were grown in the complete media at 37°C and 5% CO_2 in a humidified incubator.

Stable transfections were performed using Lipofectamine 2000 Plus (Invitrogen, California) as per manufacturer's instructions. NIH 3T3 cell lines were stably transfected with pcDNA3.1-HAPKB (AKT), pcDNA3-p110CAAX (PI3K), pcDNA3.1-c-Myc or pcDNA3.1 (empty vector), hence forth named 3T3-EV.

Cells were counted by trypan blue exclusion assay. Cells were trypsinized and left suspended in 5ml of fresh complete DMEM media. A 0.1ml aliquot of cell suspension was diluted in an equal volume of trypan blue (EM Science) and pipetted onto a hemacytometer. All eight grids on the hemacytometer were counted and the total cell concentration was calculated using following formula.

$$\text{Cell concentration (cells/ml)} = \frac{\text{Total number of cells} \times \text{dilution factor} \times 10 \times 1000}{\text{Number of quadrants}}$$

Cells were then seeded in 60mm plates (6 Well plates, Sarstedt) one day prior to transfection so that cells were 60-80% confluent at the time of transfection. 4ug of plasmid DNA was diluted in 250ul serum free medium i.e. Optimem I (Gibco). 8ul of Lipofectamine 2000 Plus was added to 250ul of Optimem I and after 5 min. of incubation it

was mixed with plasmid DNA and incubated further for 20 min. at RT. During this incubation period, complete DMEM media was removed from NIH 3T3 cells followed by a wash with 1 × phosphate buffered saline (PBS;137mM NaCl, 2.7mM KCl, 4.3mM Na_2HPO_4 $7H_2O$, 1.4 mM KH_2PO_4, pH 7.3). After 20 min. of incubation, 500ul Optimem I with plasmid DNA and lipofectamin was added to NIH 3T3 cells, incubated for 4 hrs and then the complete DMEM media was added. Cells were kept at 37°C and 5% CO_2 for 24 hrs in a humidified incubator. Transfected cells were then selected next day with 2.5mg/ml G418 sulphate for two to three weeks. The complete DMEM media with 2.5mg/ml of G418 sulphate (Bioshop) was added and cells were passaged until single colonies were observed. The cells were then transferred to 100mm plates and grown until they reached 80-90% confluency. However, pcDNA3.1-c-Myc stable clones were grown until they were 40-50% confluent. Stable cell clones were frozen down as follows: cells were frozen down in the complete DMEM media with 10% dimethyl sulfoxide (DMSO, Fisher Biotech) at a concentration of 1.5×10^{6} cells /ml. Cells were counted using trypan blue exclusion assay as described previously. The cell suspension (1ml) was dispensed in cryotubes (Nalgene) and transferred to -80°C for 3 to 5 days and then frozen down in liquid nitrogen. A vial of cells were thawed from liquid nitrogen after 2 days and cultured to ensure viability. Stable transfections and overexpression of desired protein was determined by western blotting.

Cell extracts from stably transfected cells

Cell lysates were taken from 100mm plates by removing the growth media and then washed with sterile 1×PBS. Cells were then incubated in sterile 1X trypsin–EDTA (Gibco) for 2-3 minutes in a 37°C incubator. Fresh media was then added and cells were collected by centrifugation at 1100 rpm in 15ml centrifuge tubes (Sarstedt). Cell pellets were lysed

using 200 μl of 1 ×RIPA (final concentration: 50mM Tris –Cl; pH 7.4, 1 % Triton X-100, 1 % sodium deoxycholate, 0.1% SDS, 1mM EDTA; pH 7.0, 150mM NaCl) and 1× PIC (1% Aprotonin ,1mg/ml leupeptin ,50mM NaF,1mM Na_3VO_4, 10ug/ml pepstatin in ethanol, 1mM PMSF in DMSO). Lysed resuspended pellets were kept on ice for half an hour and spun down for 20 minutes at 10000 rpm at 4°C. Protein quantification was performed by Bradford protein assay (Bio-Rad).

SDS-PAGE

4X sample buffer (for 1X :0.5M Tris –HCl (pH 6.8 at 25°C), 10% w/v SDS , 10% glycerol, 50mM 2-β-mercaptoethanol , 0.5%w/v bromophenol blue) was added to 20ug of protein and boiled for 5 min. at 95°C. Proteins were loaded onto 10% polyacrylamide gels with 4% stacking gels and separated according to the required resolutions. Gels were equilibrated in transfer buffer (25mM Tris base, 0.2M Glycin, 20% methanol; pH 8.5) and then transferred onto polyscreen PVDF transfer membranes (Perkin-Elmer life sciences) using trans-blot semi-dry transfer cell (Bio-rad) for 45 min. at 15 volts. Membranes were stained in 0.1% ponceau S solution (Sigma) for 2 minutes to visualize the protein bands and then destained in ddwater for 1 minute.

Membranes were rinsed briefly in 1X TBS/T (10mM Tris, 200mMNaCl, 0.02% sodium azide, pH 7.6 with 0.1% Tween-20) and kept in blocking buffer (1X TBS, 0.1% Tween-20, 5% nonfat dry milk) for 1 hr at RT. Membranes were then incubated with a TBS-T /primary antibody solution overnight with gentle shaking at 4°C. The primary antibodies were used at the following concentrations: pan AKT, PI3K p110α (rabbit polyclonal, 1:1000 dilution, all from Cell Signaling Technology, Beverly, Washington), and mouse monoclonal anti-Myc (1:500, Santa Cruz, USA). Membranes were washed three

times for 5 minutes each with 15ml of TBS/T and incubated with anti- rabbit IgG horseradish peroxidase (HRP) conjugated secondary antibody (1:2000, Cell Signaling Technology). Signals were detected by ECL-Plus, chemiluminescence (Western Lightning, Perkin Elmer, Woodbridge, Ontario).

REAL TIME PCR FOR eEF1A2

RNA extraction

Total RNA from the stable clones was extracted using TRIZOL reagent (Invitrogen) as per manufacture's instructions. In brief, cell extracts from 100mm plates were taken as described previously and the pellet was resuspended in 1ml of trizol reagent. Homogenized samples were then incubated for 5 min. at RT to allow complete dissociation of nucleoprotein complexes and 0.2ml of chloroform was added. Tubes were shaken vigorously and kept at RT for 2-3 min. followed by centrifugation at 12000 ×g for 15 min. at 4°C. The colorless, aqueous phase was transferred to the fresh tube and RNA was precipitated by adding 0.5ml of isopropyl alcohol. Precipitated RNA was kept at RT for 10 min. and then centrifuged at 12000 ×g for 10 min. at 4°C. After removing the supernatant, precipitated RNA was washed with 1ml of 75% ethanol. The samples were further centrifuged at 7500 ×g for 5 min. at 4°C. Partially dried RNA samples were dissolved in 50 µl of diethyl pyrocarbonate (DEPC, Sigma) treated water and stored at -80°C. Purity and quantity of RNA was determined by comparing the absorbance at 260nm to the absorbance at 280nm ($A_{260/280}$ ratio).

Preparation of cDNA and quantitative PCR

Turbo DNA-free™ (Ambion, U.S.A.) kit was used as per manufacturer's instructions to remove endogenous and / or contaminating DNA from RNA preparations. In brief, 2μg of RNA was treated with 1 µl of Turbo DNase and 5 µl of 10 ×Turbo DNase buffer in total 50 µl of reaction followed by incubation at 37°C for 1hr. 5 µl DNase inactivation reagents were further added to each sample and reaction mixtures were incubated for 1.5 min. at RT. Samples were then spun down at 10000 rpm for 1.5min and supernatants were carefully removed and transferred to the fresh tubes to proceed with further c-DNA synthesis.

Cells-to-cDNA II Kit (Ambion, U.S.A.) was used to make cDNA template as follows; 8 µl dNTP mix, 4 µl random primers (decamers) and 6 µl of nuclease free water (Ambion) were added to total 2ug of DNase free samples obtained as above. Samples were kept at 70°C for 3 min. and placed on ice for 1 min followed by addition of 4 µl 10 × RT buffer, 2 µl RNase inhibitor and 2 µl M-MLV reverse transcriptase. Samples were then incubated at 42°C for 60 min. to activate transcription followed by incubation at 92-95°C for 10 min. to denature cDNA. Samples were stored at -20°C and utilized to perform real time PCR for determining eEF1A2 expression.

Real-time PCR system depends upon the detection and quantitation of a target gene (eEF1A2) by a fluorescent reporter. In the present study, quantitative analysis of cDNA amplification was assessed by incorporation of SYBR Green (fluorescent reporter) into double-stranded (ds) DNA. The signal of SYBER Green increases in direct proportion to the amount of PCR product in a reaction. It binds to dsDNA and upon excitation emits light. Thus, as PCR product accumulates, fluorescence increases. Stock of SYBER Green was

10000× concentrated and working solution was made by dissolving 1µl of stock in 1000µl in DMSO and kept in dark place at -20°C. Real time PCR was performed using the Corbett Research real-time PCR machine, Rotor gene RG-3000model (courtesy Dr.Paul Albert's laboratory). For mouse eEF1A2, we used
5' AAGGCCGAGCGGGAACGAG 3' as the forward primer and 5' CCGCCTGGG ATGTGCCTGTAAT 3' as the reverse primer. The house keeping gene, GAPDH (Glyceraldehyde 3-phosphate dehydrogenase) was used as an internal reference gene. For mouse GAPDH, we used 5' ATCACTGCCACCCAGAA-GAC3' as the forward primer and 5' CACATTGGGGTAGGAACAC 3 ' as the reverse primer. Primers were diluted to give a final concentration of five picamoles per 25 ul of PCR reaction. All cDNA templates in 50 µl of reactions were synthesized from 2ug of DNase free RNA as mentioned above. Standard curves for eEF1A2 and GAPDH were obtained by using 2ug, 1ug, 0.5ug, 0.25, 0.125ug of cDNA template of mouse skeletal muscle and NIH 3T3 cells respectively. Mouse skeletal muscle was used as a positive control. For negative control, total RNA was extracted from 3T3-EV.

PCR mixtures for (eEF1A2 as well as GAPDH) each reaction were prepared by adding 12.5ul of 2 ×BD QTaq PCR buffer, 4ul of cDNA template, 1.5 ul of each forward and reverse primers, 0.5ul BD QTaq DNA polymerase enzyme (BD Bioscience), and 1ul SYBER Green in a total volume of 25ul. A non-template control (NTC) was used in each experiment to ensure the specificity of primers. This control contained each ingredient in the PCR mixture specified above except the sample cDNA being tested. Thermal cycling conditions were as follows: initial incubation of 3 min. at 95°C followed by 40 cycles of 20 seconds at 92°C to denature DNA, 20 seconds at 60°C annealing temperature, and 20

seconds at 72°C for amplification of DNA. Formation of primer dimers was reduced to some extent by including a last step of 85°C for 10 seconds. There was a waiting time of 30 seconds at first step and 5 seconds in between each step.

After performance of real time PCR , 5ul of each sample was electrophoresed on 1% agarose gel to confirm the product size for eEF1A2 (139kb) and GAPDH (189kb). Samples were compared using the relative comparative method. Quantification of the amount of target in unknown samples was accomplished by measuring transcripts per total cycles, and standard curves for eEF1A2 and GAPDH were used to determine starting copy number. The parameter C_T (threshold cycle) is defined as the fractional cycle number at which the fluorescence passes the fixed threshold. The entire process of calculating C_T, numbers of transcripts per total number of cycles, standard curves, and determining starting copy number for unknowns was performed automatically by the software. However, we preferred to analyze real time PCR data by using number of transcripts /copy number per total cycles. Thus, total number of transcripts/copy number per total number of cycles for eEF1A2 and GAPDH was obtained from Corbett Research system, Rotor-Gene 6.0 version of software, and then analyzed statistically. For accurate quantification of unknown samples, standard curves for eEF1A2 and GAPDH with *R* value above 0.98 was considered precise. *R* value is a correlation coefficient and it was automatically adjusted by the software. The level of target gene-expression was normalized by using internal reference gene, GAPDH. The ratio of eEF1A2 to GAPDH transcripts was analyzed to determine the significant difference in the expression of eEF1A2 levels in positive control, negative control versus unknown samples (stable clones with AKT, PI3K and c-Myc). The following formula was used to determine fold changes in eEF1A2 expression:

$$\text{Fold change in eEF1A2} = \frac{\text{Copy number of target gene (eEF1A2)}}{\text{Copy number of reference gene (GAPDH)}}$$

To determine the effect of protein expression of eEF1A2 on the protein expression of pan AKT, AKT-2, phospho-AKT, PI3K (p110 and p85), and c-Myc the following experimental approach was followed.

CULTURE OF BT-549 CELLS

BT-549 (breast ductal carcinoma; eEF1A2-negative) cells were obtained from the ATCC and grown as indicated on the ATCC website. In brief, cells were grown in RPMI media which was supplemented with 10% FBS, 1% antimycotic/antibacterial to prevent fungal and bacterial growth, 0.023 IU/ml of insulin, 5mM of sodium pyruvate, and 10mM HEPES buffer. BT-549 cells were kept in an incubator at 37°C and 5% CO_2.

BT-549 cells were transfected with pcDNA3.1_GS (Invitrogen) encoding eEF1A2 under the control of CMV. The plasmid has a C-terminal V5 tag (Gly-Lys-Pro-Ile-Pro-Asn-Pro-Leu-Leu-Gly-Leu-Asp-Ser-Thr) with a Zeocin antibiotic resistance marker. Independent BT-549 clones (BT-549-2, BT-549-5, BT-549-8) expressing different levels of the eEF1A2 protein were selected. The empty vector BT-549 (-Ev) was generated by transfecting parental cells with pcDNA3.1_GS alone.

We have used western blotting on stably transfected BT-549 cell lines to determine the effect of eEF1A2 protein expression on the protein expression of AKT(pan) , AKT-2, pAKT (phospho –AKT) , PI3K (p110 and p85), and c-Myc.

Cell extracts and SDS-PAGE:

Cell lysates were taken as described previously and protein quantification was

performed by a Bradford protein assay (Bio-Rad). 20ug of protein was loaded onto 12.5% mini-protein polyacrylamide gels with 1cm 4% stacking gels and separated according to needed resolution. SDS-PAGE analysis was performed as mentioned previously and membranes were incubated with a TBS-T /primary antibody solution overnight with gentle shaking at 4°C. The commercially available anti-rabbit primary antibodies were used at the following concentrations: panAKT, AKT-2, pAKT threonine 308, pAKT serine 473, PI3K p110α subunit, (1:1000 dilution, all from Cell Signaling Technology, Beverly, Washington), Anti-Myc (1:1000), anti-PI3kinase p85 subunit, (1:2000) (Upstate Biotech, Charlottesville, Virginia). Membranes were washed three times for 5 minutes each with 15ml of TBS/T and incubated with anti- rabbit IgG horseradish peroxidase (HRP) conjugated secondary antibody (1:2000, Cell Signaling Technology). Blots were stripped with 0.2M glycine (pH2.0) two times for 20 min. and reprobed with other primary antibodies. Mouse monoclonal anti-V5-HRP antibody (1:5000 Invitrogen, California) was used to detect V5 tagged eEF1A2 in stably transfected BT-549 cells. Membranes were reprobed with an anti-ß-actin antibody (1:12000, Sigma) to show equal loading while HRP conjugated anti-mouse (1:5000; Upstate) was used as a secondary antibody. Signals were detected by ECL-Plus, chemiluminescence (Western Lightning, Perkin Elmer, Woodbridge, Ontario).

DERIVATION OF eEF1A2 ANTIBODY

Two rabbits, 57/F and C44 (identification numbers), were immunologically challenged with a synthetic peptide, KVERKEGNASGVSLLEALDT, corresponding to human eEF1A2 residues 215-233. The peptide was conjugated to the KLH (Keyhole Limpet Hemocyanin). The peptide was synthesized by Sheldon Biotechnology Centre

(McGill) while conjugation and immunization were performed by a commercial service (Cedarline Laboratories). Terminal bleeds in 80ml of sera from each rabbit were sent to our laboratory. We stored sera at -80°C. The crude sera from both rabbits were used initially to derive eEF1A2 antibody as well as optimization of western blotting. Affinity chromatography was performed to purify the eEF1A2 specific antibody from rabbit anti-sera.

Affinity chromatography

An eEF1A2 peptide was coupled to an affi-gel 10 resin (Bio-Rad) for the purification of eEF1A2 specific antibody. Our protocol is outlined on the Mitchison laboratory web page in the protocol section (http://skye.med.harvard.edu). A resin is first activated and then coupled to the peptide antigen. The functional group of an affi-gel 10 was first converted to an amino and then to an iodoacetyl group. The eEF1A2 peptide was coupled to an affi-gel 10 resin (Bio-Rad) for affinity purification. 1ml of an affi-gel 10 resin was added to a glass-fritted funnel which was attached to a vacuum line (50ul of resin saved for further verification of resin preparation). The resin was washed with five bed volumes of 100% cold ethanol until the wet cake with resin was formed while taking precaution to not the resin dry completely. Furthermore, the resin was washed with five bed volumes of 50% cold ethanol followed by the washes with five bed volumes of cold ddH_20. Five volumes of 5% ethylene diamine was then added to the resin and incubated at RT for 15 min. The resin was washed with ten bed volumes of ddH_20 (saved 50ul resin to verify resin preparation) in order to form an amino-affi-gel.

The resin was washed with three bed volumes of 0.1M Sodium Pyrophosphate (pH7.8) and then resuspended in 0.2 volumes of 0.1M Sodium Pyrophosphate (pH7.8).

Furthermore, 20umol of IAA-NHS (Iodoacetic Acid –N-Hydroxysuccinimide Ester prepared in DMSO) was added to per ml of the resin while gently stirring with a glass rod and incubated at RT for 10 min. to block the residual iodoacetate groups. The resin was then washed with 10 volumes of 0.1M Sodium Pyrophosphate (saved 50ul resin aliquot to confirm resin preparation). The resin was resuspended as 50% slurry in 0.1M Sodium Pyrophosphate. The resin chemistry was checked as follows: resin aliquots (from step # 1, 6, 10) were resuspended in 100ul of 0.1M Sodium Pyrophosphate and 1ul of 0.1M NHS-Fluoroscein (N-hydroxysuccinimide-fluoroscein prepared in DMSO) was added and incubated for 5 min. at RT followed by centrifugation. The supernatant was discarded and the resin was washed twice with 0.1 M Sodium Pyrophosphate. Furthermore, 0.1M Sodium Pyrophosphate was added to the wet cake of resin and transferred to 15ml falcon tube. The resin was mixed gently and kept on a rotating wheel overnight at 4°C. The residual iodoacetate groups were blocked by adding 2-Mercaptoethanol (0.2% (v/v)) and the resin was incubated for 1hr at RT. At this stage, eEF1A2 peptide coupled resin was transferred and packed in 5ml columns (Bio-Rad). The resins were washed with five bed volumes of 0.1M $NaHCO_3$ followed by five bed volumes of 0.1M NaH_2CO_3 and then with five bed volume of ddH_2O. In addition, the resins were washed with five bed volumes of 0.2M glycine (pH2.0) followed by five bed volumes of 150mM NaCl. The resins were also washed with five bed volumes of 6M Guanidine buffer which was prepared in TBS buffer (20mM Tris-HCl, pH7.4, 0.15M NaCl). The resin column was re-equilibrated into 0.1 %(w/v) sodium azide buffer which was also prepared in TBS buffer (pH7.4) and stored at 4°C.

The eEF1A2 antibody was then affinity purified over the column as follows: The column was extensively washed with ~ 20ml of TBS buffer (20mM Tris-HCl, pH7.4,

0.15M NaCl). 10-15ml of eEF1A2 antibody containing serum was thawed, heat inactivated at 56°C and filter sterilized through a 0.22 μm filter. The filter serum was poured through the column at a rate of 2.5ml/5min. at RT. The serum was recirculated over the column at least for seven times. The column was washed five times with five column volumes of TBS buffer followed with 10 column volumes of the column wash buffer (0.5M NaCl, 0.2% (v/v) Triton X-100 20mM Tris-HCl, pH7.4). The column was further washed with five column volumes of TBS buffer and protein was eluted from the column using column elution buffer (0.2M Glycine-HCl, pH2.0, 0.15 M NaCl) for obtaining eEF1A2 specific antibody. Furthermore, 1ml of fractions was collected into tubes containing 100μl of Tris- Buffer (2M Tris-HCl, pH 8.5) and at least four fractions were collected and labeled as low pH fractions. Each of the fractions were spotted on PVDF membrane and stained with 0.1% Ponceau stain for 3 min. and then destained with ddH_20 until the background was reduced. The spots which turned pink usually contained protein. The column was extensively washed with TBS until the column eluted pH7.4 and then stored at 4°C with 0.1% (w/v) sodium azide prepared in TBS.

The fractions containing proteins were further dialyzed to purify proteins. The dry tubing with a cut off of 30,000 daltons was used for dialysis. It was cut in an appropriate size and treated as follows: All steps were carried out by wearing gloves when handling the tubing. Freshly made 2% (w/v) sodium bicarbonate was boiled with 1mM (w/v) EDTA and then tubing was placed in this solution for 10 min. and then cooled down in ddH_2O. Tubing was further placed in boiling ddH2O with 1mM EDTA for another 10 min. The tubing was carefully rinsed inside out with ddH2O and then one side of tubing was clipped with tubing-specific closure. Furthermore, protein sample was pipetted into this

tubing without introducing air bubbles and another end of tubing was closed off with another tubing-specific closure. The dialysis tubing containing protein was then suspended into pre-chilled dialysis buffer, TBS (20mM Tris-HCl, pH7.4, 15M NaCl), in a large beaker and incubated overnight at 4°C with gentle shaking. Dialysis buffer was replaced next day with fresh pre-chilled TBS buffer and protein was further dialyzed for another 4 hrs at 4°C. The tubing was removed from the beaker containing dialysis buffer and carefully opened one end of the tubing and pipetted the dialyzed protein solution into fresh tubes. The dialyzed protein was electrophoresed on 10% polyacrylamide gel and stained with coomasie blue stain. The specificity of the protein (eEF1A2 antibody) was verified by SDS-PADE as described earlier. The aliquots of eEF1A2 antibody (250μl) were prepared by adding 0.1% (w/v) sodium azide and stored at -20°C and 4°C.

Cell lines

To test the specificity of eEF1A2 polyclonal antibody, following cell lines were used: BT-549 cell lines stably transfected with eEF1A2 and MCF-7 (breast cancer) cells, which endogenously produces eEF1A2. It was also tested on BT-549 parental cell lines transduced (200 copies of virus/cell) with flag tagged adenovirus-eEF1A2 (Ad-1A2). For adenovirus, eEF1A2 was subcloned into *EcoRV* and *XhoI* sites of pShuttle-IRES, where the adenovirus was manufactured by the University of Ottawa. BT-549 cells were transduced with flag tagged adenovirus –eEF1A2 (Ad-eEF1A2) or with GFP control adenovirus at a MOI of 200. MCF-7 cells were grown in the complete DMEM media while BT-549 cells in the RPMI media as described previously.

Cell extraction and protein quantification were performed as described previously. SDS-PAGE and western analysis for testing eEF1A2 antibody were also performed as

mentioned earlier except the modification in few steps.

SDS-PAGE and Western blotting

20 -40 μg of protein was loaded on 12.5% gel polyacrylamide gel and the procedure was carried out until the transfer on PVDF membranes as explained earlier. Following the transfer, the membranes were immersed in a 10% blocking solution (5% (w/v) dried skim milk powder (Nestle) and 5% (w/v) bovine serum albumin (BSA, Bioshop) in TBS/T) and kept on a shaker at RT for 1.5 to 2 hrs. Following the blocking step, membranes were washed 3 times with TBS/T for 5 min. each. The affinity purified eEF1A2 specific antibody was used as a primary antibody with following concentrations: 1:100, 1:500, 1:1000, 1:2000, 1:3000, 1:4000 and 1:5000 and kept overnight on a shaker with a gentle shaking at 4°C. The primary antibody was diluted in 10% blocking solution (5% milk and 5% BSA). The anti-flag mouse (M2) monoclonal antibody was used with the concentration of 10μg/ml for Ad-eEF1A2 (positive control). Membranes were washed three times each for 6 min. and then blocked again in a 10% blocking solution for 30 to 45 min. at RT with a gentle shaking followed by two washes of TBS/T each for 3 min. Membranes were then incubated with HRP-conjugated goat anti-rabbit secondary antibody (Upstate) with the following concentrations: 1:1000, 1:2000, 1:3000, and 1:5000 at RT for 1hr with gentle shaking. Anti-mouse HRP conjugated antibody (1:5000, Upstate) was used against anti-flag primary antibody. Membranes were washed three times with TBS/T each for 7 min. Signals were detected by ECL-Plus, chemiluminescence (Western Lightning, Perkin Elmer, Woodbridge, Ontario). Primary antibody concentrations and secondary antibody concentrations (mentioned above) were tried with different combinations in order to optimize western blotting protocol for eEF1A2 antibody.

SPECIFICITY OF eEF1A2 ANTIBODY

Production of GST- recombinant proteins: eEF1A2 and eEF1A1

GST plasmids constructs

For the expression of glutathione S-transferase (GST)-eEF1A2 fusion protein ,the *EEF1A2* gene was already subcloned in the frame between *Eco RI* and *Not I* restriction sites in pGEX-4T2 (Pharmacia) and was sent to us as a pGEX-4T2-*EEF1A2* construct (courtesy Nisha Anand).

The expression of GST-eEF1A1 fusion protein was carried out in our laboratory by constructing pGEX-4T2-*EEF1A1* construct. The EEF1A1 insert was cloned out of the pcDNA3.0 vector using polymerase chain reaction (PCR). The following primers were designed such that forward primer 5'CTCGGAATTCGCCACCATGGGAAAG GAAAAGA 3' contained an *EcoRI* cut site while the reverse primer 5' TCATGC GGCCGCTCATTTAGCCTTCTGAGCTTT 3' contained a *Not I* cut site. The PCR reaction was performed in order to amplify *EEF1A1* from pcDNA3.0-*EEF1A1* plasmid and inserted into the *EcoRI* and *Not I* sites. The PCR reaction was prepared by mixing following contents in a 200ul PCR tube : 5 μl 10× PCR buffer minus $MgCl_2$ (Invitrogen), 1μl dNTP(10mM) mixture, 50mM $MgSO_4$ (Invirogen), 1 μl of each forward and reverse primers (10μM), 1 μl template DNA (pcDNA3.0-*EEF1A1*), 0.2 μl vent (New England Biolab), 38.8 μl nuclease free water (Ambion) . The PCR reaction was carried out for 30 cycles in a Biometra (Montreal Biotech Inc.) PCR system under the following thermal conditions: initial incubation of 2 min. at 94°C followed by 30 cycles of 30 seconds at 94°C to denature DNA, annealing temperature at 62°C for 30 seconds and then 72°C for

1 min for amplification.

The PCR product was run on a 1% agarose gel and the bands were visualized by staining with ethidium bromide. The insert (*EEF1A1;* 1.4 kb) was cut out of the gel under ultraviolet light with a scalpel and gel purification and /or DNA extraction was carried out by GFX columns (Amersham) according to the manufacture's instructions. The gel purified insert, *EEF1A1* was further digested with *Eco RI* and *Not I* enzymes to include sticky ends. The vector, pGEX-4T2 (Pharmacia) was also digested with *Eco RI* and *Not I* enzymes and run on 1% agarose gel and DNA was extracted from the gel by GFX columns. Ligation and transformation were carried out as described previously in 1:3 and 1:6 ratio, vector: insert in *E. Coli* DH5α and 15% glycerol stock was made and stored at -80◦c. The construct pGEX-4T2-*EEF1A1* was sequenced to ensure the proper orientation and to check any errors were introduced in the amplification process.

Expression of GST fusion proteins

GST fusion expression plasmids, pGEX-4T2-*EEF1A1* and pGEX-4T2-*EEF1A2* were transformed into competent *E.coli* BL21DE3 (pLys) strain respectively. Transformation was carried out as described earlier and transformed bacteria were grown on LB plates with 50μg/ml ampicillin. The expression of GST fusion proteins for both the constructs was performed as follows: Single colonies were picked and grown in 5ml of LB broth with 50μg/ml ampicillin overnight at 37°C. This starter culture was further inoculated in a larger scale culture i.e. 200ml. Cultures were allowed to grow with shaking at 37°C until the absorbance at λ=600 nm reached 0.6-0.8. Bacteria were then induced by incubation with 0.5mM isopropyl-β-D-thiogalactopyranoside (IPTG) at RT for 3 hrs. Bacterial cells were then collected by centrifugation at 4000× g for 10 min. at RT and bacterial lysate was

resuspended in lysis buffer (3ml for 200ml culture; 25mM HEPES pH7.9, 100mM KCl, 2mM EDTA, 20% glycerol, 2mM DTT, one tablet of protease inhibitor cocktail (per 10ml of lysis buffer; Roche). NP-40 was then added to a final concentration of 0.1%. Suspensions were distributed in 1.5ml eppendorff's tubes (3ml in 3 tubes) and sonicated at a 35% duty cycle. Suspensions were further centrifuged at 13000 × g for 10 min. at 4°C to collect cellular debris. The supernatants were transferred to fresh 15ml falcon tubes and incubated for 1.5hrs at 4°C with glutathione sepharose 4B beads (Amersham Bioscience) which were extensively washed at least 3 times in lysis buffer with 0.1% NP-40. After incubation with these beads, the precipitates were washed three times with 1ml of lysis buffer with final concentration of 0.1% NP-40. The quantification of GST fusion proteins was performed by using polyacrylamide gels and coomassie blue stain and by comparing their expression with bovine serum albumin protein standards. Specificity of eEF1A2 antibody was tested on GST fusion proteins by western blotting as described previously.

Immunoprecipitation (IP)

The BT-549-parental cells (BT-549-P) were transduced with Ad-eEF1A2 or Ad-GFP virus and cell lysates were obtained 48 hours later. The cell lysates were also obtained from untransduced BT-549-P cells. Immunoprecipitation with the flag protein was carried out by using an anti-flag M2 affinity gel (Sigma). The affinity gel was prepared as per manufacturer's instructions. Cell lysates (250μg) were added to the washed resins and final volumes were brought to 1ml by adding lysis buffer (50mM Tris- HCl, pH7.4, 150mM NaCl ,1mM EDTA, 1% triton X-100). The resins were gently agitated overnight at 4°C. The resins were further centrifuged at 7000×g for 30 seconds and supernatants were

removed. The resins were washed three times with 0.5ml TBS. The proteins were eluted by using 4× sample buffer and analyzed by western analysis as described earlier.

Immunocytochemistry

The antibody was also tested for use in immunocytochemistry on paraffin embedded MCF-7 and BT-549-EV (empty vector) cell lines. MCF-7 and BT-549-EV were grown in complete DMEM and RPMI media respectively and incubated at 37°C with 5% CO2. Both the cell lines were treated similarly as follows. Each cell line was grown in three T175 flasks(Sarstedt). Once cells became 80% confluent, cells were gently washed with sterile 1X PBS for three times and then PBS was aspirated. The cell monolayers were covered and fixed with 7ml of 10% neutral buffered formalin (For 1L of NBF, 10% formalin (37% formalin diluted 1:10), 4g NaH_2PO_4, 6.5g Na2HPO4) for 5 min. Cells were scraped and collected into labeled sterile 50ml tubes. Flasks were washed with 5ml 10% NBF to collect all cells. Cells were stored in 10% NBF at 4°C until the next step.

Cells were centrifuged at 1200rpm for 5 min. and the pellet was washed once with sterile 1x PBS and again kept in PBS and transported to the pathology laboratory. After this step, paraffin embedding was performed by the pathology laboratory at the University of Ottawa. Paraffin blocks with embedded cells and slides with fine sections were obtained from pathology laboratory and processed as follows. Sections were deparaffinized (3×5 min. toluene and 2 ×1 min. absolute alcohol) by using an automated machine in the pathology laboratory and further kept in ddH_2O. Antigen retrieval was performed by microwave method in order to restore antigen binding sites. Sections were placed in a plastic slide rack and kept in plastic staining bucket with citrate buffer (10mM Sodium citrate was adjusted to pH 6.0 with 0.1M citric acid). A single layer of boiling chips was

also placed at the bottom of bucket. Sections were boiled in a microwave on high for 5 min. Evaporated citrate buffer was replaced with hot ddH_2O and sections were kept in buffer for 10 min. at RT. The above process was performed one more time and sections were further rinsed in ddH_2O and placed in TBS.

After antigen retrieval process, sections were washed in running tap water for 5 min. and then treated with 3% H_2O_2 (30% solution, EM science, Germany) in TBS (pH7.6) for 10 min. to remove endogenous peroxidase. Sections were rinsed in TBS for 5 min. and blocked with suppressor (4% BSA, 10% Sucrose, 1 %(v/v) normal swine serum prepared in TBS, pH7.6) for 1hr at RT. Excess suppressor was decanted and sections were incubated with diluted eEF1A2 specific (primary) antibody for overnight at 4°C. An eEF1A2 antibody was diluted in primary antibody diluent (10% Sucrose, 1% BSA, 0.01% Sodium azide (w/v) prepared in TBS and filter sterilized). Primary antibody dilutions were tried as follows; 1:20, 1:30, 1:40, 1:50, 1:100, 1:200. Next day sections were brought to RT at least for 30 min. and then washed with TBS 3 × 7 min. and blocked again with 3% BSA for 1 hr at RT. Sections were then incubated with anti-rabbit, proxidase-linked secondary antibody raised in donkey (1:100, Amersham Biosciences) for 1hr at RT followed by washes with TBS three times for 7 min. and further incubated with diaminobenzidine as follows. Sections were also processed under similar conditions with only primary antibody as well as with only secondary antibody to check the background.

Diamionobenzidine (DAB, DAKO Corporation, California, U.S.A.) was used in immunohistology as a precipitating substrate for the localization of the peroxidase activity. The DAB solution was prepared in pathology laboratory by dissolving 5g of DAB in 208ml TBS (pH7.6) under fume hood in the dark and aliquoted in 2ml amounts and kept at -20°C.

Working solution of DAB was prepared by dissolving 2ml of DAB and 50μl 30% H_2O_2 into 250ml of TBS (pH7.6) and incubated for 10 min. with constant agitation in the dark. Sections were then rinsed with TBS and washed in running tap water for 5 min. Since DAB is carcinogenic, it was discarded carefully in biohazard container. Sections were dehydrated, counterstained with hematoxylin and mounted by using an automated machine in pathology laboratory. Sections were screened under high power magnification and images were taken to assess the specificity of eEF1A2 antibody.

Hypothesis:

eEF1A2 is a part of an AKT, c-Myc or PI3K-dependent oncogenic pathway.

Objectives:

1) Determine whether AKT, PI3K or c-Myc affect eEF1A2 mRNA expression

2) Determine the effect of eEF1A2 on protein expression of AKT, PI3K or c-Myc.

3) Derive an eEF1A2- specific antibody for use in breast and ovarian cancer prognosis.

RESULTS

RESULTS

DETERMINING THE EFFECT OF EXPRESSION OF AKT, PI3K AND c-MYC ON mRNA EXPRESSION OF eEF1A2

Effect of AKT on mRNA expression of eEF1A2

We generated stable cell lines expressing a constitutively active form of AKT. To confirm over-expression of AKT, a western blot was performed on the stably transfected cell lines. The blot was probed with a pan-AKT (60 kDa) antibody and showed prominent over-expression in two stable clones, AKT-1 and AKT-2, compared to the NIH 3T3 cells transfected with the empty vector, pcDNA3.1, i.e. 3T3-EV (Fig. 7A). The blot was also probed with β-actin (47 kDa) to ensure equal loading.

In order to determine the effect of AKT on eEF1A2 mRNA expression, quantitative real-time PCR (qRT-PCR) was performed on mRNA derived from the two stable clones and 3T3-EV. The schematic graph generated by the software represents normalized fluorescence on the *y* axis and the number of PCR cycles on the *x* axis. It shows amplification of eEF1A2 in mouse skeletal muscle, a positive control, after nearly 17 cycles. On the other hand, amplification of eEF1A2 in 3T3-EV, and the two stable clones, AKT-1 and AKT-2 was observed after ~23 cycles (Fig. 7B). The statistical analysis of the data is shown in figure 7C, where the *y* axis represents the fold difference in amplification of eEF1A2 in stably transfected cells compared to mouse skeletal muscle (positive control) which was set to one while the *x* axis shows the cell lines. The data showed that there was no substantial change in mRNA amplification of eEF1A2 in AKT stable cell lines compared to 3T3-EV (Fig. 7C). This data was representative of at least

Figure 7. Effect of AKT expression on mRNA expression of eEF1A2.

(A) Stable transfection with active AKT: Expression of AKT in two independently derived stably transfected NIH 3T3 cell lines, as compared to 3T3-EV control. β-actin shows equal loading.

(B) Real time PCR data represented schematically by using different colored curves. It shows amplification of eEF1A2 initiated later in AKT-1, AKT-2 stables and 3T3-EV than in a skeletal muscle.

(C) Statistical analysis of real time PCR data represented by bar graphs with standard deviations. There was no substantial fold difference in mRNA expression of eEF1A2 observed in AKT-1, AKT-2 and 3T3-EV stable cell lines. The mouse skeletal muscle (positive control) was set to one. Error bars represent standard deviation (n=3).

A)

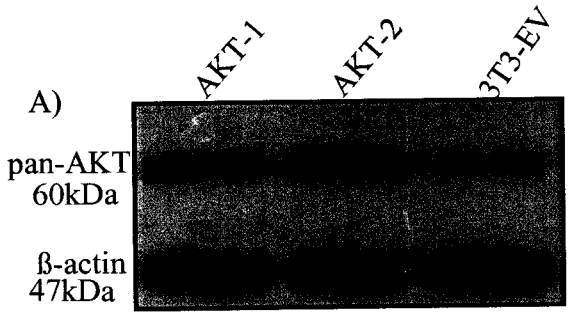
AKT-1
AKT-2
3T3-EV
pan-AKT
60kDa
ß-actin
47kDa

B)

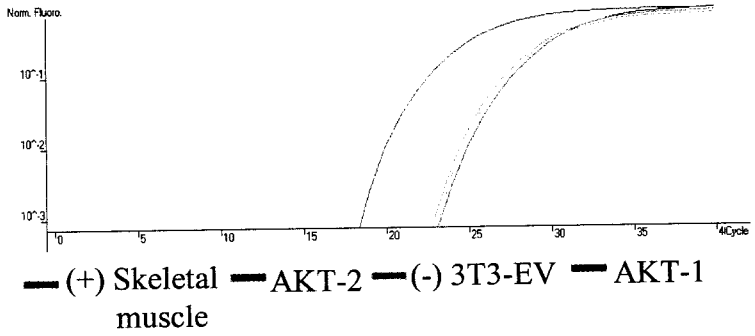
Norm. Fluoro.
10^-1
10^-2
10^-3
0
5
10
15
20
25
30
35
40Cycle
(+) Skeletal muscle
AKT-2
(-) 3T3-EV
AKT-1

C)

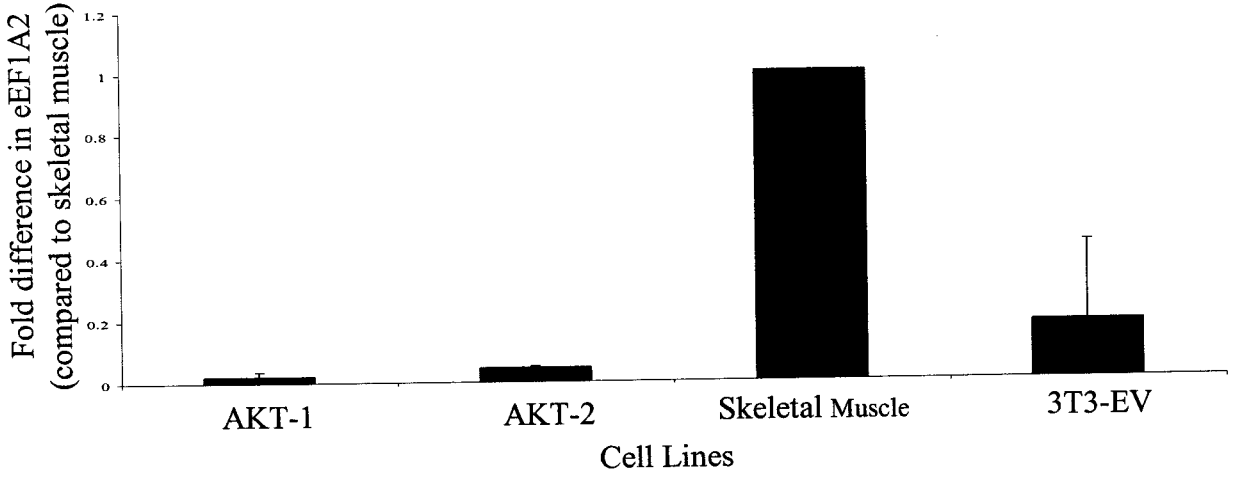
Fold difference in eEF1A2 (compared to skeletal muscle)
1.2
1
0.8
0.6
0.4
0.2
0
AKT-1
AKT-2
Skeletal Muscle
3T3-EV
Cell Lines

three independent experiments. It suggested that there was no substantial effect of AKT expression on the mRNA expression of eEF1A2.

Effect of PI3K on mRNA expression of eEF1A2

We generated stable cell lines expressing PI3K. NIH 3T3 cells, transfected with pcDNA3-p110CAAX (constitutively active PI3K), were analyzed for over-expression of PI3K catalytic subunit, p110α, by western blotting. The blot was probed with a p110α antibody and showed prominent over-expression of the 110kDa catalytic subunit in the following cell lines: PI3K-2, PI3K-3, PI3K-4 and PI3K-5 compared to negative control, 3T3-EV (Fig. 8A). However, the PI3K-1 cell line did not show over expression and seemed not to be stably transfected. The quantitative analysis and the integrated band density values were obtained from the spot denso program provided by an Alpha Imager 1220 v5.04. These values were utilized to determine consistent loading of the samples. The ratio of PI3K to β-actin (47kDa) confirmed the over-expression of PI3K in the stable clones which is depicted by arrows (Fig. 8A).

The qRT-PCR was performed on mRNA derived from the PI3K-3, PI3K-4, and PI3K-5 stable cell lines. The schematic graph created by software shows normalized fluorescence on the *y* axis and number of PCR cycles on the *x* axis. The graph illustrates the amplification of eEF1A2 in mouse skeletal muscle (positive control) after ~ 17 cycles while it initiated after 25 cycles in the PI3K-3 ,PI3K-4, 3T3-EV (negative control) and PI3K-5 cell lines (Fig. 8B). The statistical analysis of the data was depicted in the form of bar graphs where the *y* axis represents the fold difference in amplification of eEF1A2 in stably transfected cells compared to mouse skeletal

Figure 8. Effect of PI3K expression on mRNA expression of eEF1A2.

(A) Stable transfection with active PI3K: Expression of p110α in four independently derived NIH 3T3 stable cell lines. Ratio of β-actin to PI3K verifies the over expression of PI3K protein in respective cell lines represented by arrows.

(B) Real time PCR data represented schematically using different colored curves. It shows amplification of eEF1A2 started late in PI3K-3, PI3K-4, PI3K-5 stables and 3T3-EV while early in skeletal muscle.

(C) Statistical analysis of real time PCR data represented using bar graphs with standard deviations and no considerable fold difference in mRNA expression of eEF1A2 was observed in PI3K-3, PI3K-4, PI3K-5 and 3T3-EV stable cell lines. The mouse skeletal muscle (positive control) was set to one. Error bars represent standard deviation (n=3).

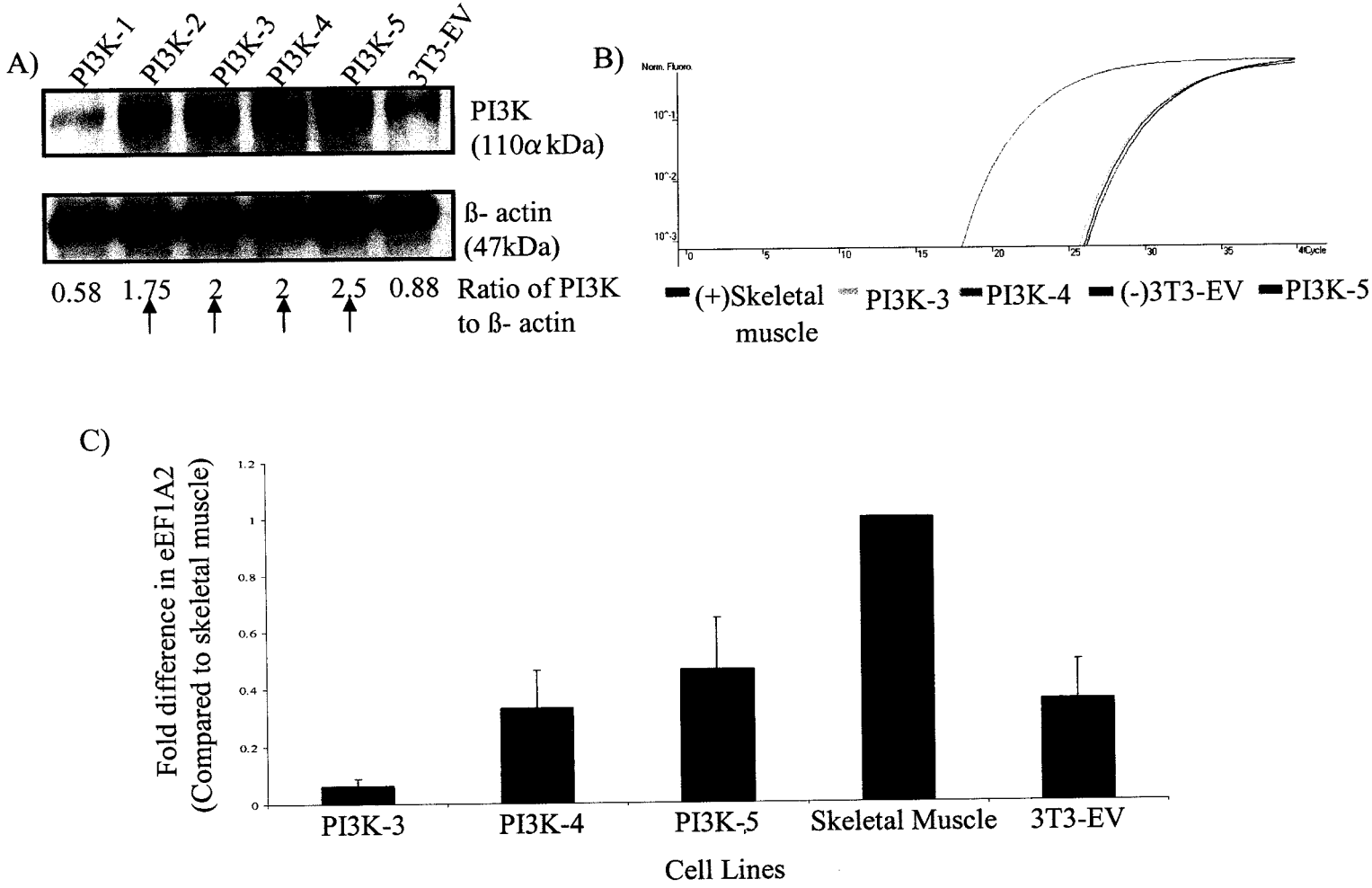
A)
PI3K-1
PI3K-2
PI3K-3
PI3K-4
PI3K-5
3T3-EV
PI3K (110α kDa)
ß- actin (47kDa)
0.58 1.75 2 2 2.5 0.88 Ratio of PI3K to ß- actin
B)
Norm. Fluoro.
(+)Skeletal muscle
PI3K-3
PI3K-4
(-)3T3-EV
PI3K-5
C)
Fold difference in eEF1A2 (Compared to skeletal muscle)
PI3K-3
PI3K-4
PI3K-5
Skeletal Muscle
3T3-EV
Cell Lines

muscle (positive control) which was set to one while the *x* axis represents the cell lines used in the experiment (Fig. 8C). This data implied that there was no substantial fold difference in eEF1A2 mRNA expression due to an over-expression of PI3K (Fig. 8C). This data was representative of at least three independent experiments.

Effect of c-Myc on mRNA expression of eEF1A2

We generated stable cell lines over expressing c-Myc. NIH 3T3 cell lines were stably transfected with a pcDNA3.1-c-Myc and the over expression of c-Myc was verified by western blotting. The blot was probed with a mouse monoclonal c-Myc antibody. It showed over expression of c-Myc (64kDa) in four stable clones: c-Myc-1, c-Myc-2, c-Myc-4, c-Myc-5 compared to control, 3T3-EV (Fig. 9A). One of the cell lines, c-Myc-3 did not over express c-Myc and seemed not be stably transfected. The loading control, β-actin (47kDa) illustrated equal loading in all the samples (Fig. 9A).

The qRT-PCR was executed for determining mRNA expression of eEF1A2 in c-Myc-1 and c-Myc-2 stables. The schematic graph generated by software represents normal fluorescence on the *y* axis while number of cycles on the *x* axis. It shows amplification of eEF1A2 in the mouse skeletal muscle (positive control) started after almost 23 cycles while it initiated in 3T3-EV after ~27 cycles (Fig. 9B). It was interesting to note that amplification of eEF1A2 in the stably transfected cells, c-Myc-1 and c-Myc-2, started after 28 cycles which was later than in 3T3-EV (Fig. 9B). The statistical analysis of the data was represented in figure 9c in the form of a bar graph, where the *y* axis represents the fold difference in mRNA amplification of eEF1A2 in stably transfected cells compared to mouse skeletal muscle (positive control) which was set to one while the *x* axis represents the cell lines (Fig. 9C). The data suggested

Figure 9. Effect of c-Myc expression on mRNA expression of eEF1A2.

(A) Stable transfection with c-Myc: Expression of c-Myc in four independently derived NIH 3T3 stable cell lines. Ratio of β-actin to c-Myc verifies the over expression of PI3K protein in respective cell lines represented by arrows.

(B) Real time PCR data represented schematically using different colored curves depicting amplification of eEF1A2 initiated earlier in c-Myc-1, c-Myc-2 stables and 3T3-EV than skeletal muscle.

(C) Statistical analysis of real time PCR data represented by bar graphs. There was no substantial fold difference in mRNA expression of eEF1A2 in c-Myc-1, c-Myc-2 and 3T3-EV stable cell lines. The mouse skeletal muscle (positive control) was set to one. Error bars represent standard deviation (n=3).

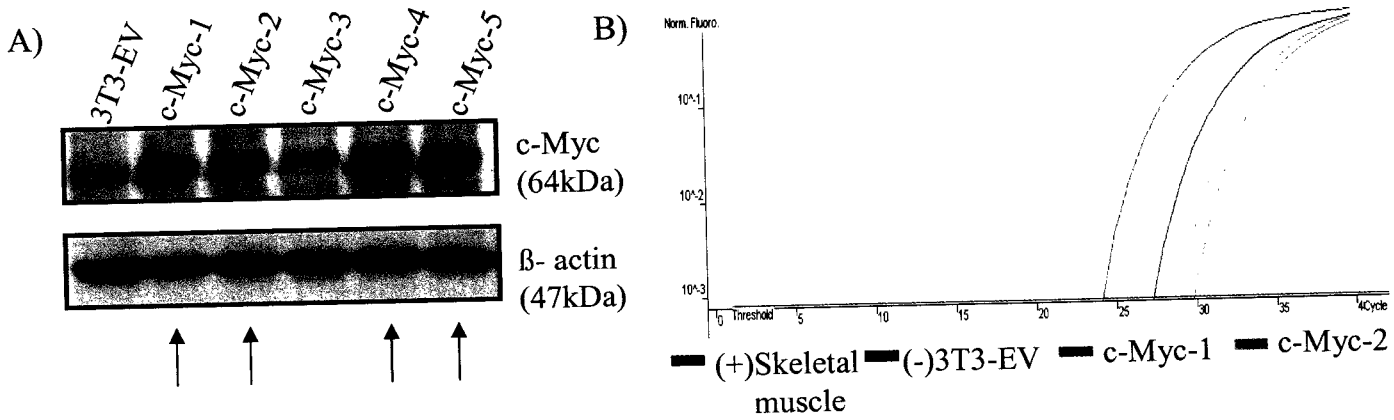
A)
3T3-EV
c-Myc-1
c-Myc-2
c-Myc-3
c-Myc-4
c-Myc-5
c-Myc
(64kDa)
ß- actin
(47kDa)
B)
Norm. Fluoro.
Threshold
Cycle
(+)Skeletal muscle
(-)3T3-EV
c-Myc-1
c-Myc-2

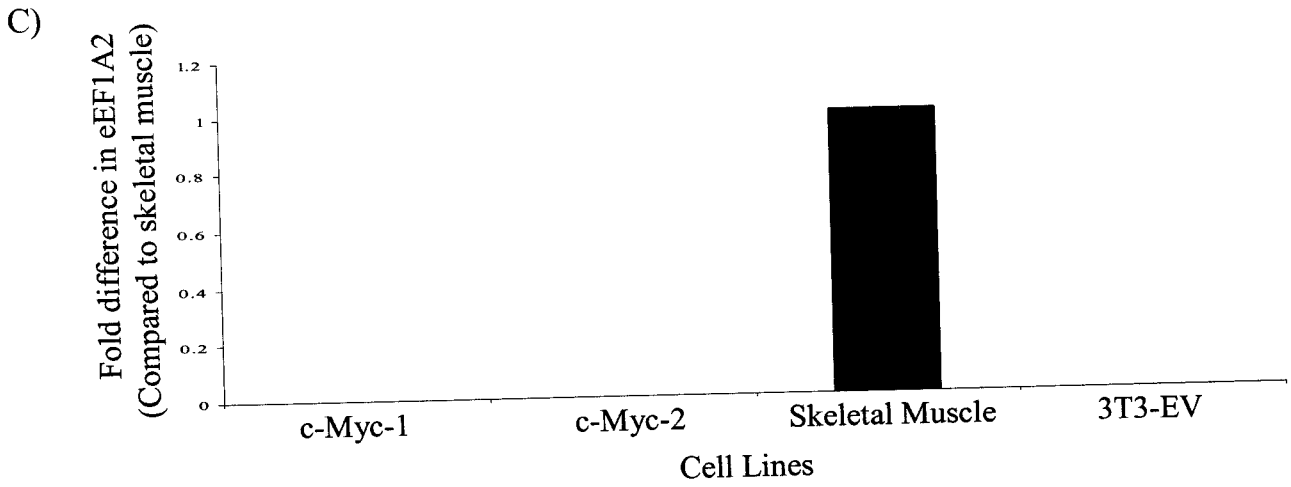
C)
Fold difference in eEF1A2
(Compared to skeletal muscle)
1.2
1
0.8
0.6
0.4
0.2
0
c-Myc-1
c-Myc-2
Skeletal Muscle
3T3-EV
Cell Lines

that there was no substantial fold difference in eEF1A2 mRNA expression due to c-Myc over-expression (Fig. 9C). This data was representative of at least three independent experiments

DETERMINING THE EFFECT OF eEF1A2 PROTEIN EXPRESSION ON PAN-AKT, AKT-2, pAKT, PI3K (p85 AND p110 SUBUNITS), AND c-MYC

Expression of eEF1A2 in BT-549 cell lines

To determine whether eEF1A2 alter protein levels of AKT, PI3K or c-Myc, we generated breast cancer cell lines over-expressing eEF1A2. Following BT-549 stables, BT-549-2, BT-549-5, BT-549-8 and as a control, BT-549-EV were used in the experiments. The levels of eEF1A2 protein were detected with an anti-V5 antibody on a western blot (Fig.10). The blot showed high expression of eEF1A2 in BT-549-2 and BT-549-5 while moderate and no expression in BT-549-8 and BT-549-EV respectively (Fig.10). β-actin (47kDa) was used to show equal loading.

Effect of eEF1A2 expression on activation and protein expression of AKT

The intracellular levels of pan-AKT and the phosphorylated AKT in the stably transfected BT-549 cells were evaluated by western analysis using pan-AKT and phospho-AKT antibodies as follows. The blot was probed with a pan-AKT antibody (60kDa) and further reprobed with serine 473 (ser473) and threonine 308 (thr308) (60kDa) antibodies to evaluate the activation of AKT (Fig.11). β-actin (47kDa) was used as a loading control (Fig.11). The blots showed substantial up regulation in the levels of AKT phosphorylation at the ser473 and thr308 residues while there was no observable change in the expression of pan-AKT (60kDa). This observation suggests

Figure 10. Expression of eEF1A2 in BT-549 cells.

Protein expression of anti-V5 tagged eEF1A2 in independent clones of BT-549 cell lines analyzed by western blotting. B-actin was used as a loading control.

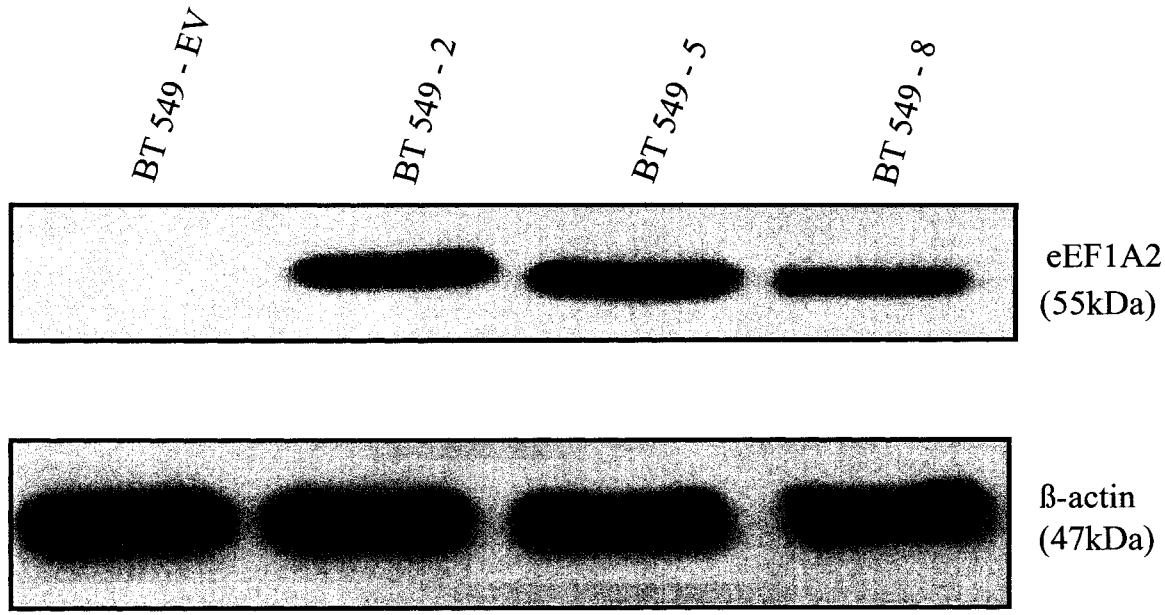
BT 549 - EV
BT 549 - 2
BT 549 - 5
BT 549 - 8
eEF1A2
(55kDa)
ß-actin
(47kDa)

Figure 11. Effect of eEF1A2 expression on protein expression of AKT and phospho AKT.

BT-549 cell lines over expressing eEF1A2 versus vector control were analyzed for pan- AKT and phospho-AKT expression by western blotting. The serine phosphorylation of AKT at position 473 and threonine phosphorylation of AKT at 308 positions were increased while pan-AKT levels were consistent relative to the empty vector control. β-actin served as a loading control. The figure is representative of at least three independent experiments.

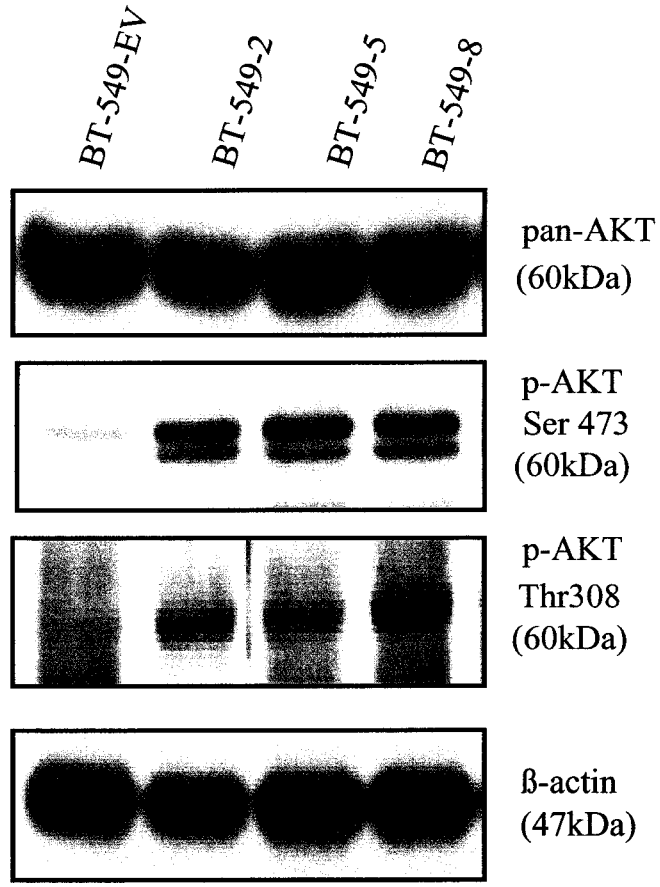
BT-549-EV
BT-549-2
BT-549-5
BT-549-8
pan-AKT
(60kDa)
p-AKT
Ser 473
(60kDa)
p-AKT
Thr308
(60kDa)
ß-actin
(47kDa)

that eEF1A2 expression did not affect the over all protein expression of AKT, however it increases the levels of phospho-AKT at ser473 and thr308 positions.

Effect of eEF1A2 expression on protein expression of AKT-2

A comparison of the endogenous levels of AKT-2 in the stably transfected BT-549 cell lines was determined by western analysis utilizing an AKT-2 antibody. The blot was probed with an AKT-2 antibody and showed no substantial change in the protein expression of AKT-2 (60kDa). An equal loading in all of the samples was verified by reprobing the blot with β-actin antibody (Fig.12).

Effect of eEF1A2 on expression on protein expression of catalytic and regulatory subunits of PI3K

The phosphoinositidol 3-kinase (PI3K) comprises two subunits; catalytic (p110) and regulatory (p85) subunit. The intracellular levels of p110 in the transfected BT-549 cell lines were assessed by western blotting. The blot, probed with a p110α antibody, demonstrated no observable changes in the levels of the p110 catalytic subunit of PI3K in stably transfected BT-549 cells over-expressing eEF1A2 compared to BT-549-EV (Fig.13).

The endogenous level of the p85, regulatory subunit in BT-549 cell lines was also determined on the same blot by western analysis. The blot probed with p85 antibody showed no substantial change in the levels of p85 subunit (Fig.13). The same blot was reprobed with an anti-V5 antibody (55kDa) to determine eEF1A2 levels in BT-549 stables. It showed high expression of eEF1A2 (55kDa) in BT-549-5, while moderate expression in BT-549-2 and weak expression in BT-549-8 compared to empty vector control (Fig.13). The equal loading was assessed by β-actin (47kDa)

Figure 12. Effect of eEF1A2 expression on protein expression of AKT-2.

AKT-2 expression in BT-549 cell lines over expressing eEF1A2 versus empty vector control was detected by using AKT-2 antibody on western blotting. β-actin used as a loading control. The figure is representative of at least three independent experiments.

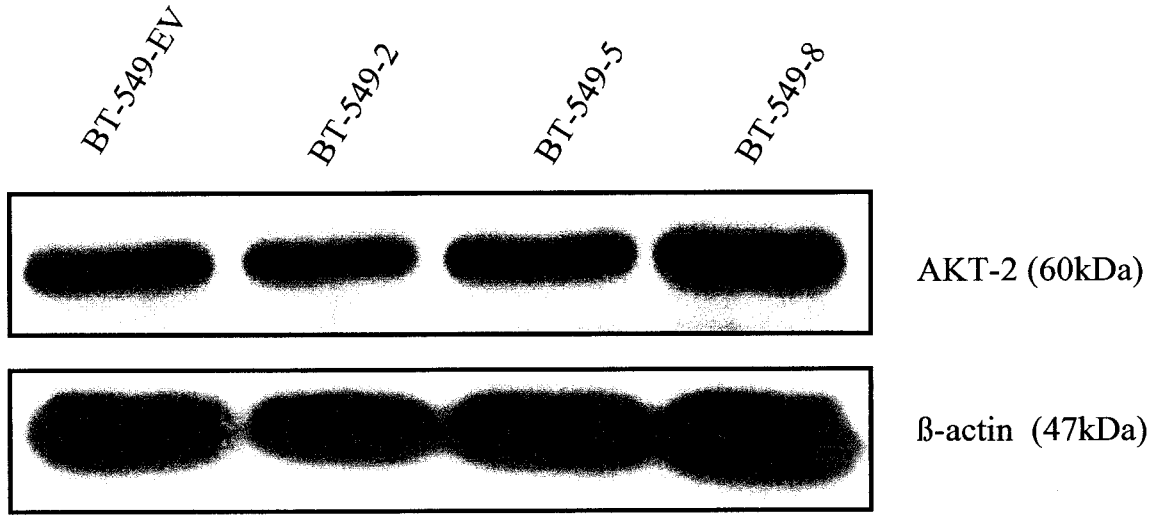
BT-549-EV
BT-549-2
BT-549-5
BT-549-8
AKT-2 (60kDa)
ß-actin (47kDa)

Figure 13. Effect of eEF1A2 expression on catalytic and regulatory subunits of PI3K.

The expression of PI3K catalytic subunit (p110α) and regulatory subunit (p85) detected by western blotting in BT-549 cell lines over expressing eEF1A2 compared to empty vector control. An anti-V5 tagged eEF1A2 protein expression in these cell lines was also depicted. β-actin used as a loading control. The figure is representative of at least three independent experiments.

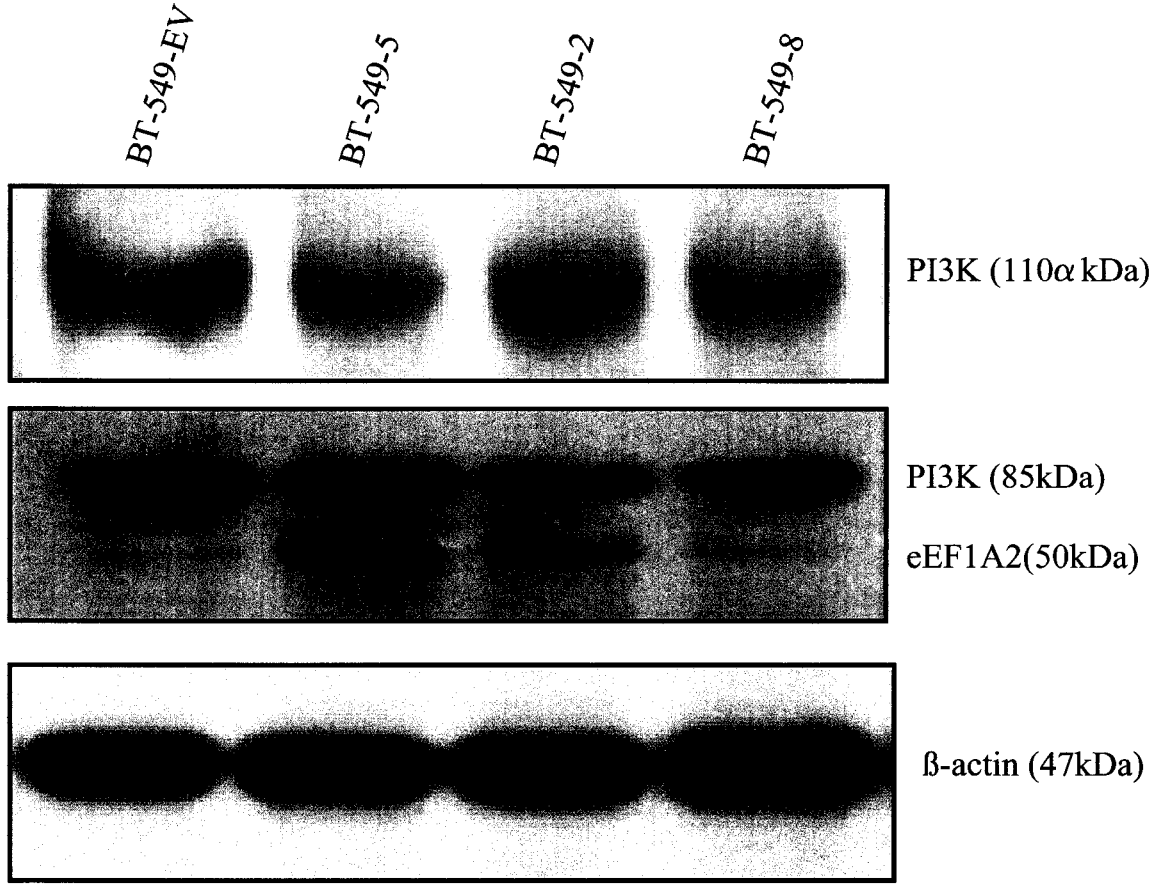
BT-549-EV
BT-549-5
BT-549-2
BT-549-8
PI3K (110α kDa)
PI3K (85kDa)
eEF1A2(50kDa)
ß-actin (47kDa)

Figure 14. Effect of eEF1A2 expression on protein expression of c-Myc.

BT-549 cell lines over expressing eEF1A2 versus vector control were analyzed for c-Myc expression by western blotting. There is no considerable change in the protein expression of c-Myc in these cell lines. β-actin was used as a loading control. The figure is representative of at least three independent experiments.

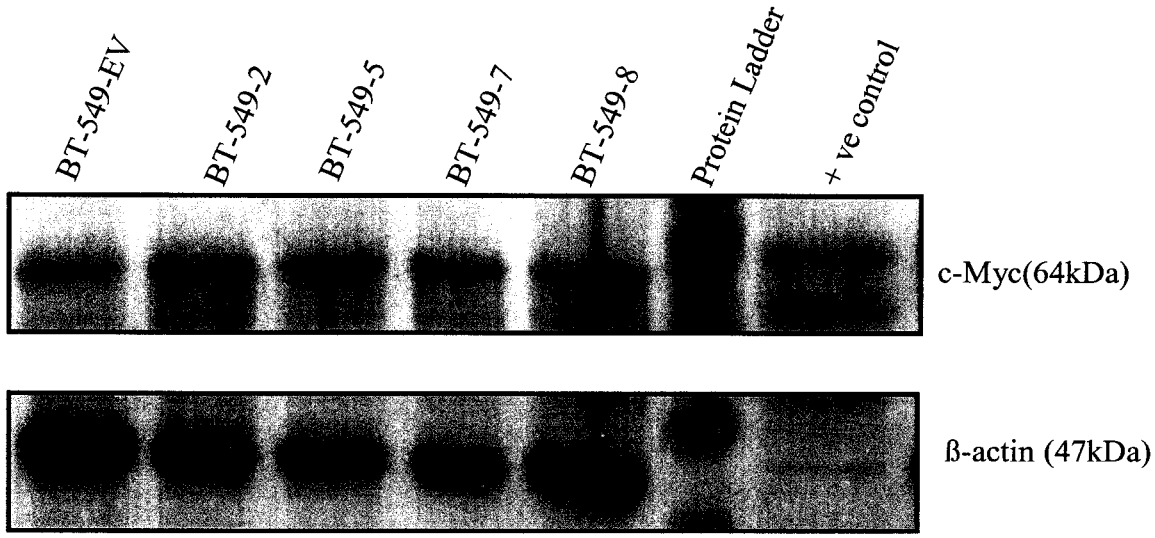
BT-549-EV
BT-549-2
BT-549-5
BT-549-7
BT-549-8
Protein Ladder
+ ve control
c-Myc(64kDa)
ß-actin (47kDa)

(Fig.13). This data implied that eEF1A2 expression did not affect protein expression of PI3K.

Effect of eEF1A2 expression on protein expression of c-Myc

The intracellular level of c-Myc in BT-549 stables was determined by western blotting. The blot, probed with an anti-Myc antibody, depicts no considerable change in the c-Myc (64kDa) protein levels in any of BT-549 stables over expressing eEF1A2 compared to the BT-549-EV (Fig.14). A positive control (human carcinoma cells) was also included in this experiment. The extent of eEF1A2 expression in BT-549-2, BT-549-5, and BT-549-8 included in this experiment was demonstrated earlier (Fig.10). The expression of eEF1A2 in BT-549-7 is similar to the BT-549-8. The blot was reprobed with β-actin (47kDa) and showed equal loading. (Fig.14).

DERIVATION OF eEF1A2 SPECIFIC ANTIBODY

Western blotting

We generated an eEF1A2 antibody by using an eEF1A2-specific peptide KVERKEGNASGVSLLEALDT. A commercial service (Cedarlane Laboratories) coupled this peptide to KLH and performed the immunization and bleeding. The affinity purified eEF1A2 antibody from two rabbits, C44 and 57/F was tested using western blotting. The BT-549 parental cell line was transduced with a flag tagged eEF1A2 in an adenoviral vector (Ad-1A2). Cell extracts were taken at times zero and 48 hours post-transduction. The zero time point samples were designated as Ad-1A2 (0) and considered as a negative control. The samples derived after 48 hours were designated as Ad-1A2 (48) and considered as a positive control sample in testing

Figure 15. Derivation of eEF1A2 antibody.

Affinity purified eEF1A2 antibody derived from C44 and 57/F rabbit sera. The antibody detected expression of eEF1A2 in flag tagged Ad-eEF1A2 (48) lanes but not in Ad-eEF1A2 (0) as compared to a positive control (Flag 48/+). The non specific high molecular weight band was appeared in all lanes except the positive control. Different dilutions of primary (eEF1A2) and secondary antibody were depicted in the figure.

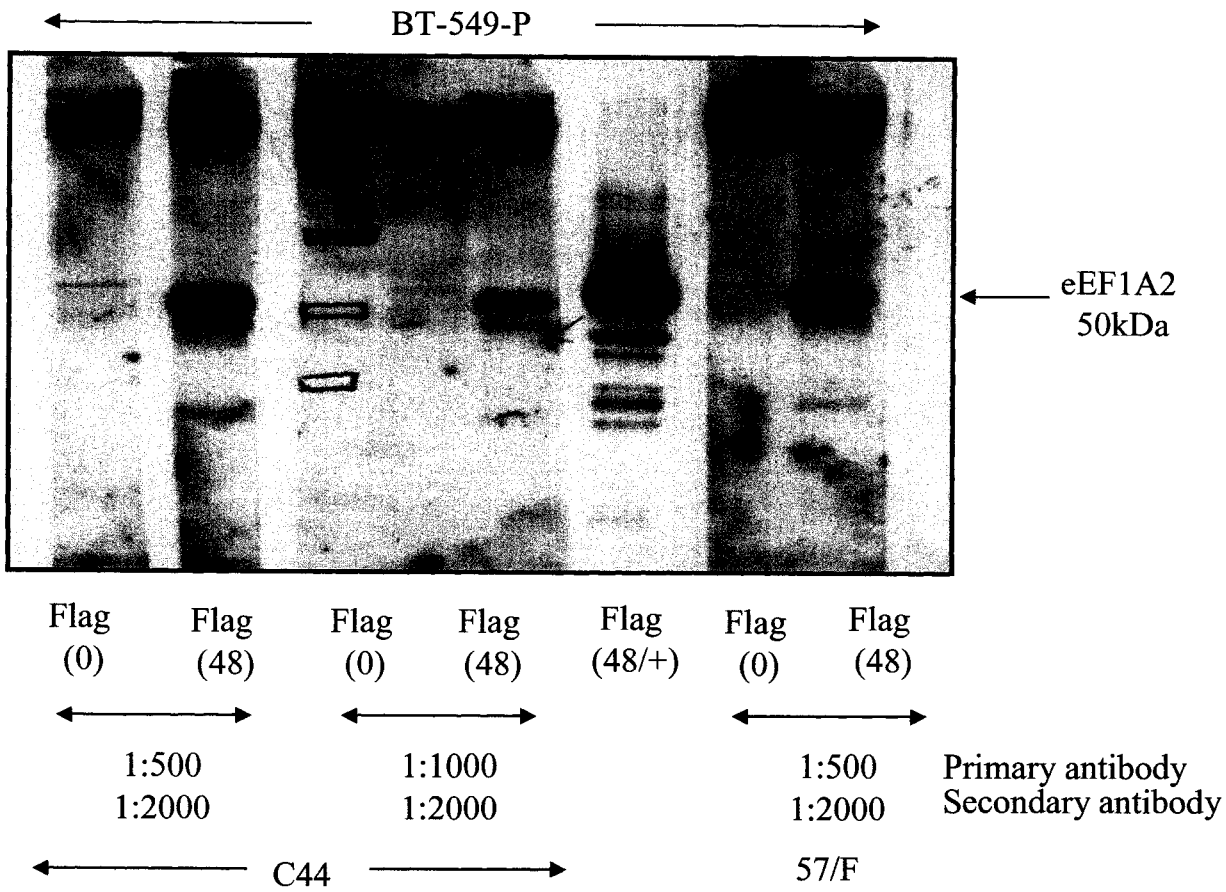
BT-549-P
eEF1A2
50kDa
Flag (0)
Flag (48)
Flag (0)
Flag (48)
Flag (48/+)
Flag (0)
Flag (48)
1:500
1:2000
1:1000
1:2000
1:500
1:2000
Primary antibody
Secondary antibody
C44
57/F

specificity of the eEF1A2 antibody. In addition, a flag tagged Ad-1A2 (48) sample was probed with a mouse anti-flag antibody and included as a positive control to verify the specificity of the eEF1A2 antibody.

The blot was probed with the eEF1A2 antibody (C44 rabbit) in 1:500 and 1:1000 dilutions and also with the antibody from the 57/F rabbit in 1:500 dilutions. The secondary anti-rabbit antibody dilution (1:2000) was kept even for all primary antibody dilutions. This blot showed a promising band around 50 kDa in Ad-1A2 (48) which was relative to the band that appeared in the positive control. A similar band did not appear in the negative control, AD-1A2 (0) (Fig.15). However, the appearance of a nonspecific high molecular weight band (~250kDa) in the blot required further optimization in the western blotting protocol.

Another blot was further probed with the eEF1A2 antibody derived from the C44 rabbit with higher dilutions; 1:2000, and 1:5000 and with a 1:3000 dilution of the 57/F rabbit. The secondary anti-rabbit antibody dilution (1:2000) was kept unchanged for all samples and the percentage of blocking solution was increased from 5% to the 10% (with equal percentage of carnation milk and BSA). This blot showed a promising band around 50kDa which was relative to the band in the positive control. The high molecular weight band around ~250kDa faded away in the 1:3000 dilution (antibody was derived from 57/F) (Fig.16). This dilution was further evaluated. One more blot was probed with the eEF1A2 antibody (1:3000) and secondary anti-rabbit antibody (1:3000) on the BT-549 parental cells transduced with Ad-eEF1A2 and Ad-GFP (Negative control) respectively (Fig.17). The western blotting in this experiment was modified by adding a blocking step (10% blocking solution) after the incubation

Figure 16. Derivation of eEF1A2 antibody.

Affinity purified eEF1A2 antibody derived from C44 and 57/F rabbit sera was further used to optimize the western blotting protocol. The antibody detected expression of eEF1A2 in flag tagged Ad-eEF1A2 (48) lanes but not in Ad-eEF1A2 (0) as compared to a positive control (Flag /+ve). The non specific high molecular weight band around 250kDa was blurred in the lane treated with 1:3000 eEF1A2 antibody dilutions.

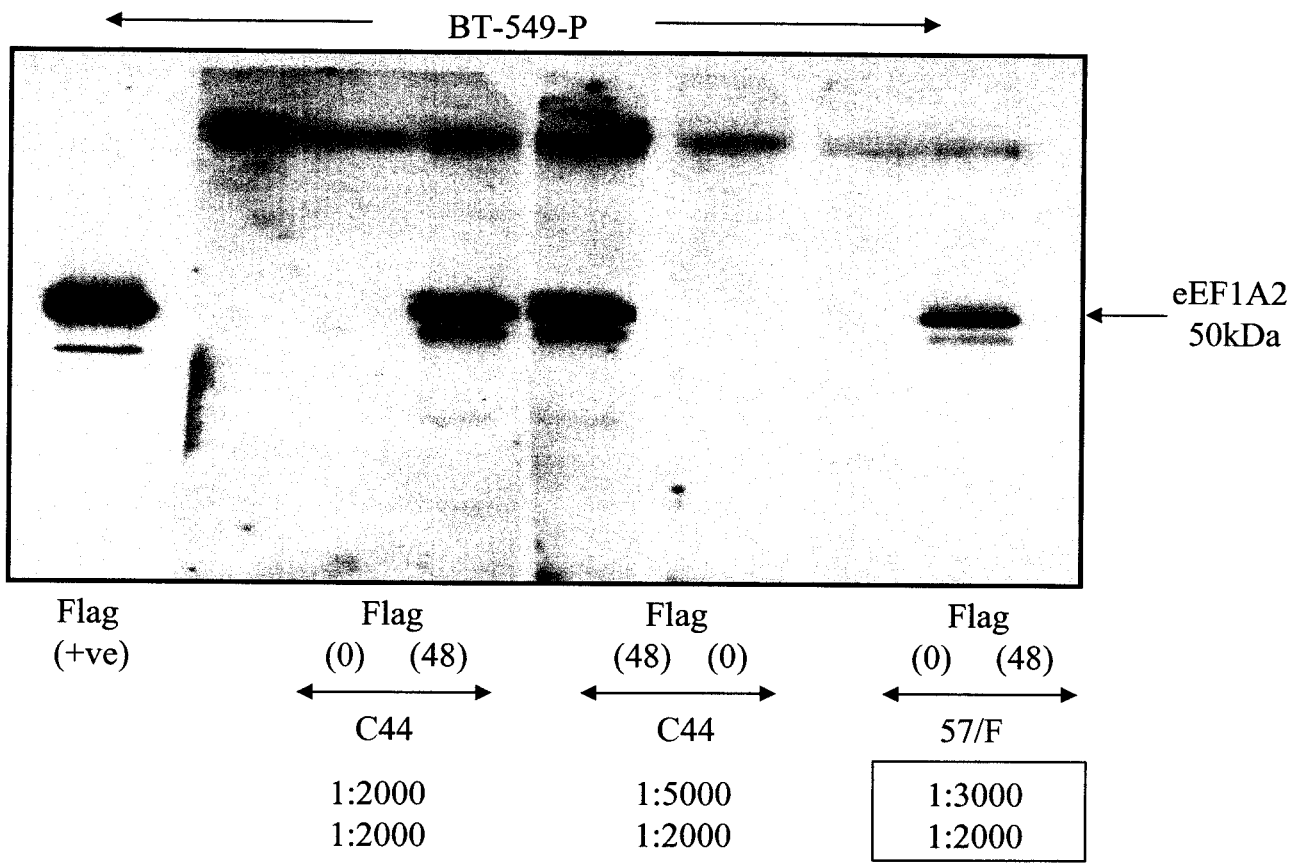
BT-549-P
eEF1A2
50kDa
Flag
(+ve)
Flag
(0) (48)
C44
1:2000
1:2000
Flag
(48) (0)
C44
1:5000
1:2000
Flag
(0) (48)
57/F
1:3000
1:2000

Figure 17. Derivation of eEF1A2 antibody (Final optimization for western blotting).

The blot was probed with eEF1A2 antibody shows prominent band in eEF1A2 expressing Ad-eEF1A2 while relative band (around 50kDa) was absent in Ad-GFP. 1:3000 dilutions were used for primary as well as secondary antibody.

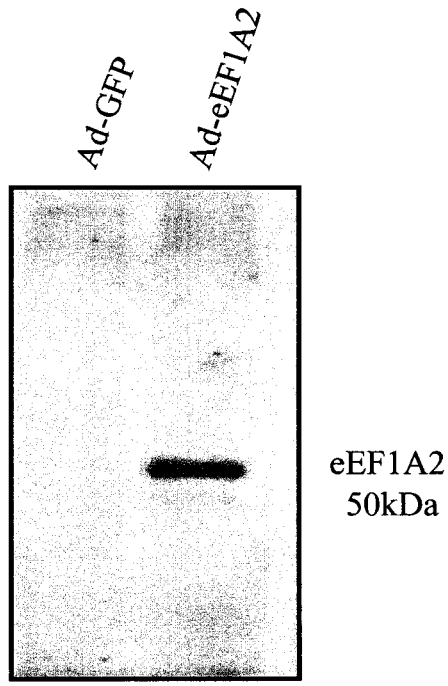

BT-549-P

1:3000 Primary antibody
1:3000 Secondary antibody

with the eEF1A2 antibody. This blot showed a promising band around 50kDa in Ad-eEF1A2 while the antibody did not pick up any band in the Ad-GFP. Moreover, the high molecular weight band was considerably blurred (Fig. 17).

To further assess the specificity of affinity purified eEF1A2, we tested this antibody on the MCF-7 cell which endogenously produces eEF1A2 as well as stably transfected BT-549 cells: BT-549-2, BT-549-5, and BT-549-8, while BT-549-EV served as a negative control. The blot was showing prominent band around 50kDA in the following cell lines: MCF-7, BT-549-2, BT-549-5, BT-549-8, all expressing eEF1A2 protein while no relative band was appeared in BT-549-EV (Fig. 18).

EVALUATION OF THE SPECIFICITY OF eEF1A2 ANTIBODY

Immunoprecipitation

The immunoprecipitation was executed on the cell extracts obtained from untransduced BT-549-parental (BT-549-P) cell lines as well as from Ad-eEF1A2 and Ad-GFP (transduced BT-549-P cell lines as mentioned earlier) to further assess the specificity of affinity purified eEF1A2 antibody. The blot comprised of six lanes where lanes one and four represented cells transduced with Ad-eEF1A2, lanes two and five represented cells transduced with Ad-GFP and lanes three and six were untransduced BT-549-P cells (Fig.19). In this experiment; lanes one, two and three were whole cell extracts (WCL) while lanes four, five and six were immunoprecipitated using an anti-flag antibody. A 50kDa band appeared in lanes number one and four, while no relative band was appeared in any other lanes (Fig.19).

Figure 18. Derivation of eEF1A2 antibody.

BT-549 cell lines stably transfected with eEF1A2 and MCF-7 were incubated with affinity purified eEF1A2 antibody and the blot shows prominent band in the lanes with MCF-7, BT-549-2, BT-549-5 and BT-549-8 cell lines versus no band in BT-549-EV control.

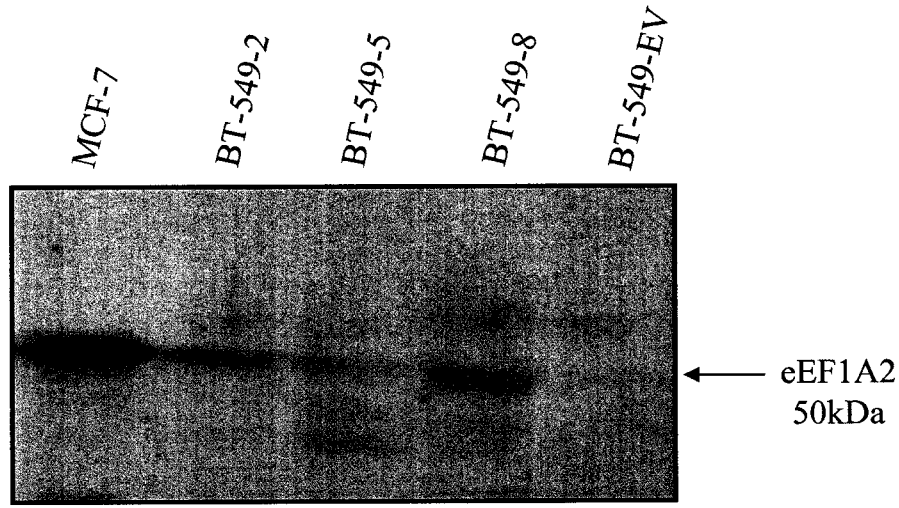
MCF-7
BT-549-2
BT-549-5
BT-549-8
BT-549-EV
eEF1A2
50kDa

Figure 19. Immunoprecipitation.

Immunoprecipitation assay demonstrating specificity of eEF1A2 antibody. The blot was probed with eEF1A2 antibody. First three lanes show whole cell lysates (WCL) of Ad-eEF1A2, Ad-GFP and BT-549-parental cell lines respectively. The prominent band was appeared in Ad-eEF1A2 lanes (1 and 4) but not in the lanes 2,5 or 3,6. Lane 4, 5 and 6 were pulled down with flag antibody. Lane 4 was comprised of Ad-eEF1A2 and shows prominent band while no band (around 50kDa) was present in lane 5 and 6 comprised of Ad-GFP and BT-549-parental cell lysates respectively.

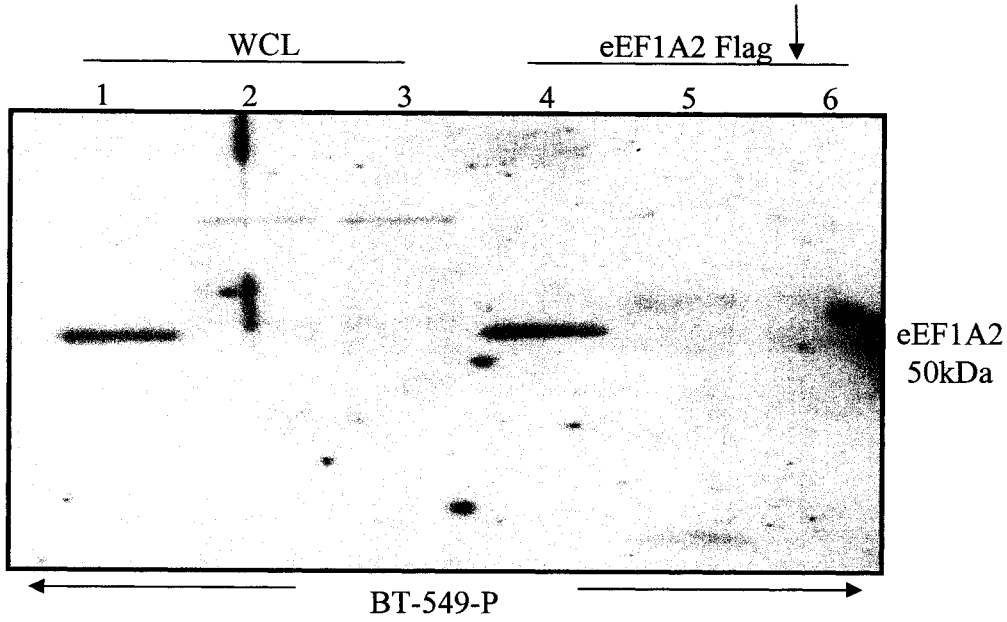

1, 4 : Ad-eEF1A2

2, 5 : Ad-GFP

3, 6 : BT-549-P(untransduced)

This experiment further validated the specificity of the eEF1A2 antibody.

eEF1A2 siRNA and eEF1A2 antibody

Another experiment was performed on MCF-7 cells cultured in the complete DMEM media with different concentrations of serum; 5% and 0% (in the absence of serum) and treated with siRNA against eEF1A2 and negative siRNA respectively. The blot probed with eEF1A2 antibody showed prominent band around 50kDa in all the lanes containing MCF-7 cells treated with negative siRNA (lane 1 and 3). These cell lines were designated as follows: -ve siRNA5% and -ve siRNA0% respectively (Fig. 20). Interestingly, eEF1A2 antibody picked up the band around 50kDa but with the reduced eEF1A2 expression in the lanes comprised of MCF-7 cells treated with siRNA (lane 2, and 4). These cell lines were assigned as: eEF1A2 siRNA 5% and eEF1A2 siRNA 0% respectively (Fig. 20). This experiment assured specificity of the affinity purified polyclonal eEF1A2 antibody.

GST constructs and eEF1A2 antibody

The specificity of eEF1A2 antibody was further verified by using GST-eEF1A2 and GST-eEF1A1 fusion proteins. The ponceau S staining of a PVDF membrane shows a band around 75kDa in the GST-eEF1A2 (lane2) and GST-eEF1A1 (lane 4) lanes (Fig. 21A). The membrane also illustrates the band around 25kDa in a GST fusion protein lane (lane 3). MCF-7 was included as a positive control in the lane five (Fig. 21A). The blot was further incubated with the eEF1A2 antibody and a prominent band (75kDa) was present in the GST-eEF1A2 lane while the equivalent band was not present in the GST-eEF1A1 lane (Fig. 21B). However, a band around 50kDa was visible in the positive control lane of MCF-7 (Fig. 21B). These data

Figure 20. Specificity of eEF1A2 antibody (The eEF1A2-siRNA and eEF1A2 antibody).

The blot was probed with eEF1A2 antibody. It demonstrates that eEF1A2 antibody recognized the reduction in eEF1A2 protein levels in eEF1A2 siRNA treated MCF-7 cells (Lane 2, 4), incubated with different percentages of serum versus MCF-7 cells treated with negative siRNA (Lanes 1, 3). β-actin shows equal loading.

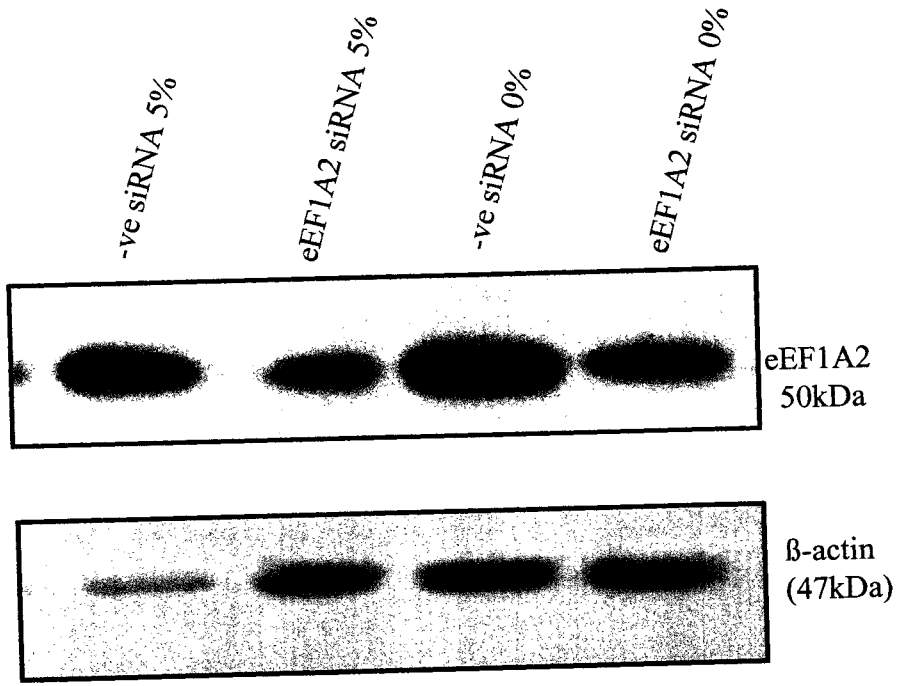
-ve siRNA 5%
eEF1A2 siRNA 5%
-ve siRNA 0%
eEF1A2 siRNA 0%
eEF1A2
50kDa
ß-actin
(47kDa)

Figure 21. Specificity of eEF1A2 antibody.

The western blot was performed to test cross reactivity of eEF1A2 anti-sera against eEF1A1 protein.

(A) The blot was stained with ponceau S solution and it shows band at around 75kDa in GST-eEF1A2 (second lane) and GST-eEF1A1 (fourth lane) respectively. The third lane with GST protein shows band around 25kDa. The first lane with protein ladder was used as a molecular weight marker. MCF-7 cell line in fifth lane was used as a positive control.

(B) The blot above was further probed with eEF1A2 antibody. The prominent uppermost band around 75kDa appeared in the GST-eEF1A2 lane but the eEF1A2 antibody did not pick up relative band in the GST-eEF1A1 lane. The lane with MCF-7 shows prominent band around 50kDa.

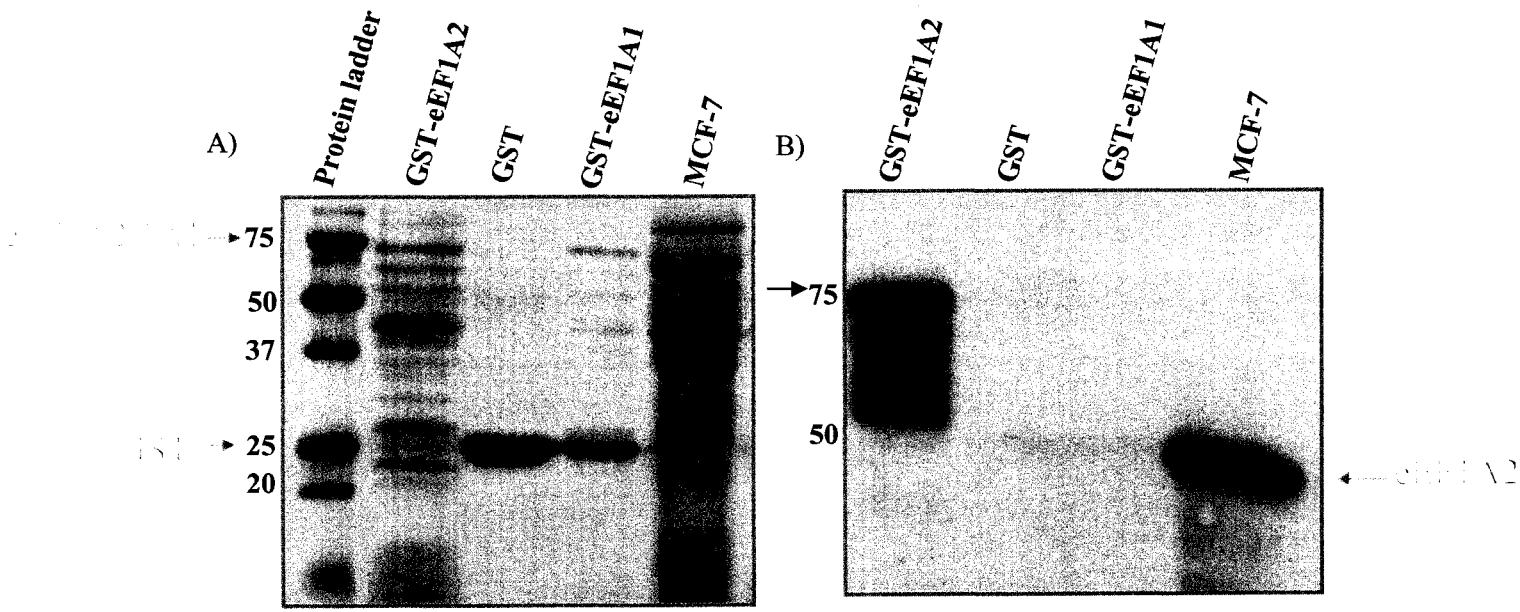
A)
Protein ladder
GST-eEF1A2
GST
GST-eEF1A1
MCF-7
75
50
37
25
20
B)
GST-eEF1A2
GST
GST-eEF1A1
MCF-7
75
50

Figure 22. Immunocytochemistry.

The paraffin embedded sections of MCF-7 and BT-549-EV were incubated with eEF1A2 antibody and stained with DAB.

(A) Section with MCF-7 cells stained with DAB and hematoxylin, show brown coloration in the cytoplasm after staining with DAB which denotes the positive signal for eEF1A2 antibody.

(B) Section with BT-549 EV used as a negative control and stained with DAB and hematoxylin. The cytoplasm of these sections does not show brown coloration. Signal for eEF1A2 antibody was not observed in these sections.

(C-D) Sections with MCF-7 and BT-549-EV were served as a control to determine background coloration. These were incubated with only HRP conjugated secondary antibody and stained with DAB and hematoxylin.

A) MCF-7

B) BT-549-EV

C) MCF-7 (Only secondary)

D) BT-549-EV (Only secondary)

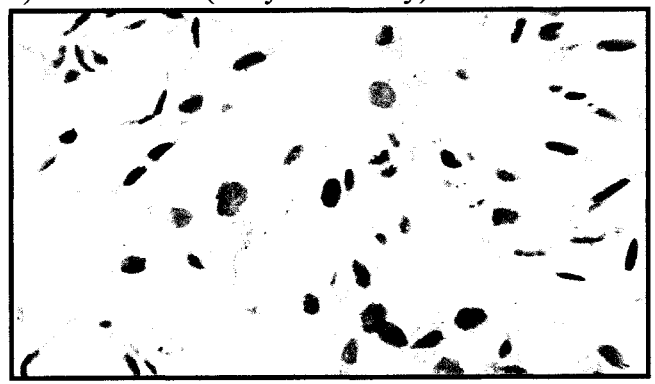

further confirmed the specificity of our eEF1A2 antisera.

Immunocytochemistry

The affinity purified anti-rabbit polyclonal eEF1A2 antibody was also tested for use in immunocytochemistry on paraffin embedded MCF-7 and BT-549-EV cell lines. Diaminobenzidine (DAB) is a brown colored precipitating substrate used for the detection of peroxidase activity. Positive staining with the eEF1A2 antibody was determined by the appearance of brown color in the cytoplasm. The MCF-7 cell lines were used as a positive control while BT-549-EV as a negative control. In addition, both the cell lines were also stained with the secondary antibody (1:100) alone and compared to the positive as well as negative test samples. The sections were incubated with the eEF1A2 antibody in a 1:50 dilution while the anti-rabbit secondary antibody was used at a 1:100 dilution (Fig. 22). The section with the MCF-7 cell line clearly shows the prominent brown color in the cytoplasm (Fig. 22A). On the other hand, the cytoplasm of BT-549-EV cells did not show considerable brown coloration (Fig. 22B). The nucleus of all the cells were stained blue because of the hematoxylin counter staining. The sections of MCF-7 (Fig. 22C) and BT-549-EV (Fig. 22D) were also stained with the secondary antibody alone (1:100) and these cells did not show significant brown color or background noise. The images of all the sections were captured under the high power magnification (40×).

DISCUSSION

Discussion

Many studies have been conducted on transcriptional regulation in oncogenesis. However, an emerging field of interest is the relationship between translational control and tumorigenesis. Protein translation factors can regulate cell growth, cell survival and tumorigenesis (Thornton *et al.* 2003; Sonenberg, 1993). For example, the expression of protein initiation factor, eIF4E is increased in primary breast cancer (Antony *et al.* 1996). Similarly, the amplification of protein elongation factor, *EEF1A2*, was observed in one third of primary ovarian tumors and its over-expression enhanced focus formation in Rat1 fibroblasts. In addition, eEF1A2 can stimulate anchorage-independent growth in soft agar and induce tumorigenicity in various mouse and human cell lines. (Anand *et al.* 2002). These experiments suggest that eEF1A2 is a putative oncogene. However, the mechanism by which eEF1A2 enhances cell growth and tumorigenicity is yet undetermined.

Numerous data suggest interactions between the signaling pathways controlling cell proliferation and components of the protein synthesis machinery (Rhoads, 1999). Because eEF1A2 is a translational elongation factor, it may increase the production of proteins that activate cell growth or lead to an overall increase in protein translation which may result in cell proliferation. In the present study, we were mainly interested in investigating the possible involvement of eEF1A2 in signal transduction pathways comprised of known oncogenes. Therefore, we hypothesized that eEF1A2 is a part of an AKT, c-Myc or PI3K-dependent oncogenic pathway.

DETERMINING THE EFFECT OF AKT, PI3K AND c-MYC EXPRESSION ON mRNA EXPRESSION OF eEF1A2

NIH 3T3, mouse fibroblast cells do not express eEF1A2 at a detectable level. It has been seen that the over-expression of exogenous eEF1A2 can transform NIH 3T3 cells *in vitro* as well as *in vivo* (Anand *et al.* 2002). In order to determine the effect of AKT, PI3K or c-Myc expression on the mRNA expression of eEF1A2, we have engineered NIH 3T3 cells to derive stable cell lines expressing AKT, PI3K or c-Myc respectively. In this scenario, it would be preferable to detect the target gene at the level of mRNA expression. The over-expression of eEF1A2 mRNA transcripts in human cancer cell lines and tissues was detected by quantitative real time PCR (qRT-PCR) (Joseph *et al.* 2004). In the present study, we used qRT-PCR to determine the mRNA expression of eEF1A2 in stable cell lines over-expressing AKT, PI3K and c-Myc, respectively. This experimental approach facilitated us to determine if eEF1A2 was one of the major downstream targets of the AKT, c-Myc or PI3K-dependent pathways.

Effect of AKT expression on mRNA expression of eEF1A2

We used a constitutively active, AKT for generating stable clones in NIH 3T3 cells. Active AKT contains a mutation within the autoinhibitory pleckstrin homology region, where the serine 473(ser 473) and threonine 308 (thr308) residues were substituted to aspartic acid residue (Ignatoski *et al.* 2003; Vojtek *et al.* 2003; Alessi *et al.* 1996a). The phophorylation of ser473 and thr308 residues is required for the full activation of AKT (Hara *et al.* 2005; Chan *et al.* 1999) (Fig. 5). Upon activation, AKT detaches from the plasma membrane and translocates to the nucleus where it activates transcription factors and /or stimulates certain cell regulatory targets in the cytosol (Meier *et al.* 1997). The

constitutively active AKT can relocate to the plasma membrane independent of PI3K activation.

In the present study, we speculated that eEF1A2 could be a downstream target of AKT. In this scenario, eEF1A2 might regulate or be regulated by down stream targets of AKT that are related to cell survival and proliferation. Over-expression of AKT could affect cell cycle regulators such as cyclin D1 (Hanada *et al.* 2004; Lawlor and Alessi, 2001) or transcription factors such as forkhead and NF-κB (Agarwal *et al.* 2004). Thus AKT has many downstream targets; however whether all these targets are directly phosphorylated by AKT remains yet inconclusive (Fig. 5). We wanted to explore the possibility that eEF1A2 interacts with one of these downstream targets and contributes to tumorigenesis. For example, eIF4E has already been recognized as an important human oncogene (Mamane *et al.* 2004; De Benedetti and Harris, 1999). Moreover, eIF4E, an mRNA cap-binding protein, mediates mTOR-dependent cell cycle regulation and is a downstream target of AKT. This pathway is emerging as a critical player in the etiology of cancer (Fingar *et al.* 2004; Nielsen *et al.* 1995). A growing emphasis has been placed on upstream and downstream targets of the mTOR pathway. It has been reported that AKT activates the ribosome recruiting machinery via mTOR and stimulates translation of key elements which can lead to tumorigenesis (Hay and Sonenberg, 2004). While following our hypothesis, we can also rule out the possible contribution of eEF1A2 in the mTOR pathway which is downstream of the AKT pathway.

In the current study, we created stables in which levels of AKT protein expression are increased. The isoforms of AKT (AKT-1, AKT-2 and AKT-3) are similar in structure and size and have similar substrate specificity (Chan *et al.* 1999) and the over-expression of

each isoform is crucial in various cancers (Katso *et al.* 2001). Therefore, a pan-AKT antibody was used to detect all three isoforms of AKT in the stable and control cell lines. We further performed qRT-PCR to investigate changes in eEF1A2 mRNA expression levels in the AKT stable cell lines (Fig. 7B-C). The schematic graph showed no substantial differences in the number of PCR cycles utilized for amplifying eEF1A2 in the AKT-1, AKT-2 and 3T3-EV (negative control) stable cell lines compared to mouse skeletal muscle (positive control) where eEF1A2 amplification started at an earlier PCR cycle (Fig. 7B). The statistical analysis depicted by bar graphs suggested that there was no substantial fold difference in the mRNA amplification of eEF1A2 in the AKT stable cell lines (Fig. 7C). The variations in fold difference in the two stable cell lines versus 3T3-EV were due to loading variations. Moreover, all stable cell lines were independently derived at different time points. These results were confirmed in triplicate, with RNA extracted at different time points and this data suggests that eEF1A2 is unlikely to be a downstream target of AKT.

One of the key upstream effectors of AKT is the heterodimeric lipid kinase, phosphoinositide 3-kinase (PI3K) (Fujita *et al.* 2002). However, interactions between PI3K and serine threonine kinases like AKT are not fully understood and should be further explored. PI3K is involved in many cellular activities such as cell proliferation, survival, vesicle trafficking and cytoskeletal organization. The dysregulation of PI3K signaling can occur by over-expression of PI3K protein level or an increase in kinase activity (Jimenez *et al.* 2000). We investigated whether eEF1A2 was a downstream target of the PI3K-dependent pathway.

PI3K is a member of phosphoinositide family. It has been documented that phosphoinositides and their derivatives interact with a variety of cellular proteins through

lipid-protein or protein-protein interactions (Chan *et al.* 1999). Recently, it has been shown that eEF1A2 interacts with M4, a member of the muscarinic acetylcholine receptor family, which mainly belongs to the G-protein-coupled receptor (GPCR) super family (McClatchy *et al.* 2002). Moreover, D-3 phosphorylated phosphoinositides can bind to domains of exchange factors which regulate heterotrimeric guanosine triphosphate (GTP) binding proteins or G proteins (Cantley, 2002). Because eEF1A2 is a GTP-binding protein, it is possible that there can be a connection between PI3K and eEF1A2.

Effect of PI3K expression on mRNA expression of eEF1A2

PI3K generates specific inositol lipids as secondary lipid messengers such as PI(3,4,5) P3 (PIP_3) and PI(3,4)P2(PIP_2). These further stimulate signal transductions by translocating AKT to the plasma membrane (Fig.5). At the plasma membrane, the conformational changes in AKT convert it into a substrate for phosphoinositide – dependent kinasel (PDK1) (Cantrell D.A., 2001; Vanhaesebroeck and Alessi, 2000). The PI3K/PDK1/AKT pathway has also been reported to be an important pathway in oncogenesis (Cantley, 2002). It has been observed that the major kinase activity from brain extracts depicted the ability of partially purified PDK1 to phosphorylate AKT at serine 473 residue (Vanhaesebroeck and Alessi ,2000; Stokoe *et al.* 1997) in the presence of PIP_3 (Delcommenne *et al.* 1998). Moreover, Stokoe and colleagues suggested that PDK2 may also be involved in these interactions. Since eEF1A2 is highly expressed in brain, it might be involved in similar types of interactions and could be exerting similar and /or additional kinds of cellular effects. It has also been claimed that a serine threonine kinase, integrin-linked kinase (ILK) can also phosphorylate ser473 of AKT in vitro as well as when over-expressed in cells by an indirect mechanism (Vanhaesebroeck and Alessi, 2000; Chan *et al.*

1999; Lynch *et al.* 1999) and appears to be involved in PI3K –mediated invasion (Dedhar *et al.* 1999). We have speculated that over-expression of PI3K might affect the mRNA expression of eEF1A2 and regulate cellular transformations through a PI3K-dependent pathway. This proposition was verified on stably transfected NIH 3T3 cells over-expressing the p110CAAX motif corresponding to a constitutively active PI3K.

The p110 subunit of PI3K is constitutively active and can phosphorylate several different phosphoinositides after being recruited to the cell surface by p85, a regulatory subunit (Nagoshi *et al.* 2005; Vanhaesebroeck and Waterfield, 1999). The Myc-tagged PI3K p110, a catalytic subunit (active PI3K) containing the membrane targeting CAAX motif was adequate to enhance the downstream effectors of PI3K (Fujita *et al.* 2002; Bar-Sagi, 2001). This construct was used in the current study to generate stable clones in NIH 3T3 cells. Cells expressing p110CAAX were shown to increase levels of serine-phosphorylated AKT (Ignatoski *et al.* 2003). The amplification of the p110 subunit of PI3K was observed in PI3K-mTOR pathways reported to be involved in various human cancers (Fry, 2001). On the other hand, constitutively active PI3K can also regulate Rac- and Rho-mediated cytoskeletal responses of membrane "ruffling" and formation of actin stress fibers (Arrieumerlou *et al.* 1998). More precisely, the production of PIP_3 can activate Rac, which plays a principle role in remodeling the actin cytoskeleton in response to chemotactic reagents (Cantley, 2002). It has been reported that eEF1A proteins from several species and genera associate with the cellular actin network (Yang *et al.* 1990) and these studies further supported our hypothesis. More interestingly, one of the key targets for PI3K/PDK1 is S6K1 kinase which upon phosphorylation governs protein synthesis as well as cell growth (Pullen *et al.* 1998). It has been documented that growth factor stimulation can lead to

S6K1 activation at its hydrophobic motif either via mTOR or through a mTOR- independent PI3K-PDK1 signaling inputs (Holland *et al.* 2004; Vanhaesebroeck and Alessi, 2000). The main substrate of the S6Ks is the ribosomal protein S6. More importantly, S6 has been localized to the small head region of the 40S subunit of the ribosome (Holland *et al.* 2004), where it can cross-link to a number of translational components present in or at the tRNA/mRNA binding site (Nygard and Nilsson, 1990). Furthermore, S6 phosphorylation was theorized to be involved in the translation of a specific class of mRNAs which is a TOP (terminal oligopyrimidine) tract in the 5' untranslated region (5' UTR) mRNA (Jefferies *et al.* 1997). Interestingly, it has been recently documented that these 5' TOP class of mRNAs comprise ribosomal proteins such as elongations factors: eEF1A1 and eEF1A2 (Holland *et al.* 2004). Furthermore, since eEF1A2 is one of the 5' TOP gene encoded proteins, this evidence further supports our speculation that eEF1A2 can be a downstream target of the PI3K-dependent pathway and can consequently exert tumorogenic characteristics.

We used active PI3K (p110CAAX motif) to derive stably transfected cell lines as mentioned earlier. The protein expression of the p110 catalytic subunit was detected by the p110α antibody. We used a p110α antibody to detect over-expression of PI3K because the stable clones were created by using p110CAAX motif. The over-expression of p110α in four independently derived stable clones compared to 3T3-EV control is shown by arrows (Fig. 8A). The eEF1A2 mRNA expression in the three stable clones, PI3K-3, PI3K-4 and PI3K-5 was detected by qRT-PCR. The ratio of PI3K to β-actin for PI3K-2 stable cell line was low compared to rest of the stable cell lines (Fig. 8A), and hence it was not evaluated by qRT-PCR. The qRT-PCR results were represented schematically and statistically as bar graphs (Fig. 8B-C). The amplification of eEF1A2 started earlier in skeletal muscle while it

was initiated approximately at the same number of PCR cycles in stably transfected cells as well as the 3T3-EV control(Fig. 8B). This data suggested that there was no substantial change in the eEF1A2 amplification in response to PI3K. The statistical analysis depicted by bar graphs suggested that there was no substantial fold difference in the amplification of eEF1A2 in the PI3K stable cell lines (Fig. 8C). The variations in fold difference in three PI3K stable cell lines versus 3T3-EV were due to loading variations. In addition, all stable cell lines were independently derived at different time points. These results were confirmed in triplicate, with RNA extracted at different time points and this data suggests that eEF1A2 is unlikely to be a downstream target of PI3K. PI3Ks exhibit protein kinase activity as well as lipid kinase activity (Walker *et al.* 1999). Our findings can be verified in future by determining the effect of PI3K kinase activity on eEF1A2 expression. However, it has been documented that eEF1A could act as an activator of PI4-kinase (Kahns *et al.* 1998). In this scenario, eEF1A2 may have a key role upstream of PI3K. This possibility was explored later on in the current project.

Effect of c-Myc expression on mRNA expression of eEF1A2

Another well known oncogene, c-Myc was also examined in the current study. It is a transcription factor involved in diverse cellular processes. It can mediate the induction of transcription cofactors which leads to an overall increase in transcriptional activity (Pelengaris *et al.* 2002). In spite of recent progress, it is still not well understood as to how c-Myc's transcriptional activity at the molecular level translates into the growth-promoting properties of the c-Myc protein. It has been documented that c-Myc expression induces cell growth by increasing expression of eIF4E (Rosenwald, 1996). Accordingly, the possibility arises whether c-Myc interacts with other components of protein synthetic machinery such

as eEF1A2. This led to our hypothesis that eEF1A2 could be one of the downstream targets of c-Myc in mediating cellular transformations. Several genes show up-regulation in response to c-Myc expression. However, it remains unclear whether increased expression is a direct consequence of Myc-Max transactivation or an indirect outcome of Myc-induced cell cycle progression (Facchini and Penn, 1998). For example, ectopic expression of c-Myc can up-regulate the protein and mRNA levels of cyclin A with delayed kinetics (Steiner *et al.* 1995). However, it is unclear whether this induction imitates a direct or indirect mechanism. Thus, the identification and characterization of c-Myc targets should provide insight into c-Myc function in both normal and neoplastic cell growth. It was stated that c-Myc has the ability to undergo protein-protein interactions and further alter gene transcription (Facchini and Penn, 1998). These findings were supported by numerous studies claiming that the helix–loop-helix domain of c-Myc can mediate protein–protein interactions (Liao and Dickson, 2000; Packham and Cleveland, 1995). Furthermore, the localization of c-Myc is debatable. It has been noted that c-Myc tends to be nuclearized in colon, testis, liver and ovary neoplasms, while cytoplasmic localization was also observed in many malignant tumors (Yuen *et al.* 2001). eEF1A proteins are present in the cytoplasm (Bohnsack *et al.* 2002; Lee *et al.* 1993). It has been documented that eEF1A acts as a major nuclear export substrate of RanBP21/exportin 5 (Bohnsack *et al.* 2002) and this suggests eEF1A2, one of the isoforms of eEF1A, may function similarly. We hypothesized that eEF1A2 may interact with c-Myc in two possible ways. It could be regulating MAX by channeling it to homodimerize with c-Myc and thus activating transcription factors in the nucleus or it could be directly or indirectly activating cyclin dependent kinases (Dang, 1999) via interacting with c-Myc. To explore these possibilities we speculated that eEF1A2 is a

key downstream target of the c-Myc pathway.

It has been reported that ectopic expression of c-Myc endorses cell-cycle progression and condenses the G_1 phase in cycling Rat fibroblasts cells (Eilers *et al.* 1991). In addition, CB33, a human lymphoid cell line, is also transformed by stable transfection with a plasmid expressing c-Myc (Gu *et al.* 1993) although the precise molecular basis for c-Myc activity remains unknown. c-Myc expression can also regulated post transcriptionally at the level of protein translation as well as mRNA stability. In addition, it was documented that exogenous expression of Myc also immortalizes primary mouse embryo fibroblasts while assisting oncogenic alleles of RAS in the transformation process (Thornton *et al.* 2003; Lutz *et al.* 2002; Facchini and Penn, 1998). eEF1A2 induced focus formation in Rat cells was similar to the RAS ^{val12} stimulated foci (Anand *et al.* 2002). These findings further supported our speculation that eEF1A2 could possibly be playing key role as a downstream target of c-Myc pathway and thus regulate cell transformations.

In the current study, we generated stable cell lines over-expressing c-Myc. The over-expression of c-Myc was detected in four independently derived NIH 3T3 stable cell lines versus 3T3-EV stable cell line (Fig. 9A). The stable cell lines, c-Myc-1 and c-Myc-2 were evaluated for eEF1A2 expression by qRT-PCR (Fig. 9B-C). These stables were over-expressing c-Myc at higher levels than the rest of stables (Fig. 9A). Interestingly, the amplification of eEF1A2 in c-Myc stables was initiated after the 3T3-EV (Fig. 9B). The statistical analysis of this data represented by bar graphs showed no mRNA expression of eEF1A2 in these stable cell lines (Fig. 9C) and these findings were again consistent with the schematic data (Fig. 9B). These evidences suggest that eEF1A2 is unlikely to be a downstream target of c-Myc pathway.

eEF1A2 is expressed in a tissue specific manner in terminally differentiated cells (Lee *et al.* 1993). On the other hand, c-Myc expression is higher in proliferating cells and reduced in terminally differentiated cells (Naidu *et al.* 2002; Johansen et al. 2001). This data was consistent with the findings where down regulation of c-Myc expression leads to the terminal differentiation of cells and permanent withdrawal from the cell cycle (Facchini and Penn, 1998; Rao and Anderson, 1997). Since eEF1A2 is expressed in terminally differentiated neuronal cells (Chambers *et al.* 1998), it is unlikely to be regulated by c-Myc. Our data is consistent with these findings and suggest that eEF1A2 is unlikely to be present downstream of the c-Myc pathways.

The findings in this current study suggest that eEF1A2 is unlikely to be a down stream target of AKT, c-Myc or PI3K-dependent pathways. The second part of our study was designed to address whether eEF1A2 was an upstream mediator of these oncogenes. We hypothesized that expression of eEF1A2 can affect protein expression of AKT, PI3K or c-Myc. We used BT-549 cells stably over- expressing eEF1A2 and the control, empty vector (Fig.10) and investigated the effect of eEF1A2 expression on protein expression of AKT, AKT-2, phospho-AKT, PI3K and c-Myc respectively by performing western blot on these cell lines.

DETERMINING THE EFFECT OF eEF1A2 EXPRESSION ON THE PROTEIN EXPRESSION OF AKT, pAKT, AKT-2, PI3K AND c-MYC

Effect of eEF1A2 expression on protein expression of AKT, AKT-2 and phospho-AKT (pAKT)

It has been documented that eEF1A2 can stimulate the rate of apoptosis in eEF1A2-

/- *wasted* mice (Potter *et al.* 1998). The ectopic expression of eEF1A2 has also been shown to protect against caspase-3 mediated apoptosis (Ruest *et al.* 2002). These evidences suggest that eEF1A2 can be a potential key player in cell survival. Numerous studies document that AKT activation can stimulate downstream targets that lead to cell survival (Hanada *et al.* 2004; Agarwal *et al.* 2004; Lawlor and Alessi, 2001). We investigated the potential role of eEF1A2 in promoting cell survival via AKT and speculated that eEF1A2 can affect protein expression and / or activation of AKT. Over-expression of AKT-2 is observed in 10-20% of ovarian cancers (Knuefermann *et al.* 2003) and it also contributes to tumor cell progression (Arboleda *et al.* 2003). Therefore, we determined the expression of AKT-2 levels in BT-549 stables versus empty vector. We found that the expression of eEF1A2 did not affect protein expression of AKT-2 at substantial levels (Fig.12). In order to rule out the changes in the expression of overall AKT protein in BT-549 stables over-expressing eEF1A2, we used a pan-AKT antibody. We demonstrated that eEF1A2 expression did not affect the levels of pan-AKT in these cell lines at considerable levels (Fig.11). However, it was interesting to note that eEF1A2 expression considerably upregulates the phosphorylation of serine 473 (Fig.11) and threonine 308 (Fig.11) residues of AKT in the BT-549 stable cell lines relative to the empty vector control (Fig.11). These findings suggest that eEF1A2 is not affecting overall protein expression of AKT, but it is likely to be activating AKT. This data is consistent with the speculation that eEF1A2 directly or indirectly activates AKT.

The signal transduction pathways leading to AKT activation are considered to be an important avenue in understanding tumorigenesis. The upstream regulation of AKT phosphorylation is known to be mediated by phosphatidylinositol signaling (Dedhar *et al.*

1999; Vanhaesebroeck and Alessi, 2000; Lynch *et al.* 1999). It has been documented that an eEF1A-like protein can directly activate PI4K in carrot cells (Kahns *et al.* 1998; Yang et al. 1990). It will be interesting to study the interactions between eEF1A2 and PI4K in mediating cell growth. Thus, the identification of eEF1A2 as an upstream activator of AKT suggests a probable mechanism by which eEF1A2 can promote cell growth and tumorigenicity. It has also been reported that the increase in AKT activity without simultaneous increase in its protein expression may have a "broader" effect on oncogenesis (Knuefermann *et al.* 2003). This effect may be related to tumor aggressiveness and /or its resistance towards anti-cancer agents. Our investigation of eEF1A2 as an upstream regulator of AKT activation is an avenue for future research because AKT plays a key role in multiple signaling pathways regulating cell growth. Thus, these findings indicate that eEF1A2 can possibly promote cell growth via AKT activation either by stimulating one of the upstream regulators of AKT or by increasing the activity of upstream kinases. It has been shown that the phosphorylation of ser473 as well as thr308 residues of AKT is essential for the complete activation of AKT (Hara *et al.* 2005). Interestingly, we demonstrated the upregulation of phosphorylated AKT at both residues. In order to fully understand the mechanics, we should further look at the known upstream activators of AKT such as PDKs and ILK. Vanhaesebroeck and Allessi documented that PDKs in rat brain extracts mainly phosphorylates AKT at ser473 residue and they also speculated that ILK may do the same although through an indirect mechanism (Vanhaesebroeck and Allessi, 2000). In addition, Stokoe and colleagues also hypothesized that AKT can be activated at ser473 residue by PDK2 (Stokoe *et al.*1997). Thus, it may be possible that eEF1A2 could be involved in ILK-or PDK- mediated AKT activation.

We also determined the protein levels of the catalytic and regulatory subunits of PI3K. However, it would be interesting to determine PI3K activity in eEF1A2 expressing cells. This will help to explore the probable role of eEF1A2 in mediating PI3K/AKT pathway in regulating cell growth and tumorigenesis. Moreover, MCF-7 cells, which endogenously express eEF1A2, are also estrogen responsive. Estrogen receptors govern most of the biological effects of estrogen in breast and ovarian cancers. It has been documented that eEF1A2 expression is increased in breast and ovarian cancers (Anand *et al.* 2002). Therefore, it would also be interesting to verify whether eEF1A2 expression and AKT activation correlates with estrogen response.

Effect of eEF1A2 expression on protein expression of catalytic (p110) and regulatory (p85) subunits of PI3K

The increase in AKT activity is regulated by upstream regulatory signals produced by over-expression or mutational activation of Ras oncogenes which activates AKT through PI3K (Knuefermann *et al.* 2003). In this objective, we determined whether eEF1A2 is promoting cell growth and tumorigenicity by affecting protein expression of PI3K subunits. PI3K is a heterodimer of a regulatory (p85) and catalytic (p110) subunits (Jimenez *et al.* 2000). We determined the effect of eEF1A2 expression on the protein expression of p110 as well as p85 subunits of PI3K (Fig.13). The regulatory subunit of PI3K is involved in actin cytoskeleton dynamics. In addition, PDGF mediated cdc42 activation can regulate p85α and consequently regulate actin cytoskeletal dynamics (Jimenez *et al.* 2000). The NH_2–terminal of p85 contains a Bcr homology (BH) domain which is homologous to the Rho guanosine triphosphatase activating protein domain of Bcr (Okkenhaug and Vanhaesebroeck, 2001). This BH domain is involved in stimulating cdc42 to bind with p85α thus protecting GAP

activity of cdc42 (Okkenhaug and Vanhaesebroeck, 2001). The guanine nucleotide exchange factors are essential for the activation of Cdc42 and this activity is often regulated by an upstream signal. PI3K can bind to domains of exchange factors which regulate GTP binding proteins (Cantley, 2002) and since eEF1A2 is a GTP-binding protein (Kahns *et al.* 1998), eEF1A2 may be mediating cdc42-like pathways through interactions with the regulatory subunit of PI3K and participating in cytoskeletal rearrangements. Therefore, we investigated the effect of eEF1A2 expression on protein expression of p85. We found that expression of eEF1A2 did not substantially affect the protein expression of the p85 subunit in the BT-549 stable cell lines (Fig.13). This data suggests that eEF1A2 is unlikely to be regulating the regulatory subunit of PI3K.

The p85 subunit associates with p110 and this complex is essential for transporting p110 to its lipid substrates in the membrane, thus regulating recruitment of PI3K to tyrosine - phosphorylated proteins (Okkenhaug and Vanhaesebroeck, 2001; Walker *et al.* 1999). After being transported to the plasma membrane, the p110 catalytic subunit binds to Ras, gets stabilized, and further stimulates the catalytic activity of the p110-p85 complex (Cantrell, 2001). Ras proteins are involved in cell replication and growth. eEF1A proteins can upregulate the production of Ras proteins, and eEF1A2 might be involved in similar regulatory mechanisms. It has been documented that the p85 subunit is required to stabilize p110. Similarly Ras can be substituted for p85 for a similar purpose (Rodriguez-Viciana *et al.* 1994). The amplification of the gene, *PIK3CA*, which encodes p110α, has been observed in ovarian and cervical cancers (Paez *et al.* 2003). Therefore, we investigated the effect of eEF1A2 expression on the protein expression of p110α. In addition, constitutively active p110α immortalizes rodent cells and these cells show the characteristics of oncogenic

transformation (Klippel *et al.* 1998). Since p110α is amplified in human cancers, we investigated the effect of eEF1A2 expression on the protein expression of p110 α and found that there is no substantial effect of eEF1A2 expression on the expression of p110α (Fig.13). This data is consistent with the p85 subunit findings. It has been documented that the p85α is essential to prevent the degradation of p110α while p110α can regulate the expression of p85α (Okkenhaug and Vanhaesebroeck, 2001). In addition, the catalytic subunits of PI3K are unstable when regulatory subunits are limiting (Yu *et al.* 1998). In this scenario, the upregulation in p85 subunit will also lead to the p110 upregulation. Together, these findings lend further support to our findings. As reported earlier, eEF1A-like protein acts as an activator of PI4-kinase (Kahns *et al.* 1998). In this possibility, eEF1A2 may interact with PI4K instead of PI3K. This possibility will be explored as a new research avenue in the future.

Effect of eEF1A2 expression on protein expression of c-Myc

c-Myc expression is deregulated in the development of experimentally induced tumors (Kato and Dang, 1992) and considered to be one of the potent regulators of cell growth (Yagi *et al.* 2002). The c-Myc proto-oncogene is amplified and /or over-expressed in ~15% of all human tumors (Yagi *et al.* 2002) and its gene amplification or protein over-expression in breast cancer vary between ~50-100% (Blancato *et al.* 2004). Cytokines or mitogens phosphorylate Myc at the amino–terminus through the Ras signaling pathway by stabilizing the protein and enhancing the transcription and translation of Myc by promoting cell proliferation (Huang, 2004). It was previously mentioned that eEF1A proteins can upregulate the protein expression of c-Myc in order to activate cell growth and proliferation (Lee, 2003). These findings encouraged us to speculate that eEF1A2 is deregulating cell

growth via c-Myc regulation.

We investigated whether the expression of eEF1A2 affects protein expression of c-Myc and speculated that eEF1A2 expression may upregulate c-Myc expression at protein levels. The isoforms of c-Myc express 62kDa to 67kDa of proteins (Liao and Dickson, 2000; Facchini and Penn, 1998). The commercially obtained positive control shows the 62kDa and 67kDa isoforms of c-Myc (Fig.14). Moreover, we found that eEF1A2 expression does not substantially affect protein expression of c-Myc (Fig.14). These findings are consistent with data that over-expression of Myc blocks cellular differentiation (Huang, 2004), while eEF1A2 tends to be expressed in differentiated cells (Chambers *et al.* 1998). These contradictory features of c-Myc and eEF1A2 suggest that eEF1A2 may not be exerting tumorigenic characteristics via c-Myc pathway. In addition, Mad or Mxil proteins are predominantly expressed in differentiated cells (Huang, 2004). These proteins bind to c-Myc and antagonize transcription activity of c-Myc (Lutz *et al.* 2002). This data supports our findings that eEF1A2 is neither present downstream or upstream of c-Myc in exerting cell growth and tumorigenesis.

To summarize, so far we found that AKT, PI3K or c-Myc oncogenes are not affecting mRNA expression of eEF1A2. On the other hand, eEF1A2 is not affecting protein expression of AKT, PI3K or c-Myc, however it is likely to be activating AKTat ser(473) and thr(308) positions. The goal of the current study is based on determining mechanism by which eEF1A2 enhances cell growth and tumorigenesis. We investigated that eEF1A2 is likely to be exerting tumorigenic characteristics by activating AKT.

DERIVATION OF eEF1A2 SPECIFIC ANTIBODY

Amplification of *EEF1A2* is observed in breast and ovarian cancer (Anand *et al.* 2002). The major goal behind derivation of the eEF1A2 antibody is to use this antibody as a potential prognostic marker in breast and ovarian tumours. The tissue specific eEF1A2 is highly similar to its isoform, eEF1A1 therefore the antibody analysis of eEF1A2 becomes critical (Tomlinson *et al.* 2005). An anti-eEF1A2 antibody is not available commercially. These facts encouraged us to derive an eEF1A2 specific antibody. In the current study, we designed the eEF1A2 specific peptide in such a way that the amino acid sequence of this peptide was not similar and conserved in eEF1A1. This approach is important in reducing the further possibility of cross reactivity with the eEF1A1 isoform. The eEF1A2 peptide was used to generate polyclonal antibodies that target unique epitopes of eEF1A2 protein. The peptide was conjugated to immunogenic carrier KLH to increase size and immunogenicity of the peptide. Animals generally used for polyclonal antibody production include chickens, goats, guinea pigs, horses, and sheep (ACEC, 1998). However, we used the rabbit, the most commonly used laboratory animal (Stanley *et al.* 1995). Furthermore, apart from the cost and convenience involved in it, rabbits can also produce vigorous antibody responses and thus it is easy to obtain high titer of the eEF1A2 antibody. In addition, rabbits have a relatively long life span and are easy to handle (ACEC, 1998). Two rabbits, 57/F and C44, were used in order to reduce potential total failure resulting from non-responsiveness to antigens of individual animals. Affinity purification was then performed on eEF1A2 anti-sera to remove the bulk of the non-specific immunoglobulin fractions, whereas enriching the fraction of immunoglobulin that specifically reacts with the eEF1A2 antigen.

Immunoaffinity purification can provide monospecific antibodies with similar homogenity as well as antigen binding specificity as monoclonal antibodies (Field *et al.* 1998). The specificity was accomplished by covalently coupling the eEF1A2 peptide to an affi-gel 10 affinity column. The eEF1A2 anti-sera were passed through the column and eEF1A2 specific antibodies were adsorbed on coupled resins and then eluted by using low affinity elution buffer. In this process, non-specific antibodies were allowed to pass through the column, thus leaving only the antibody towards eEF1A2. In this way, a monospecific antibody towards eEF1A2 was purified from a complex mixture of polyclonal antibodies by saving cost and time over monoclonal antibody purification. The specificity of the affinity purified eEF1A2 antibody derived from two rabbits was further determined by Western blotting.

Optimization of western blotting

The specificity of the eEF1A2 antibody was determined by using the cell extracts from BT-549 parental cells transduced with flag tagged Ad-eEF1A2 (Ad-1A2) (Fig.15, 16), MCF-7 cells and BT-549 cells stably transfected with eEF1A2 (Fig.18). MCF-7 cells endogenously produce eEF1A2 and used as a positive control. However, initially the specificity of eEF1A2 antibody was determined by comparing the relative band obtained with the commercially available anti-flag antibody (positive control) (Fig.15, 16). In addition, we also included BT-549 parental cells transduced with Ad-GFP virus (Fig.17) as a negative control. The addition of controls in above experiments helped us to confirm the specificity of eEF1A2 antibody. The optimal dilution of an eEF1A2 antibody was assessed (Fig.17) by including several modifications in western blotting protocol. For example, we used different combinations of dilutions in primary as well as secondary antibodies (Fig.15,

16, 17). Antibody dilutions were made in the 10% blocking solution comprising 5% carnation milk and 5% BSA. The increase in the percentage of blocking solution helped us to eliminate the non-specific bands (Fig.15). However, the high molecular weight band was resistant to any of the above modifications (Fig.16). The prolonged washing steps could only fade away the high molecular weight band in a 1:3000 dilution of eEF1A2 antibody, but it was not completely eliminated (Fig.16). Interestingly, the inclusion of blocking step after primary antibody dilution eliminated the non specific band (Fig.17). It means that the high molecular weight band and background noise was likely to be because of the secondary antibody.

The specificity of eEF1A2 antibody

The specificity of eEF1A2 was further evaluated by immunoprecipitation assay. The right size (50kDa) prominent band in flag immunoprecipitated Ad-eEF1A2 cell extract further verified the specificity of eEF1A2 antibody (Fig.19). The specificity was also confirmed on MCF-7 cells treated with the siRNA against eEF1A2 and negative siRNA respectively. Because the siRNAs against eEF1A2 work in specific manner, the MCF-7 cells treated with these siRNAs showed the reduction in eEF1A2 expression. This reduction was detected specifically by the eEF1A2 antibody and therefore the specificity of eEF1A2 antibody is reassured (Fig. 20). The eEF1A1 and eEF1A2 share more than 90% amino acid homology (Anand *et al.* 2002) and we designed our peptide specific to the eEF1A2 protein. The eEF1A2 peptide was designed using 215-233 residues because of the considerable difference (differences are underlined) between it and the corresponding eEF1A1 sequence (KVTRKDGNASGTTLLEALDC). Furthermore, we verified the specificity and potential cross reactivity of eEF1A2 anti-sera against ubiquitously expressed

eEF1A1. We used GST constructs expressing eEF1A2 and eEF1A1 proteins respectively. The pGEX4T-2- GST fusion protein system allows high level of expression and purification of fusion proteins from bacterial and eukaryotic cell extracts (Kaplan *et al.* 1997). The eEF1A2 anti-sera neither reacted with the epitope from the GST-eEF1A1 nor with the GST protein (Fig. 21B). This suggests that our antibody is only specific to the eEF1A2 protein and does not cross react with eEF1A1. The multiple bands (less than 75kDa) in the GST-eEF1A2 lane (Fig. 21B) are either because of the internal methionine residues or due to the degraded protein products. This data is important for using our antibody on cells as well as tissue samples. In that scenario, the eEF1A2 antibody will not pick up signals from ubiquitously distributed eEF1A1.

In summary, the eEF1A2 antibody is efficient to detect the denatured epitope of eEF1A2 protein and hence can be used in western blotting application. However, it was still undetermined whether this affinity purified eEF1A2 antibody could also be used on tissue sections. The eEF1A2 antibody isolated by another group was used on breast tumor samples and reported that eEF1A2 is moderately to strongly express in two-thirds of breast tumors (Tomlinson *et al.* 2005). The major goals of the current objective are also based on deriving an eEF1A2 antibody to use on breast as well as on ovarian tumor samples by tissue microarrays. We performed immunocytochemistry to evaluate the specificity and potential of eEF1A2 anti-sera to further use on tissue samples. The samples used in the current study were embedded in paraffin because it provides and retains better morphological details as well as resolution. Paraffin is thus an excellent embedding medium because it can be heated to liquid state and quickly turned to a solid state for maximum structural support in sectioning process. The immunocytochemistry was performed on the paraffin embedded

MCF-7 and BT-549-EV cells. MCF-7 cells endogenously produce eEF1A2 and were used as a positive control, while BT-549-EV cells do not produce eEF1A2 and were used as a negative control. It has been documented that the eEF1A proteins are comprised of 1-3% of the cytoplasm (Bohnsack *et al.* 2002). We performed DAB staining on MCF-7 and BT-549-EV cells to visualize the brown colored staining in the cytoplasm of cells (Fig. 22A-B). The brown coloration was considered as a positive signal appeared due to the eEF1A2 antibody (Fig.22A). DAB is the chromogen precipitating substrate and the end product is a brown coloration. It is used in numerous studies (Oostendorp *et al.* 2004; Sweetwyne *et al.* 2004; Garcia *et al.* 2002) on tissue as well as cell sections. The endogenous peroxidase activity in the cells was eliminated by pre-incubating sections with 3% hydrogen peroxide and then sections were treated with HRP-conjugated secondary antibody followed by DAB substrate. The optimal eEF1A2 antibody dilution (20 -50 fold) was determined by evaluating the strongest specific eEF1A2 (antigen) staining with the lowest non-specific background. The sections of MCF-7 and BT-549-EV cells were treated with the HRP conjugated anti-rabbit secondary antibody and then stained with DAB (Fig. 22C-D). These sections were considered as a control for determining background noise in MCF-7 and BT-549-EV cells. Since MCF-7 and BT-549-EV cells are two different types of cell lines, these were treated with the secondary antibody alone and this served as a control.

The immunostaining on cell sections implied that we could use the eEF1A2 antibody as a potential prognostic marker especially in the breast and ovarian tumours where *EEF1A2* copy number is amplified. We are planning to use the eEF1A2 antibody on tissue microarray samples comprised of ovarian and breast cancer tissues. Tissue microarrays are a powerful tool for studying tumor samples for the levels of gene and protein expression of

potential oncogenes (Keller and Yao, 2002). It has been documented that tissue microarrays performed on biopsies for determining the protein expression can be analyzed by conventional immuno histochemistry (IHC) using specific antibodies. The protein expression obtained by IHC was seen to be consistent with the RNA expression (Macgregor and Squire, 2002). *EEF1A2* mRNA expression was shown to be higher in some established ovarian cell lines compared to normal ovarian epithelial cells (Anand *et al.* 2002). Tissue microarray technology for DNA and RNA detection is expensive for routine use (Macgregor and Squire, 2002). The breast and ovarian tissues showing amplification in *EEF1A2* copy number can be analyzed for eEF1A2 protein expression by conventional IHC using our antibody. The use of our eEF1A2 antibody will thus be cost saving and, in the future, may help us to design eEF1A2 as an economical and a potential prognostic marker for analyzing and classifying tumors in the progression of cancer and the consequent outcome of the patient. In the future, we also anticipate that the eEF1A2 antibody will be used to map the regions of eEF1A2 that interact with various residential cell regulatory factors. This approach will also strengthen our understanding of how eEF1A2 influences tumorigenesis *in vivo*. It may be helpful in establishing eEF1A2 as a possible target for therapeutic interventions.

LIST OF REFERENCES

ACEC: Use of adjuvants in the production of polyclonal antibodies (1998) The University of Newcastle, animal care and ethics committee, Newcastle, Australia.

Abbott, C.M., Proud, C.G. (2004) Translation factors: in sickness and in health. *Trends Biochem Sci*, **29**, 25-31.

Agarwal, A., Das, K., Lerner, N., Sathe, S., Cicek, M., Casey, G., Sizemore, N. (2004) The AKT/IκB kinase pathway promotes angiogenic /metastatic gene expression in colorectal cancer by activating nuclear factor –κB and β-catenin. *Oncogene*, **Dec 13**, 1-11.

Alessi, D. R., Andjelkovic, M., Caudwell, B., Cron, P., Morrice, N.,Cohen, P., Hemmings, B.A. (1996a) Mechanism of activation of protein kinase B by insulin and IGF-1. *EMBO J*, **15**, 6541-6551.

Anand, N., Murthy, S., Amann, G., Wernick, M., Porter,L.A., Cukier,I. H., Collins, C., Gray, J.W., Diebold, J., Demetrick, D.J., Lee, J. M. (2002) Protein elongation factor EEF1A2 is a putative oncogene in ovarian cancer. *Nat Genet*, **31**, 301-305.

Antony,B., Carter,P., DeBenedetti, A. (1996) Overexpressionofthe proto-oncogene/translation factor 4E in breast –carcinoma cell lines. *Int J Cancer*, **65**, 858-863.

Arboleda, M. J., Lyons, J. F., Kabbinavar, F. F., Bray, M.R., Snow, B.E., Ayala, R., Danino, M., Karlan, B.Y., Slamon, D. J. (2003) Overexpression of AKT-2/protein kinase Bβ leads to up-regulation of β1 integrins ,increased invasion,and metastasis of human breast and ovarian cancer cells. *Cancer Res*, **63**,196-206.

Arrieumerlou, C., Donnadieu, E., Brennan, P., Keryer, G., Bismuth,G., Cantrell,D., Trautmann,A. (1998) Involvement of phosphoinositide 3-kinase and Rac in membrane ruffling induced by IL-2 in T cells. *Eur J Immunol*, **28**, 1877-1885.

Bar-Sagi D. (2001) A Ras by any other name. *Mol Cell Biol,* **21**, 1441-1443.

Blancato, J., Singh, B., Liu, A., Liao, D.J., Dickson, R.B. (2004) Correlation of amplification and overexpression of the c-Myc oncogene in high-grade breast cancer: FISH, in situ hybridization and immunohistochemical analyses. *Br J Cancer*, **90**, 1612-1619.

Bohnsack, M.T., Regener, K., Schwappach, B., Saffrich, R., Paraskeva, E., Hartmann, E., Gorlich D. (2002) Exp5 exports eEF1A via tRNA from nuclei and synergizes with other transport pathways to confine translation to the cytoplasm. *EMBO J*, **21**,

6205–6215.

Cantley, L.C. (2002) The phosphoinositide 3-kinase pathway. *Science*, **296**, 1655-1657.

Cantrell, D.A. (2001) Phosphoinositide 3-kinase signalling pathways. *J Cell Sci*, **114**, 1439-1445.

Chambers, D.M., Peters, J., Abbott, C.M. (1998) The lethal mutation of the mouse wasted (*wst*) is a deletion that abolishes expression of a tissue –specific isoform of translation elongation factor 1α, encoded by the *Eef1a2* gene. *Proc Natl Acad Sci USA*, **95**, 4463-4468.

Chan, T.O., Rittenhouse, S.E., Tsichlis, P. N. (1999) AKT/PKB and other D3 phosphoinositide-regulated kinases :Kinase activation by phosphoinositide – dependent phosphorylation. *Annu Rev Biochem*, **68**, 965-1014.

Chang, Y.W., Traugh, J. A. (1997) Phosphorylation of elongation factor 1 and ribosomal protein S6 by multipotential S6 kinase and insulin stimulation of translational elongation. *J Biol Chem*, **272**, 28252-28257.

Condeelis, J. (1995) Elongation factor 1α translation and the cytoskeleton. *Trends Biochem Sci*, **20**, 169-170.

Dang, C.V. (1999) c-Myc target genes involved in cell growth ,apoptosis and metabolism. *Mol Cell Biol*, **19**, 1-11.

Datta, S.R., Brunet, A., Greenberg, M.E. (1999) Cellular survival: a play in three Akts. *Genes Dev*, **13**, 2905-2927.

De Benedetti, A., Harris, A.L. (1999) eIF4E expression in tumors:its possible role in progression of malignancies. *Intl J Biochem Cell Biol*, **31**, 59-72.

Dedhar, S., Williams, B., Hannigan, G. (1999) Integrin- linked kinase (ILK): a regulator of integrin and growth –factor signaling. *Trend Cell Biol*, **9**, 319-323.

Delcommence, M., Tan, C., Gray, V., Rue, L., Woodgett, J., Dedhar, S. (1998) Phosphoinositide 3-OH kinase –dependent regulation of glycogen synthase kinase 3 and protein kinase B/AKT by the integrin –linked kinase. *Proc Natl Acad Sci USA*, **95,** 11211-11216.

Dever,T.E., Glynias,M. J., Merrick,W.C. (1987) GTP-binding domain: three consensus sequence elements with distinct spacing. *Proc Natl Acad Sci USA*, **84**, 1814-1818.

Eilers, M., Schirm, S., Bishop, J.M. (1991) The MYC protein activates transcription of the alpha-prothymosin gene. *EMBO J*, **10**,133-141.

Facchini, L. M., Penn L.Z. (1998) The molecular role of Myc in growth and transformation: recent discoveries lead to new insights. *FASEB J*, **12**, 633-651.

Faridi ,J.,Wang,L., Endermann,G., Roth, R.A. (2003) Expression of constitutively active Akt-3 in MCF-7 breast cancer cells reverses the estrogen and tamoxifen responsivity of these cells in vivo. *Clin CancerRes*, **9**, 2933-2939.

Field, C. M., Oegema, K., Zheng, Y., Mitchison, T. J., Walczak, C.E. (1998) Purification of cytoskeletal proteins using peptide antibodies. *Methods Enzymol*, **298**, 525-541.

Fingar, D.C., Richardson,C.J., Tee,A.R., Cheatham, L., Tsou,C., Blenis, J. (2004) mTOR controls cell cycle progression through its cell growth effectors S6K1 and 4E-BP1/eukaryotic translation initiation factors 4E. *Mol Cell Biol*, **24**, 200-216.

Frangioni, J.V., Neel, B.G. (1993) Solubilization and purification of enzymatically active glutathione S-transferase (pGEX) fusion proteins. *Anal Biochem*, **210**,179-187.

Franke,T.F. (1999) A difficult Akt to follow. *Neural Notes*, **5**, 3-7.

Fry, M.J. (2001) Phosphoinositide 3-kinase signaling in breast cancer: how big a role might it play? *Breast Cancer Res*, **3**, 304-312.

Fujita, N., Sato, S., Ishida, A., Tsuruo, T. (2002) Involvement of Hsp90 in signaling and stability of 3-phosphoinositide –dependent kinase -1. *J Biol Chem*, **277**, 10346-10353.

Fulton, D., Gratton,J.P., McCabe, T.J., Fontana, J., Fujio,Y., Walsh, K., Franke, T.F., Papaetropoulos, A., Sessa, W.C. (1999) Regulation of endothelium-derived nitric oxide production by the protein kinase Akt. *Nature*, **399**, 597-601.

Garcia, M.L., Herreras, J. M., Dios, E., Argueso,P., Almaraz, A. (2002) Evaluation of lectin staining in the diagnosis of fungal keratitis in an experimental rabbit model. *Mol Vis*, **8**, 10-16.

Gewin, L., Galloway, D.A. (2001) E Box-Dependent Activation of Telomerase by Human Papillomavirus Type 16 E6 Does Not Require Induction of c-*myc*. *J Virol*, **75**, 7198-7201.

Gingras, A., Raught, B., Sonenberg, N. (1999) eIF4 initiation factors: Effectors of mRNA recruitment to ribosomes and regulators of translation. *Annu Rev Biochem*, **68**,

913-963.

Gopalkrishnan, R.V., Su, Z.Z., Goldstein, N.I., Fishsher, P.B. (1999) Translational infidelity and human cancer: role of the PTI-1 oncogene. *Int J Biochem Cell Biol*, **31**, 151-162.

Grandori, C., Cowley, S. M., James, L. P., Eisenman, R. N. (2000) The Myc/Max/Mad network and the transcriptional control of the cell behavior. *Annu Rev Cell Dev Biol*, **16**, 653-699.

Gu, W., Cechova, K., Tassi, V., Dalla-Favara, R. (1993) Opposite regulation of gene transcription and cell proliferation by c-Myc and Max. *Proc Natl Acad Sci USA*, **90**, 2935–2939.

Guo, Q. M., Malek, R. L., Kim, S., Chiao, C., He, M., Ruffy, M., Sanka, K., Lee, N. H., Dang, C.V., Liu, E.T. (2000) Identification of c-Myc Responsive Genes Using Rat cDNA Microarray. *Cancer Res*, **60**, 5922-5928.

Hanada, M., Feng, J., Hemmings, B.A. (2004) Structure ,regulation and function of PKB/AKT –a major therapeutic target. *Biochim Biophys Acta*, **1697**, 3-16.

Hara, S., Oya, M., Mizuno, R., Horiguchi, A., Marumo, K., Murai, M. (2005) AKT activation in renal cell carcinoma : contribution of a decreased PTEN expression and the induction of apoptosis by an AKT inhibitor. *Ann Oncol*, **16**, 928-933.

Hay, N., Sonenberg, N. (2004) Upstream and downstream of mTOR. *Genes Dev*, **18**, 926-1939.

Hershey, J.W. (1991) Translational control in mammalian cells. *Annu Rev Biochem*, **60**, 717-755.

Holland, E.C., Sonenberg, N., Pandolfi, P.P., Thomas, G. (2004) Signaling control of mRNA translation in cancer pathogenesis. *Oncogene*, **23**, 3138-3144.

Hotokezaka,Y.,Tobben,U., Hotokezaka, H., Leyen, K.V., Beatrix, B., Smith, D.H., Nakamura, T.,Wiedmann, M. (2002) Interaction of the Eukaryotic Elongation Factor 1A with Newly Synthesized Polypeptides. *J Biol Chem*, **277**, 18545-18551.

Huang, Z. (2004) Stress signaling and Myc downregulation. *Cell Cycle*, **3**, 593-596.

Hurlin, P.J., Queva, C., Koskinen, P.J., Steingrimsson, E., Ayer, D.E. (1995b) Mad3 and Mad4: novel Max-interacting transcriptional repressors that suppress c-Myc dependent transformation and are expression during neural and epidermal differentiation. *EMBO J*, **14**, 5646-5659.

Ignatoski, K.M.W., Livant, D.L., Markwart, S., Grewal, N.K., Ethier, S.P. (2003) The Role of Phosphatidylinositol 3'-Kinase and its Downstream Signals in erbB-2-Mediated Transformation. *Mol Cancer Res*, **1**, 551-560.

Igney, F.H., Krammer, P.H. (2002) Death and anti-death: tumour resistance to apoptosis. *Nat Rev Cancer*, **2**, 277-288.

Jefferies, H.B., Fumagalli, S., Dennis, P.B., Reinhard, C., Pearson, R. B., Thomas, G. (1997) Rapamycin suppresses 5'TOP mRNA translation through inhibition of p70s6k. *EMBO J*, **16**, 3693-3704.

Jimenez ,C., Portela, R.A., Mellado, M., Rodriguez- Frade, J. M., Collard, J., Serrano, A., Martinez-A, C., Avila, J., Carrera, A.C. (2000) Role of the PI3K regulatory subunit in the control of actin organization and cell migration. *J Cell Biol*, **151** 249-261.

Johansen, L.M., Iwama, A., Lodie, T.A., Sasaki, K., Felsher, D.W., Golub, T.R., Tenen, D.G. (2001) c-Myc is a critical target for C/EBPα in granulopoiesis. *Mol Cell Biol*, **21**, 3789-3806.

Joseph, P., O'Kernick, C.M., Othumpangat, S., Lei, Y., Yuan, B., Ong, T. (2004) Expression profile of eukaryotic translation factors in human cancer tissues and cell lines. *Mol Carcinogenesis*, **40**, 171-179.

Kahns, S., Lund, A., Kristensen, P., Knudsen, C.R., Clark, B.F.C., Cavallius, J., Merrick, W.C. (1998) The elongation factor 1 A-2 isoform from rabbit: cloning of the cDNA and characterization of the protein. *Nucleic Acids Res*, **26,** 1884-1890.

Kandel, E.S., Hay, N. (1999) The regulation and activities of the multifunctional serine/threonine kinase AKT/PKB. *Exp Cell Res*, **253**, 210-229.

Kandl, K.A., Munshi, R., Ortiz, P.A., Anderson, G.R., Kinzy, T.G., Adams, A.E.M., (2002) Identification of a role for actin in translational fidelity in yeast. *Mol Genet Genomics*, **268**, 10-18.

Kaplan,W., Husler, P., Klump, H., Erhardt, J., Sluis-Cremer, N., Dirr, H. (1997) Conformational stability of pGEX-expressed *Schistosoma japonicum* glutathione S-transferase: A detoxification enzyme and fusion –protein affinity tag. *Protein Sci*, **6**, 399-406.

Kapp, L.D., Lorsch, J. R. (2004) The molecular mechanics of eukaryotic translation. *Annu Rev Biochem*, **73**, 657-704.

Kato, G. J., Dang, C.V. (1992) Function of the c-Myc oncoprotein. *FASEB J*, **6** 3065-3072.

Katso, R., Okkenhaug, K., Ahmadi , K., White, S., Timms, J., Waterfield, M.D. (2001) Cellular function of phosphoinositide 3-kinases : implications for development, homeostasis and cancer. *Annu Rev Cell Dev Biol*, **17**, 615-675.

Keller, E.T., Yao, Z. (2002) Application of high-throughput methods to cancer metastases. *J Musculoskelet Neuronal Interact*, **2**, 575-578.

Khwaja, A. (1999) AKT is more than just a Bad kinase. *Nature*, **401**, 33-34.

Klippel, A., Escobedo, M.A., Wachowicz, M.S., Apell,G., Brown, T.W., Giedlin, M.A., Kavanaugh, W.M., Williams, L.T. (1998) Activation of phosphatidylinositol 3-kinase is sufficient for cell cycle entry and promotes cellular changes characteristics of oncogenic transformation. *Mol Cell Biol*, **18**, 5699-5711.

Knuefermann, C., Lu,Y., Liu, B., Jin, W., Liang, K.,Wu, L., Schmidt, M., Mills, G.B., Mendelsohn, J., Fan, Z. (2003) HER2/PI-3K/AKT activation leads to a multidrug resistance in human breast adenocarcinoma cells. *Oncogene,* **22**, 3205-3212.

Krasilnikov, M.A. (2000) Phosphatidylinositol-3 kinase dependent pathways: the role in control of cell growth, survival, and malignant transformation. *Biochemistry*, **65**, 59-67.

Kubokura, H., Koizumi, K., Yamamoto, M., Tanaka, S. (1999) Chromosome 8 copy number and the c-Myc gene amplification in non-small cell lung cancer ,analysis by interphase cytogenetics. *J Nippon Med Sch,* **66**, 107-112.

Lamberti, A., Caraglia, M., Longo, O., Marra, M., Abbruzzese, A., Arcari, P. (2004) The translation elongation factor 1A in tumorigenesis, signal transduction and apoptosis: Review article. *Amino Acids*, **26**, 443-448.

Lawlor, M.A., Alessi, D.R. (2001) PKB/AKT: a key mediator of cell proliferation, survival and insulin responses? *J Cell Sci*, **114**, 2903-2910.

Lee, J. M. (2003) The role of protein elongation factor eEF1A2 in ovarian cancer. *Reprod Biol Endocrinol*, **1**, 69.

Lee, S., Wolfraim, L.A., Wang, E. (1993) Differential expression of S1 and elongation factor-1 alpha during rat development. *J Biol Chem*, **268**, 24453-24459.

Li , B.D., Gruner, J.S., Abreo, F., Johnson, L.W., Yu, H., Nawas, S., McDonald, J. C., DeBenedetti, A. (2002) Prospective study of eukaryotic initiation factor 4E protein elevation and breast cancer outcome. *Ann surg*, **235**, 732-738.

Liao, D.J., Dickson, R.B. (2000) c-Myc in breast cancer. *Endocr Relat Cancer*, **7**, 143-164.

Liu, C. H.L., Liu, S., Wang, E. (1993) Expression of an EF-1α-like rat cDNA, S1, in *E.Coli* and production of a rabbit polyclonal antiserum to the recombinant protein. *Biochem Biophys Res Commun*, **195**, 1371-1378.

Lund, A., Knudsen, S. M.,Vissing, H., Clark, B., Tommerup, N. (1996) Assignment of human elongation factor 1 alpha genes:EEF1A maps to chromosome 6q14 and EEF1A2 20q13.3. *Genomics*, **36**, 359-361.

Lutz, W., Leon, J., Eilers, M. (2002) Contributions of Myc to tumorigenesis. *Biochim Biophys Acta*, **1602**, 61-71.

Lynch, D. K., Ellis, C.A., Edwards, P.A.W., Hiles, I. D. (1999) Integrin-linked kinase regulates phosphorylation of serine 473 of protein kinase B by an indirect mechanism. *Oncogene*, **18**, 8024-8032.

Macgregor, P.F., Squire, J.A. (2002) Application of microarray to the analysis of gene expression in cancer. *Clin Chem*, **48** , 1170-1177.

Mamane,Y., Petroulakis, E., Rong, L., Yoshida, K., Ler, L.W., Sonenberg, N. (2004) eIF4E- from translation to transformation. *Oncogene*, **23**, 3172-3179.

Mansilla, F., Friis, I., Jadidi, M., Nielsen, K. M., Clark, B.F.C., Knudsen, C.R. (2002) Mapping the human translation elongation factor eEF1H complex using the yeast two-hybrid system. *Biochem J*, **365**, 669-676.

Marte, B. M., Downward, J. (1997) PKB/AKT: connecting phophoinositide 3-kinase to cell survival and beyond. *Trends Biochem* Sci, **22**, 355-358.

McClatchy, D.B., Knudsen, C.R., Clark, B. F., Khan, R.A., Hall, R. A., Levey, A.I. (2002) Novel interaction between the M4 muscarinic acetylcholine receptor and elongation factor 1A2. *J Biol Chem*, **277**, 29268-29274.

Meier, R., Alessi, D.R., Cron, P., Andjelkovic, M., Hemmings, B. A. (1997) Mitogenic activation, phosphorylation and nuclear translocation of protein kinase B β. *J Biol Chem,* **272**, 30491-30497.

Munshi, R., Kandl, K.A., Carr-Schmid, A., Whitacre, J. L., Adams A. E. M., Kinzy, T.G. (2001) Overexpression of translation elongation factor 1A affects the organization and function of the actin cytoskeleton in yeast. *Genetics*, **157**, 1425-1436.

Nagoshi, T., Matsui, T., Aoyama, T., Leri, A., Anversa, P., Wataru, O., Monte, F., Gwathmey, J. K., Grazette, B.H., Kass, D.A., Champion, H.C., Rosenzweig, A. (2005) PI3K rescues the detrimental effects of chronic Akt activation in the heart

during ischemia/reperfusion injury. *J Clin Invest,* **July 7**, 1-11.

Naidu, R., Waheb, N.A., Yadav, M., Kannankutty, M. (2002) Protein expression and molecular analysis of c-Myc gene in primary breast carcinomas using immunohistochemistry and differential polymerase chain reaction. *Int J Mol Med,* **9**,189-196.

Nakatani, K., Sakaue, H., Thompson, D.A., Weigel, R. J., Roth, R. A. (1999) Identification of a human Akt3 (protein kinase Bγ) which contains the regulatory serine phosphorylation site. *Biochem Biophys Res Commun*, **257**, 906-910.

Nielsen, F.C., Ostergaard, L., Neilsen, J., Christiansen, J. (1995) Growth-dependent translation of IGF-II mRNA by a rapamycin-sensitive pathway. *Nature*, **377**, 358-362.

Nygard, O., Nilsson, L. (1990) Translational dynamics. Interactions between the translational factors, tRNA and ribosomes during eukaryotic protein synthesis. *Eur J Biochem*, **191**, 1-17.

Okkenhaug, K., Vanhaesebroeck, B. (2001) New responsibilities for the PI3K regulatory subunit p85α. *Sci STKE*, **65**, 1-5.

Olive, D.M. (2004) Quantitative methods for the analysis of protein phosphorylation in drug development. *Expert Rev Proteomics*, **1**, 327-341.

Oostendorp, J., Hylkema, M. N., Luinge, M., Geerlings, M., Meurs, H., Timens, W., Zaagsma, J., Postma, D.S., Boddeke, H.W., Biber,K. (2004) Localization and Enhanced mRNA Expression of the Orphan Chemokine Receptor L-CCR in the Lung in a Murine Model of Ovalbumin-induced Airway Inflammation. *J Histochem Cytochem*, **52**, 401-410.

Ouyang, Y., Zhang, X., He, Q,. Wang, G., Siesjo, B. K., Hu, B. (2000) Differential phosphorylation at Ser473 and Thr308 of AKT-1 in rat brain following hypoglycemic coma. *Brain Res*, **876**, 191-195.

Paez, J.G., Sellers, W.R. (2003) PI3K/PTEN/AKT pathway. A critical mediator of oncogenic signaling. *Cancer Treat Res*, **115**, 145-67

Peckham, G., Cleveland, J.L. (1995) c-Myc and apoptosis. *Biochim Biophys Acta*, **1242**, 11-28.

Pelengaris, S., Khan, M., Evan, G. (2002) c-MYC: more than just a matter of life and death. *Nat Rev Cancer*, **2**, 764-776.

Plisiecka-Halasa, J., Karpinska, G., Szymanska, T., Ziolkowska, I., Madry, R., Timorek, A., Debniak, J., Ulanska, M., Jedryka, M., Chudecka-Glaz, A., Klimek, M., Rembiszewska, A., Kraszewska, E., Dybowski, B., Markowska, J., Emerich, J., Pluzanska, A., Goluda, M., Rzepka-Gorska, I., Urbanski, K., Zielinski, J., Stelmachow, J., Chrabowska, M., Kupryjanczyk, J. (2003) P21 WAF1, P27KIP1, TP53 and C-MYC analysis in 204 ovarian carcinomas treated with platinum-based regimens. *Ann Oncol*, **14**, 1078-1085.

Potter, M., Bernstein, A., Lee, M.J. (1998) The wst gene regulate multiple forms of thymocyte apoptosis. *Cell Immunol*, **188**, 111-117.

Pullen, N., Dennis, P.B., Andjelkovic, M., Dufner, A., Kozma, S.C., Hemmings, B., Thomas, G. (1998) Phosphorylation and activation of p70s6k by PDK1. *Science*, **279**, 707-710.

Ransom-Hodgkins, W., Brglez, I., Wang, X., Boss, W.F. (2000) Calcium –regulated proteolysis of eEF1A. *Plant Physiol*, **122**, 957-965.

Resar, L.M., Dolde, C., Barrett, J.F., Dang, C.V. (1993) B-myc inhibits neoplastic transformation and transcriptional activation by c-myc. *Mol Cell Biol*, **13**, 1130-1136.

Rhoads, R.E. (1999) Signal transduction pathways that regulate eukaryotic protein synthesis. *J Biol Chem,* **274**, 30337-30340.

Rao, M.S., Anderson, D.J. (1997) Immortalization and controlled in vitro differentiation of murine multipotent neural crest stem cells. *J Neurobiol*, **32**, 722-746.

Rodriguez-Viciana, P., Warne, P.H., Dhand, R., Vanhaesebroeck, B., Gout, I., Fry, M. J., Waterfield, M.D., Downward, J. (1994) Phosphatidylinositol -3-OH kinase as a direct target of Ras. *Nature*, **370**, 527-532.

Rosenwald I.B. (1996) Upregulated expression of the genes encoding translation initiation factors eIF-4E and eIF-2alpa in transformed cells. *Cancer Lett*, **102**,113-123.

Ruest, L-B., Marcotte, R., Wang, G. (2002) Peptide elongation factor eEF1A2 -2/S1 expression in cultured differentiated myotubes and its protective effect against caspase-3 mediated apoptosis. *J Biol Chem*, **277**, 5418-5425.

Samuels, Y., Wang, Z., Bardlli, A., Silliman, N., Ptak, J., Szabo, S., Yan, H., Gazdar, A., Powell, S. M., Riggins, G. J., Willson, J. K.V., Markowitz, S., Kinzler, K.W., Vogelstein, B., Velculescu, V.E. (2004) High frequency of mutations of the PIK3CA gene in human cancers. *Science*, **304**, 554.

Sheikh, S. S. El., Domin, J., Tomtitchong, P., Abel, P., Stamp, G., Lalani, E. (2003)

Topographical expression of class IA and class II phosphoinositide 3-kinase enzymes in normal human tissues is consistent with a role in differentiation. *BMC Clin Pathol*, **3**, 1-14.

Shiina, N., Gotoh,Y., Kubomura, N., Iwamatsu, A., Nishida, E. (1994) Microtubule severing by elongation factor 1 α. *Science*, **266**, 282-285.

Sonenberg, N. (1993) Translation factors as effectors of cell growth and tumorigenesis. *Curr Opin Cell Biol*, **5**, 955-960.

Stanley, S., Dias, J.A., D'Arcangelis, D., Mannella, C. A. (1995) Peptide-specific Antibodies as Probes of the Topography of the Voltage-gated Channel in the Mitochondrial Outer Membrane of *Neurospora crassa. J Biol Chem*, **270**, 16694-16700.

Steelman ,L.S., Pohnert, S.C., Shelton, J.G., Franklin, R.A., Bertrand, F. E., McCubrey, J.A. (2004) JAK/STAT,RAF/MEK/ERK,PI3K/AKT and BCR-ABL in cell cycle progression and leukemogenesis. *Leukemia*, **18**,189-218.

Steiner, P., Philipp, A., Lukas, J., Godden-Kent, D., Pagano, M., Mittnacht, S., Bartek, J., Eilers, M. (1995) Identification of a Myc-dependent step during the formation of active G1 cyclin-cdk complexes. *EMBO J*, **14**, 4814–4826.

Stephens, L., Anderson, K., Stokoe, D., Erdjument-Bromage, H., Painter, G. F., Holmes, A.B., Gaffney, P. R. J., Reese, C. B., McCormick,F., Tempst, P., Coadwell, J., Hawkins, P.T. (1998) Protein kinase B kinases that mediate phosphatidylinositol 3,4,5-triphosphate-dependent activation of protein kinase B. *Science*, **279**, 710-714.

Stokoe, D., Stephens, L.R., Copeland, T., Gaffney, P. R., Reese, C.B., Painter, G.F., Holmes, A.B., McCormick, F., Hawkins, P.T. (1997) Dual role of phosphatidylinositol 3, 4, 5-triphosphate in the activation of protein kinase B. *Science*, **277**, 567-570.

Sun, M., Wang, G., Paciga, J. E., Feldman, R. I., Yuan, Z., Ma, X., Shelley, S.A., Jove, R., Tsichlis, P.N., Nicosia, S.V., Cheng, J.Q. (2001) AKT1/PKBα kinase is frequently elevated in human cancers and its constitutive activation is required for oncogenic transformation in NIH3T3 cells. *Am J Pathol*, **159**, 431-437.

Sweetwyne, M.T., Brekken, R.A., Workman, G., Bradshaw, A.D., Carbon, J., Siadak, A.W., Murri, C., Sage, E. H. (2004) Functional Analysis of the Matricellular Protein SPARC with Novel Monoclonal Antibodies. *J Histochem Cytochem*, **52**, 723-733.

Thomas-Tikhonenko, A., Viard-Leveugle, I., Dews, M., Wehrli, P., Sevignani, C., Yu, D., Ricci, S., el-Deiry, W., Aronow, B., Kaya, G., Saurat, J.H., French, L.E.

(2004) Myc- transformed epithelial cells down-regulate clusterin ,which inhibits their growth in vitro and canrcinogenesis in vivo. *Cancer Res*, **64**, 3126-3136.

Thornton, S., Anand, N., Purcell, D., Lee, J. (2003) Not just for housekeeping: protein initiation and elongation factors in cell growth and tumorigenesis. *J Mol Med*, **81**, 536-548.

Tomlinson, V. A., Newbery, H. J., Wray, N. R., Jackson, J., Larionov, A., Miller, W. R., Dixon, J. M., Abbott, C. M. (2005) Translation elongation factor eEF1A2 is a potential oncoprotein that is overexpressed in two-thirds of breast tumours. *BMC Cancer*, **5,** 113.

Vanhaesebroeck, B., Alessi, D.R. (2000) The PI3K-PDK1 connection: more than just a road to PKB. *Biochem J*, **346**, 561-576.

Vanhaesebroeck, B., Leevers, S. J., Khatereh, A., Timms, J., Katso, R., Driscoll, P. C., Woscholski, R., Parker, P. J., Waterfield, M. D. (2001) Synthesis and function of 3-phosphorylated inositol lipids. *Annu Rev Biochem*, **70**, 535-602.

Vanhaesebroeck, B., Waterfield, M. D. (1999) Signaling by distinct classes of phosphoinositide 3-Kinases. *Exp Cell Res*, **253**, 239-254.

Vivanco, I., Sawyers, C. L. (2002) the phosphatidylinositol 3-Kinase –AKT pathway in human cancer. *Nature Rev Cancer*, **2**, 489-501.

Vojtek , A.B,. Taylor, J., DeRuiter, S. L.,Yu, J., Figueroa, C., Kwok, R., Turner, D.L. (2003) Akt regulates basic helix-loop –helix transcription factor –coactivator complex formation and activity during neuronal differentiation. *Mol Cell Biol,* **23,** 4417-4427.

Walker, E. H., Perisic, O., Ried, C., Stephens, L., Williams, R.L. (1999) structural insights into phosphoinositide 3-kinase signaling. *Nature*, **402**, 313-320.

Wang,Y. H., Liu, S., Zhang, G., Zhou, C. Q., Zhu, H.X., Zhou, X.B., Quan, L.P., Bai, J. F., Xu, N. Z. (2005) Knockdown of c-Myc expression by RNAi inhibits MCF-7 breast tumor cells growth in vitro and in vivo. *Breast Cancer Res*, **7**, R220-R228.

Watanabe,T., Imoto, I., Katahira, T., Hirasawa, A., Ishiwata, I., Emi, M., Takayama, M., Sato, A., Inazawa, J. (2002) Differentially regulated genes as putative targets of amplification at 20q in ovarian cancers. *Jpn J Cancer Res*, **93**,1114-1122.

Watkins, S. J., Norbury, C. J. (2002) Translation initiation and its deregulation during tumorigenesis. *Br J Cancer*, **86**, 1023-1027.

Waterfield, M. D., Downward, J. (1994) Downward phosphatidylinositol -3-OH kinase as

a direct target of Ras. *Nature*, **370**, 527-532.

Yagi, K., Furuhashi, M., Aoki, H., Goto, D., Kuwano, H., Sugamura, K., Miyazono, K., Kato, M.(2002) c-Myc is a downstream target of the Smad pathway. *J Biol Chem*, **277**, 854-861.

Yang, F., Demma, M., Warren, V., Dharmawarshane, S., Condeelis, J. (1990) Identification of an actin-binding protein from Dictyostelium as elongation factor1α. *Nature*, **347**, 494-496.

Yu, J., Zhang, Y., Mcllroy, J., Rordorf-Nikolic, T., Orr, G. A., Backer, J. M. (1998) Regulation of the p85/p110 phosphatidylinositol 3'-kinase:stabilization and inhibition of the p110α catalytic subunit by the p85 regulatory subunit. *Mol Cell Biol*, **18**, 1379-1387.

Yuen, M., Wu, P., Lau, J., Lai, C. (2001) Expression of c-Myc, c-Fos and c-Jun in hepatocellular carcinoma. *Cancer*, **91**, 106-112.

Zdychova, J., Komers, R. (2005) Emerging role of Akt kinase/protein kinase B signaling in pathophysiology of diabetes and its complication. *Physiol Res*, **54**, 1-16.